AUTONOMIC CONTROL OF CORONARY BLOOD FLOW IN CONTROL AND HEART FAILURE OVINE MODELS

Mridula Pachen

A thesis submitted in fulfilment of the requirements for the degree of Doctor of Philosophy in Cardio-renal Physiology, the University of Auckland, 2021.

Abstract

Carotid bodies (CBs) are the main peripheral chemoreceptors that are strategically located at the bifurcation of the common carotid artery. They are the primary sensors of systemic hypoxia, and their stimulation elicits powerful reflex responses such as respiratory, autonomic, and cardiovascular adjustments critical for body homeostasis. Recent studies suggest that CB chemosensitivity is higher in patients with heart failure (HF) and animal models of HF. Activation of the CB is presumed to activate both the sympathetic and parasympathetic nerves to the heart but this has not been directly determined. In addition, the role of the CB in modulating coronary blood flow (CoBF) is unclear. I hypothesized that activation of the CB would increase directly recorded cardiac SNA, which would then lead to coronary vasodilation. I tested this in the conscious control animals. I also hypothesized that inactivation of the CB via hyperoxia would cause a reduction in CoBF in both control and HF groups.

Experiments were conducted in conscious sheep implanted with electrodes to record cardiac SNA and diaphragmatic electromyography (dEMG), flow probes to record CoBF and cardiac output (CO) and a catheter to record mean arterial pressure (MAP). To eliminate the contribution of metabolic demand on coronary flow, the heart was paced at a constant rate during CB chemoreflex stimulation.

Intra-carotid potassium cyanide (KCN) injection resulted in a significant increase in directly recorded cardiac SNA as well as a dose-dependent increase in MAP and CoBF. The increase in CoBF was augmented in the HF group when the influence of metabolic vasodilation was abolished. The increase in CoBF and coronary vascular conductance (CVC) to intracarotid KCN injection was abolished after propranolol infusion in the control group but not the HF group. The pressor response to activation of the CB was abolished by pre-treatment with intravenous atropine in both groups. My data suggests that CB-mediated increases in CoBF are

mediated by an increase in cardiac SNA in the control group but not the HF group. Inactivation of the CBs using hyperoxia caused a significant decrease in MAP and CoBF in the HF group.

To further examine the influence of pulmonary afferents, I used a novel airflow therapy, high nasal flow (HNF) and investigated the MAP, renal blood flow (RBF), and renal vascular conductance (RVC) responses to HNF in conscious normotensive and hypertensive sheep. HNF caused a significant decrease in blood pressure and increase in RVC in both groups. Taken together my studies suggest that CBs play an essential role in modulating blood flow to the heart and that HNF can be beneficial in conditions where the CB is hyperactive without causing impairment of blood flow to vital organs.

Acknowledgement

It is my pleasure to acknowledge the roles of many individuals who were instrumental in completing my PhD study.

First of all, I would like to express my sincere gratitude and profound respect to my supervisor Dr. Rohit Ramchandra who has helped and encouraged me at all stages of my thesis work with great patience and immense care. I sincerely enjoyed working in a research environment that stimulates critical thinking and initiative, which he created. Dr. Rohit's skilful guidance, knowledge, innovative ideas, and immense patience are greatly appreciated. Above all, his overwhelmed attitude to help his students was solely responsible for accomplishing my work.

I would like to acknowledge the valuable input of my co-supervisor, Dr. Carolyn Barrett, who contributed her intellectual comments and contribution that helped shape the final version of this thesis.

I would like to acknowledge Dr. Nigel Lever, an interventional cardiologist, who performed the microembolization surgery and contributed to drafting the published papers.

I thank profusely to my lab colleagues: Dr. Yonis Abukar, Bindu George, Dr. Julia Shanks, Dr. Robert Chen, Charlotte Hamilton, Dylan Pen, Dr. Joshua Chang, and Chris Sohn. It was a great pleasure working with incredibly friendly people with whom I could share many ideas, thoughts, laughs, and quality fun time. Special thanks must go to Dr. Yonis Abukar for training and helping me with experiments, surgeries, data analysis, and Bindu George for helping me from my initial stage of my PhD with experiments and surgeries. Similarly, Linley Nisbet, Maree Schollum, Vanessa Hawkins, and Melanie Hyslop of the Vernon Jansen Unit, University of Auckland deserve praise for their excellent technical assistance, animal care and welfare.

I would like to express my gratitude to Professor. Julian Paton, Dr. James Fisher, Dr. Fiona McBryde, and Dr. Sarah-Jane Guild, as well as everyone else in the CVARC (Cardiovascular Autonomic Research Cluster) family, for their advice and encouragement.

My most profound appreciation belongs to my parents, sisters, and my beloved husband, Mr. Riyesh Poolanchalil, for their unwavering encouragement, assistance and support throughout my research period. I would also like to mention BioRender software to create all figures in this thesis and my husband for his assistance.

Lastly, this research would not have been possible without the generous support of the University of Auckland Faculty Research Development Fund, the Maurice and Phyllis Paykel Trust, Fisher and Paykel Healthcare, Health Research Council of New Zealand, and Heart Foundation of New Zealand.

Table of Contents

List of Figures

List of Tables

Glossary

To aid ease of reading, less common abbreviations are reiterated at their first use in each chapter

ACE	Angiotensin-converting enzyme
Ach	Acetylcholine
Ang II	Angiotensin II
ANOVA	Analysis of variance
AT1	Angiotensin II type 1
BP	Blood pressure
Ca2+	Calcium ion
CB	Carotid body
CO	Cardiac output
CoBF	Coronary blood flow
CPAP	Continuous positive airway pressure
CVC	Coronary vascular conductance
dEMG	Diaphragmatic electromyography
EF	Ejection fraction
FS	Fractional Shortening
HF	Heart Failure
HNF	High nasal flow
HR	Heart rate
HTN	Hypertension
i.m.	Intramuscular
i.v.	Intravenous
KCN	Potassium cyanide
Kg	Kilogram
K+	Potassium ion
L	Litre
MAP	Mean arterial pressure

ME	Microembolization
mg	Milligram
min	Minutes
mL	Millilitre
mmHg	Millimetre of mercury
Na^+	Sodium ion
NTS	Nucleus tractus solitarius
$PaCO_2$	Partial pressure of carbon dioxide
PaO_2	Partial pressure of oxygen
PNS	Parasympathetic nervous system
RAAS	Renin-angiotensin-aldosterone system
RBF	Renal blood flow
RVC	Renal vascular conductance
RVLM	Rostral ventrolateral medulla
SD	Standard deviation
Sec	Seconds
SNA	Sympathetic nerve activity
SNS	Sympathetic nervous system
SV	Stroke volume
α1	alpha-1
α2	alpha-2
β1	beta-1
β2	beta-2
2K1C	2-kidney, 1-clip model
ºC	Degree Celsius
%	Percentage
<	Less than
>	More than
±	Plus or minus

Chapter 1: Introduction

1.1 Heart failure

1.1.1 *Epidemiology of Heart Failure in New Zealand*

Heart failure (HF) is defined as a complex clinical syndrome that can occur from any structural or functional cardiac disorder that impairs the ability of the ventricle to fill or eject blood or both (Hunt, 2005; Jessup et al., 2009). Moreover, heterogeneous aspects of HF have limited therapeutic advances in the field. HF is associated with poor quality of life, frequent hospitalization, high mortality, and morbidity rate (Cowie, 2001; McMurray et al., 2012). One-year mortality rates after the initial first hospitalization for HF are between 25 and 35% (Schaufelberger et al., 2004). The burden of HF is increasing and is associated with increasing health care expenditures (Savarese et al., 2017).

The prevalence of HF is over 26 million worldwide (Savarese et al., 2017). Cardiovascular disease places a significant burden on the New Zealand health system as well. More than 165,000 people in New Zealand are affected by heart disease, and every 90 minutes, one New Zealander dies from cardiovascular disease (Ministry of Health, 2013). Each year, there are about 12,000 hospitalizations, of approximately 5,500 patients, for HF (Wasywich et al., 2007). In 2011-12 approximately $501 million was spent on hospitalization (Del Rio et al., 2013b) indicating a huge economic burden. Although there has been a decrease in mortality through the 1990s, the mortality rate for HF and hospitalization is higher in New Zealand (Doughty et al., 1995; Riddell, 2005).

HF is of particular concern in New Zealand since it disproportionately affects Māori, with proportionally more deaths per 100 000 in Māori. HF among Māori occurs at an average of 10-15 years earlier than for Pākehā (non-Māori). Alarmingly, the HF mortality rate is approximately 8 times higher among Māori males aged 45-64 years than among non-Māori and

approximately 3.5 times higher among Māori aged 65 years and over (Ministry of Health, 2013). Similar excess mortality is observed for Māori females (Carr et al., 2002). Hospitalization for HF is 4 times higher among Māori compared with non-Māori with the disparity greater for females: hospital admissions for HF among Māori females is about 4.5 times as high as that among non-Māori females (Ministry of Health, 2011).

The incidence of HF continues to increase as the population ages, (Butler, 1997). According to national population projections, in New Zealand with a population of 5 million people, it is estimated that the proportion of the population over the age of 65 years will increase from 18% in 2021, to 21-26% in 2048 and 24-34% in 2073 (Stats, 2016).Considering that the prevalence of HF is approximately 10% among those aged 65 years and older (Bloomfield, 2017), it can be assumed that the number of people affected by HF will increase by around 50% over the next few decades. This increase in prevalence would increase the burden on healthcare systems imposed by HF.

Improvement in primary prevention of HF will result in a reduction in the disease incidence, while better medical treatment would lead to better survival, which in turn increases the prevalence of HF (Roger, 2013). Incidence and survival play a key role in the emergence of the hospitalization burden among patients with HF (Roger, 2013). Studies have reported that β-blocker therapy is one key factor to improve the survival rate (Barker et al., 2006). Also, data from previous studies have observed that while survival after HF diagnosis used to remain relatively poor, improvements have been observed since the late 1990s (Jhund et al., 2009; Yeung et al., 2012). Despite improved survival of recent decades, mortality and morbidity from HF remain high meaning improved treatment options are needed.

1.1.2 *Pathophysiology of heart failure and compensatory mechanisms*

HF is caused by myocardial dysfunction and often results in left ventricular (LV) hypertrophy and/or dilation (Cohn et al., 2000). HF has been broadly sub classified based on prevailing LV ejection fraction (LVEF). There are two main categories: HF with preserved EF (LVEF≥50%), and HF with reduced EF (HFrEF, in which the LVEF is ≤40%) (Yancy et al., 2017). I will be addressing HFrEF for the remainder of this thesis. HFrEF is a major public health concern with substantial morbidity, and mortality and the cause of death can be challenging to ascertain (Murphy et al., 2020). The heart fails to pump blood to deliver oxygen at a rate equivalent to the demand for tissue metabolism (America, 2010). The cause of this diminished CO in HFrEF is usually decreased contractility of the myocardium. Myocardial infarction (MI) and ischaemic heart disease resulting from partial blockage of the coronary vessels represents one of the leading causes of HF (Swedberg et al., 2005).

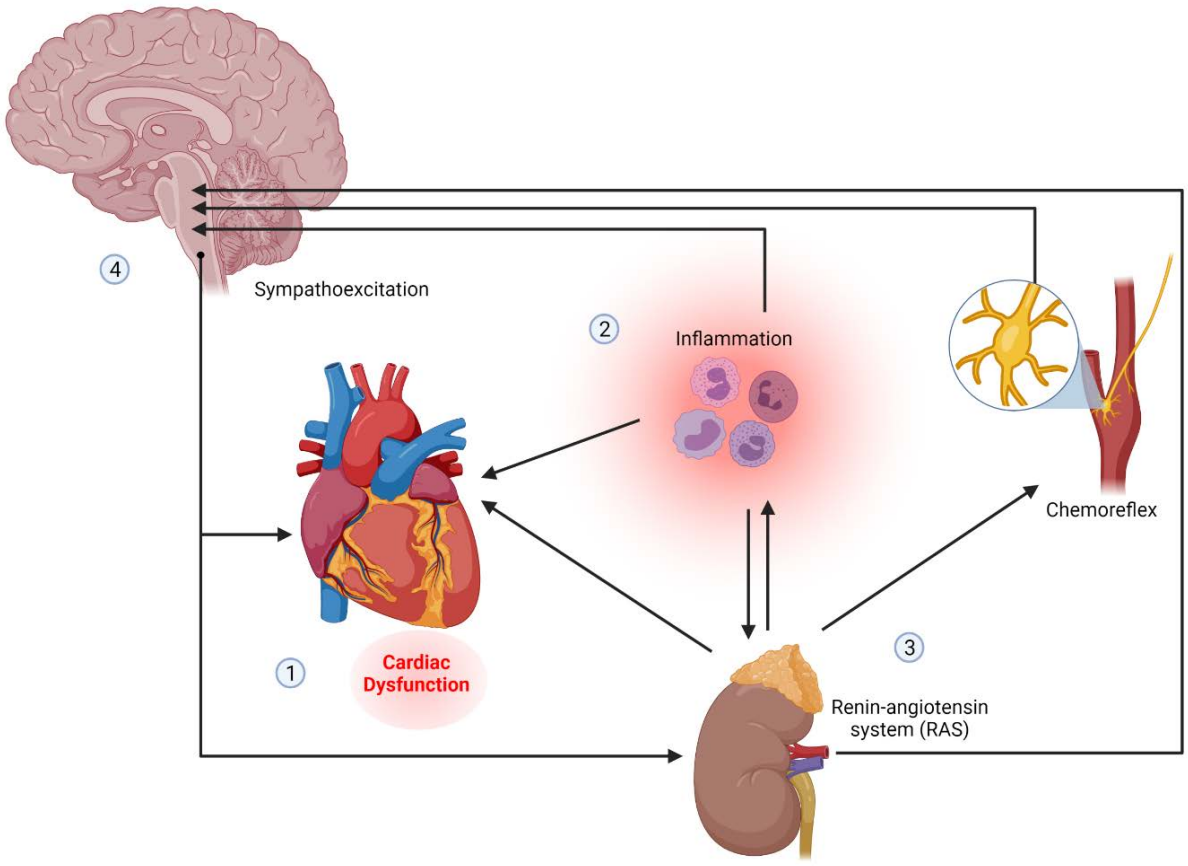

Figure 1 Main hallmarks of HF.

The main hallmarks of HF include (1) Cardiac dysfunction (2) systemic inflammation (3) activation of renin–angiotensin system and (4) autonomic imbalance, characterized by increased sympathetic activity and parasympathetic withdrawal.

People who live with heart disease have a reduced quality of life since autonomic dysfunction, and disordered breathing patterns are commonly observed in patients with HF and are thought to contribute to disease progression (Esler et al., 1998; Haack et al., 2014; Ponikowski et al., 1997; Schultz et al., 2015; Triposkiadis et al., 2009b). Studies have shown that breathing instability or oscillatory breathing patterns play a significant role in contributing to the autonomic imbalance in the HF state (Andrade et al., 2015; Díaz et al., 2020; Giannoni et al., 2008). Importantly, both autonomic dysfunction and breathing instability in HF have been

associated with altered chemoreflex function (Del Rio et al., 2013a; Marcus et al., 2014d; Zucker, 2006). Since peripheral chemoreflex is an essential topic in my study, its role and function in control and HF will be discussed in detail later in the Introduction.

To better understand the pathophysiology of HF, it is important to understand cardiac physiology. The most common causes of HF include hypertension (HTN), coronary artery disease, diabetes mellitus, obesity, cardiomyopathy and family history of cardiac diseases (Fletcher et al., 2001; Rogers et al., 2015). According to the New York Heart Association (NYHA) Functional Classification, the severity of HF is graded based on the physical activity, shortness of breath, and/or angina pain (American Heart Association, 2011) (Table 1).

Table 1 New York Heart Association (NYHA) functional classification of the severity of HF (American Heart Association, 2011)

Class I	No symptoms with ordinary activity
Class II	Slight limitation of physical activity Comfortable at rest, but ordinary physical activity results in fatigue, palpitation, dyspnea, or angina
Class III	Marked limitation of physical activity Comfortable at rest, but less than ordinary physical activity results in fatigue, palpitation, dyspnea, or angina
Class IV	Unable to carry out any physical activity without discomfort Symptoms of cardiac insufficiency may be present even at rest

The amount of blood pumped by the heart in a minute is called CO, which is, in turn, the product of heart rate (HR) and stroke volume (SV) and is generally 4 -8L/min at rest (Kemp et al., 2012). SV is defined as the amount of blood ejected by the ventricle in a heartbeat. In HFrEF, also called LV systolic dysfunction, SV is typically reduced, which will therefore reduce CO (Klabunde, 2011; Mohrman et al., 2014). The circulatory changes caused by an impaired cardiac pump function are sensed by peripheral arterial chemoreceptors and baroreceptors (Hartupee et al., 2017). As a result, these sensory receptors activate compensatory mechanisms that lead to changes in HR and cardiac contractility, salt and water retention, and total peripheral resistance in an attempt to maintain cardiovascular homeostasis (Triposkiadis et al., 2009a).

One of the main characteristics of HF is cardiac dysfunction (Figure 1) (Azad et al., 2014; Yancy et al., 2017). The decreased CO due to LV dysfunction leads to global hypoperfusion. Also, LV dysfunction coupled with compensatory mechanisms discussed below results in an increase in the amount of blood in the LV and, consequently, increases end-diastolic and end-systolic volumes (Kemp et al., 2012). The end-diastolic volume further causes an increase in LV end-diastolic pressure (LVEDP), which causes an increase in left atrial pressure and thereby pressures in the lung capillaries. This elevated lung pressure forces fluid out of the pulmonary capillaries, leads to pulmonary oedema and is clinically observed as symptoms of dyspnoea (Kantor et al., 2010; Kemp et al., 2012).

The compensatory mechanisms to the reduction in CO include activation of the sympathetic (adrenergic) nervous system (Kishi, 2012; Xu et al., 2015) and renin-angiotensin-aldosterone system (RAAS) (Figure 1), which maintain CO through increased salt and water retention (Sciarretta et al., 2009; Suzuki et al., 2004). Activation of SNS and RAAS releases epinephrine and norepinephrine, which causes an increase in peripheral vascular resistance as well as positive inotropic and chronotropic effects. This redistribution of blood flow by peripheral vasoconstriction and central vasodilation helps to maintain blood flow to vital organs

(Tanai et al., 2015). The changes in other systems, such as loss of parasympathetic tone and increased resistance to natriuretic peptides, are also characteristics in the HFrEF condition (Floras, 1993). These responses are collectively known as neurohormonal activation (Floras, 1993; Packer, 1992a) and will be discussed in the next few sections.

1.2 Sympathetic nervous system

1.2.1 *Structure and function*

The sympathetic nervous system (SNS) is an integral part of the autonomic system and plays a fundamental role in the maintenance of blood pressure (BP) and cardiovascular function. Preganglionic neurons of the SNS originate from the thoracic and lumbar (T1 to L2) regions of the spinal cord (McCorry, 2007; Wehrwein et al., 2011). The cell bodies are distributed in four areas of the grey matter in the spinal cord. The preganglionic neuron may exit the spinal cord and synapse with postganglionic neurons in the same levels of the spinal cord from which it originates or travels upwards or downwards in the ganglion chain to synapse with postganglionic neurons at other levels. In fact, a single preganglionic neuron may synapse with multiple postganglionic neurons in many various ganglia (McCorry, 2007).

1.2.2 *Sympathetic and parasympathetic neurons and receptors*

The preganglionic axons of the SNS are short and synapse with postsynaptic neurons found within sympathetic ganglia (Figure 2). Unlike the SNS, the axons of the preganglionic neurons of the parasympathetic nervous system (PNS) are quite long. The neurotransmitter used at the preganglionic sympathetic neurons is acetylcholine (ACh). This ACh activates nicotinic receptors, and the nerve fibers that release ACh are referred to as cholinergic fibers. The postganglionic neurons then travel to their effector sites, release epinephrine and norepinephrine (catecholamines) (McCorry, 2007).

These nerve fibers that release norepinephrine are referred to as adrenergic fibers. Most sympathetic postganglionic fibers release norepinephrine except sweat glands and the arrectores pili muscle (Shibasaki et al., 2010). These neurotransmitters then act on the adrenergic receptors such as alpha-1, alpha-2, beta-1 and beta-2 (α1, α2, β1 and β2 respectively) (Figure 2) (Strosberg, 1993). Cholinergic receptors are also found in PNS. Nicotinic cholinergic receptors stimulate parasympathetic postganglionic neurons to release their chemicals. Muscarinic receptors are mainly connected with parasympathetic functions and are located in peripheral tissues such as glands and smooth muscle (McCorry, 2007).

1.2.3 *Receptor sub-types and downstream actions*

The neurotransmitters and the circulating catecholamines bind to specific receptors on the cell membrane of the effector tissue (Triposkiadis et al., 2009a). All adrenergic and muscarinic receptors are coupled to G proteins and second messengers, which carry out the intracellular effects (McCorry, 2007). These receptors may be either inhibitory or excitatory, depending on the tissue on which it is located. The more abundant adrenergic receptors are alpha receptors, and of the 2 subtypes, α1 receptors are the most widely distributed on the effector tissues. Stimulation of these receptors causes smooth muscle contraction, resulting in vasoconstriction (Strosberg, 1993).

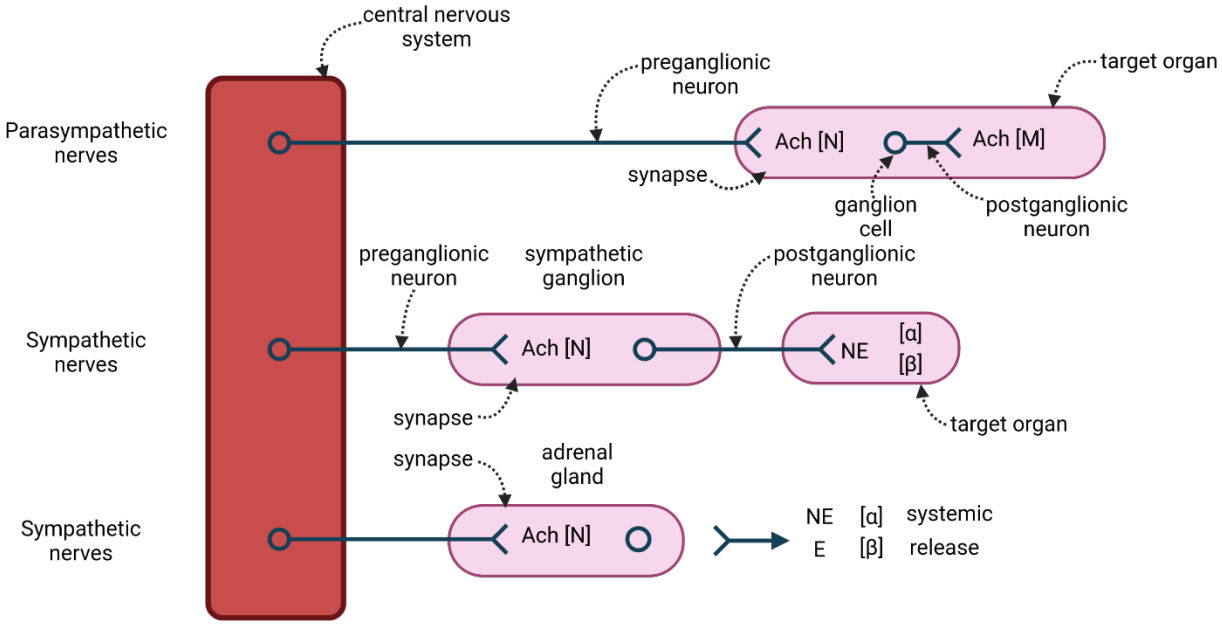

Figure 2 Autonomic ganglia and receptors

[N] Nicotinic acetylcholine receptor – located on the postganglionic neurons of the sympathetic and parasympathetic cell bodies. [M] Muscarinic receptor – found on all parasympathetic effector cells and some sympathetic effector cells. [α1, α2, β1, β2] Adrenergic receptors – located on most sympathetic effector cells Ach – Acetylcholine, E – Epinephrine, NE - Norepinephrine

Likewise, whether beta receptors are excitatory or inhibitory depends on the tissue on which they are found, stimulation of β2-receptor causes relaxation of vascular smooth muscle resulting in vasodilation. In the heart, β1-receptors are excitatory, and stimulation leads to increased HR, increased force of contraction, and rate of conduction. Therefore, sympathetic activation causes an increase in cardiac contractility and HR and hence increases CO (Strosberg, 1993).

The cardiac sympathetic nerve fibers are located subepicardially and travel along the routes of the major coronary arteries representing the predominant autonomic component in the ventricles (Zipes, 2008). The parasympathetic fibers run with the vagus nerve subendocardially after crossing the atrioventricular groove and are mainly present in the atrial myocardium and also present in the ventricular myocardium (Coote, 2013; Zipes, 2008). In addition, the sympathetic outflow to the heart and peripheral circulation is regulated by cardiovascular reflexes, mainly from aortic arch and carotid baroreceptors (SNS inhibition), cardiopulmonary baroreceptors (Bezold-Jarisch reflex, SNS inhibition), and peripheral chemoreceptors (SNS activation) (Malliani et al., 1983; Schwartz et al., 2011; Zhang et al., 2014). I have focused on the CB chemoreceptors in the HF state and this is discussed in detail in my study chapters.

1.2.4 *Heart Failure and SNS Hyperactivity*

As mentioned previously, myocardial dysfunction is associated with activation of the neurohumoral system. The neural limb of this response is represented by the SNS which is activated by a lot of afferent reflexes and hormones including low and high-pressure baroreceptors to increase SNA and thereby maintain CO (Tanai et al., 2015). The humoral limb is represented by increased secretion of hormones, most importantly the RAAS (Dzau et al., 1981). The sympathetic hyperactivity in HF is attributed to abnormalities in cardiovascular reflexes. The sympathoexcitatory reflexes, including the cardiac sympathetic afferent reflex and the arterial chemoreceptor reflex, are enhanced (Grassi et al., 1995).

The sensitivity of the baroreflex control of muscle SNA (MSNA) and renal SNA has been reported to be reduced in patients with HF and animal models of HF (Grassi et al., 1995; Liu et al., 2000; Mark, 1995). However, studies have found that the arterial baroreflex control of MSNA in patients with HF and baroreflex control of renal SNA in anaesthetized dogs with HF is preserved (Dibner-Dunlap et al., 1996; Dibner-Dunlap et al., 1989; Zucker et al., 1985).

Also, a study in conscious sheep with HF has concluded that the baroreflex control of cardiac sympathetic nerve activity (cardiac SNA) was not significantly changed (Watson et al., 2007). The sympathetic baroreflex control is complex and may vary between sympathetic beds. For instance, the sympathetic outflow to skeletal or renal vascular beds is strongly influenced by baroreceptor inputs, whereas the sympathetic outflow to the skin is little affected (Wallin et al., 2007).

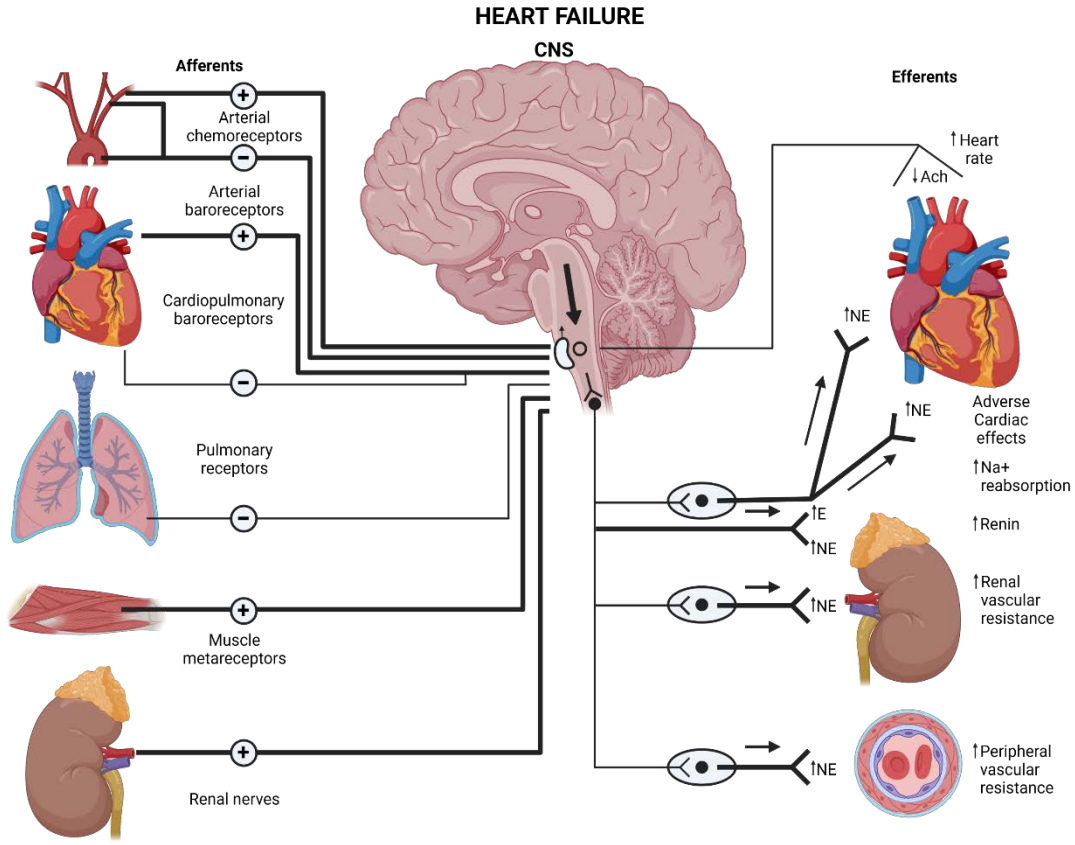

Figure 3 Mechanisms for sympathetic activation and parasympathetic withdrawal in HF

As HF progresses, the amount of input effecting sympatho-inhibition by stimulating ventricular and atrial mechanoreceptor nerve afferents decreases (thin line). In contrast, inhibitory modulation of efferent sympathetic nerve traffic by arterial baroreceptors (thick line) is maintained. Efferent vagal HR responses to arterial baroreflex perturbations are reduced (thin line) and excitatory (+) afferent input increases (thick lines). The net response to this altered balance consists of a generalized increase in sympathetic nerve traffic, weakened parasympathetic and sympathetic control of HR, and impaired reflex sympathetic regulation of vascular resistance. In advanced HF, there is an increase in sympathetic nerve traffic to the heart, kidney, skeletal muscle, adrenal, and other vascular beds (thick arrow shafts, thick lines). Ach = acetylcholine; CNS = central nervous system; E = epinephrine; Na^+ = sodium; NE = norepinephrine

Previous studies have indicated that the increase in SNA to the heart occurs earlier and to a greater extent than that to other organs (Esler et al., 1988; Hasking et al., 1986). Studies using noradrenaline (NA) spillover, a radiotracer technique that gives an index of organ-specific SNA, suggest that sympathetic drive to the human heart with HF is increased more than sympathetic activity to other organs such as kidneys, lungs, gut, or liver (Esler et al., 1988; Hasking et al., 1986; Rogers et al., 2015). The increase in NA spillover in the heart occurs earlier in the development of HF than other organs (Rundqvist, 1997). However, since cardiac NA spillover is an indirect measure of cardiac SNA, it is important that direct recordings of cardiac SNA in HF are examined to confirm the extent to which SNA is increased in HF.

Pacing- and infarction-induced animal models of HF have demonstrated using direct recordings of renal sympathetic nerve activity (Renal SNA) that activity in the renal nerves is increased (DiBona et al., 1994; Liu et al., 1999b), as is renal norepinephrine (NE) spillover in humans with HF (Hasking et al., 1986). Direct recording of cardiac SNA and renal SNA in HF sheep showed that the resting levels of sympathetic activity in both nerves were similar and close to their maximum levels (Ramchandra et al., 2009). Furthermore, direct recordings of muscle SNA in human HF have also confirmed that sympathetic activity is dramatically increased (Ferguson et al., 1992; Grassi et al., 1995).

The activation of the sympathetic nervous system also causes some negative impact in the HF condition and is shown to be detrimental. For instance, catecholamines (epinephrine and norepinephrine) released due to sympathetic stimulation increase HR and contractility (Chaggar et al., 2009). Sympathetic overactivation of the heart can cause lethal cardiac arrhythmias, myocardial ischaemia, and myocardial toxicity, leading to hypertrophy and cell death (Esler et al., 1998; Mann et al., 1992; Packer, 1992b). It is likely to account for the relationship between

autonomic dysfunction and sudden cardiac death in HF (Vaseghi et al., 2008). Moreover, norepinephrine causes down-regulation of β1-adrenergic receptors or uncoupling of β2-adrenergic receptors (Insel, 1996), and this may be associated with baroreceptor dysfunction and augmentation of sympathetic activity (Jackson et al., 2000). In addition, chronic sympathetic activation leads to further stimulation of RAAS system to further increase pre-load (Jhund et al., 2016).

Taken together, autonomic imbalance is characterized by increased sympathetic activity and parasympathetic withdrawal (Figure 3) contribute to the progression of HF (Floras et al., 2015). This thesis has a particular emphasis on oscillatory breathing pattern which in HF has been associated with altered chemoreflex function (Del Rio et al., 2013a; Marcus et al., 2014d; Zucker, 2006). In a previous human study, 60% of patients with HF displayed increased ventilatory responses to hypoxia when compared with controls (Giannoni et al., 2008). In support of this concept, animal studies have shown that tonic and hypoxia-induced afferent activity recorded from the CB chemoreceptors is enhanced in experimental HF (Del Rio, 2015; Del Rio et al., 2013a), suggesting that peripheral chemoreceptors may play a key role in HF. The role of the CB chemoreceptors will be discussed further in the Introduction.

1.2.5 *Renin-angiotensin-aldosterone system (RAAS)*

The reduction in CO and decreased blood volume in HF activates the RAAS (Dzau et al., 1981) which leads to increased plasma concentrations of renin, plasma angiotensin II, and aldosterone (Chatterjee, 2005; Dzau et al., 1981). Renin converts a precursor molecule, angiotensinogen to angiotensin I, which is then converted by angiotensin-converting enzyme (ACE) to angiotensin II (Jackson et al., 2000; Leung et al., 2003). Angiotensin II (Ang II) is a potent vasoconstrictor of the renal, and systemic circulation (Brunner-La Rocca et al., 2001). It

stimulates the release of noradrenaline from sympathetic nerve endings, inhibits vagal tone, and enhances aldosterone secretion (Rogers et al., 2015).

In addition to the altered neural inputs from baroreceptors and chemoreceptors, Ang II is another potential driver for the raised level of SNA in HF (Figure 4). Ang II acts on the brain and several areas of the central nervous system, that may augment ganglionic transmission, facilitation of norepinephrine release presynaptically, and regulation of postjunctional effects of norepinephrine (DiBona et al., 1995b; Reid, 1992; Sun et al., 1999a; Zucker et al., 2001). Moreover, increased levels of circulating Ang II may increase SNA by actions on circumventricular organs of the forebrain (Figure 4) (Liu et al., 1999a).

As mentioned previously, Ang II may facilitate sympathetic neurotransmission by a stimulatory action on sympathetic ganglia, by increasing neurotransmitter release at sympathetic nerve endings and inhibiting NA uptake at sympathetic nerve terminals (Dampney et al., 2002; Reid, 1992). These facilitatory actions of Ang II are suggested to operate only when SNA is high (Reid, 1992), so they may be important in HF. Therefore, ACE inhibitors and AT1 receptor blocker have been widely used in the management of patients with HF (Dibner-Dunlap et al., 1996; DiBona et al., 1995a; Egan et al., 1993; Grassi et al., 1997; Liu et al., 1999a; Ma et al., 1997; Young et al., 2004). Treatments that reduce the effects of the RAAS, including ACE inhibitors, have been shown to improve the overall condition of patients with HF and reduce hospitalization and mortality rates (Grassi et al., 1997; Lohse et al., 2003; Miller, 2003). The reported effects of treatment with ACE inhibitors on SNA in patients with HF are inconsistent, with both reductions and no change being reported (Dibner-Dunlap et al., 1996; Grassi et al., 1997).

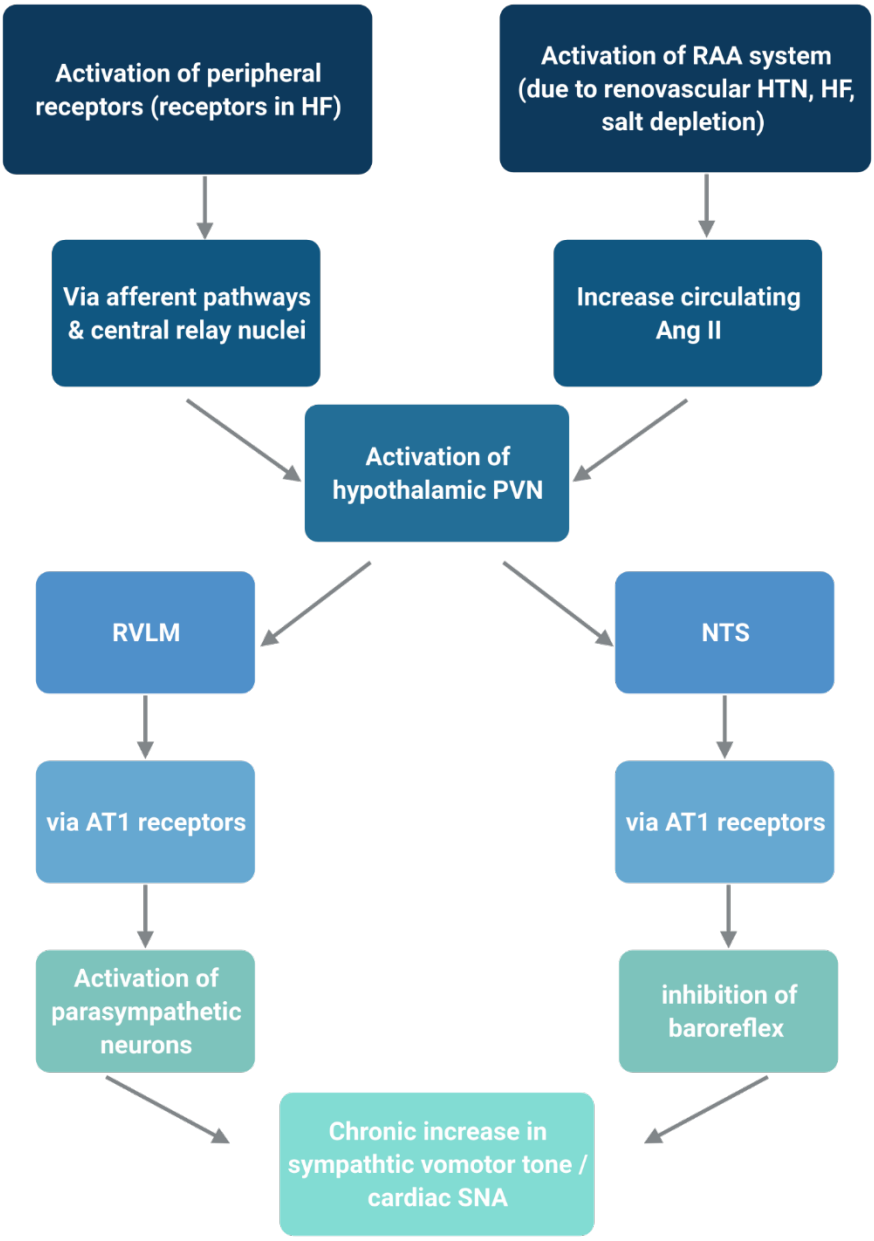

Figure 4 Central mechanisms result in a sustained increase in sympathetic nerve activity

Figure shows the presumed mechanisms that result in a sustained increase in sympathetic vasomotor and sympathetic cardiac activity elicited by various forms of chronic stimulation are depicted in this diagram. AngII = angiotensin II; CVO = circumventricular organs; PVN = paraventricular nuclei; NTS = nucleus tractus solitarius; RVLM = rostral ventrolateral medulla

In animal studies using rabbits and rats with HF, the findings have been more consistent, with intravenous infusion of AT_1 receptor antagonists being shown to decrease renal SNA and improve the arterial baroreflex regulation of HR and renal SNA (DiBona et al., 1995a; Murakami et al., 1997; Murakami et al., 1996). The finding that the increase of baroreflex sensitivity by an AT_1 receptor antagonist in HF rabbits was blocked by lesion of the area postrema suggests that, in HF, the baroreflex desensitization by Ang II resulted from an action on this circumventricular organ (Abukar et al., 2018; Liu et al., 1999a).

In addition to the previous paper examining the area postrema, there is good evidence that Ang II has potent actions on other areas of the central nervous system, and it is noted that the concentration of Ang II in the cerebrospinal fluid increases in chronic HF (Zucker et al., 2004). Studies in conscious sheep have shown that centrally administered Ang II caused an increase in cardiac SNA and a decrease in renal SNA (Watson et al., 2004). In anaesthetized and conscious rats in HF, it has been shown that the blockade of AT1 receptors in the brain normalized the baroreflex relationship between arterial pressure and renal SNA and arterial pressure and HR (DiBona et al., 1995a; Ramchandra et al., 2012; Zhang et al., 1999).

Aldosterone also plays a pivotal role in the HF cascade, which leads to sodium and water retention and increases potassium excretion (Rogers et al., 2015). Aldosterone leads to impairment of arterial compliance and causes increased pulmonary vascular resistance (PVR) and, in turn, HTN (Jackson et al., 2000). These can lead to pulmonary and vascular congestion, which contributes to the set of symptoms that characterize HF (Rogers et al., 2015). The constant sympathetic nerve stimulation with the synergistic effects of the catecholamine release, combined with the fluid overload and decreased compliance associated with HF, can lead to ventricular remodelling (Fletcher et al., 2001).

1.3 Peripheral chemoreceptors

The peripheral (arterial) and central chemoreceptors are sensory organs responsible for homeostatic control of arterial Po_2 (PaO_2), arterial Pco_2 ($PaCO_2$) and pH (Gonzalez et al., 1994). Peripheral chemoreceptors consist of carotid and aortic bodies and some clusters along the thoracic and abdominal vagus route (Marshall, 1994; Prabhakar et al., 2004), supplied with sensory fibers, and receive a rich sympathetic efferent supply from the superior cervical (carotid bodies) and stellate ganglion (aortic bodies), and parasympathetic efferent nerve supply (O'Regan et al., 1982). The sensory (afferent) nerve supplies of the carotid and aortic bodies run in the glossopharyngeal and vagus nerves, respectively, through the sinus and aortic nerve branches. These branches of nerves also carry the afferent fibers from the carotid sinus and aortic arch baroreceptors (Marshall, 1994).

Peripheral chemoreceptors are essential for maintaining oxygen homeostasis. They detect changes in arterial blood oxygen and activates reflexes that are essential for maintaining homeostasis during hypoxia (Prabhakar et al., 2004). They stimulate cardiorespiratory changes, such as increased BP and breathing immediately after hypoxia onset (O'Regan et al., 1982). For this review, CB chemoreceptors will be discussed in detail, as this is the central focus of my studies.

1.3.1 *The carotid body chemoreceptor: the peripheral master regulator*

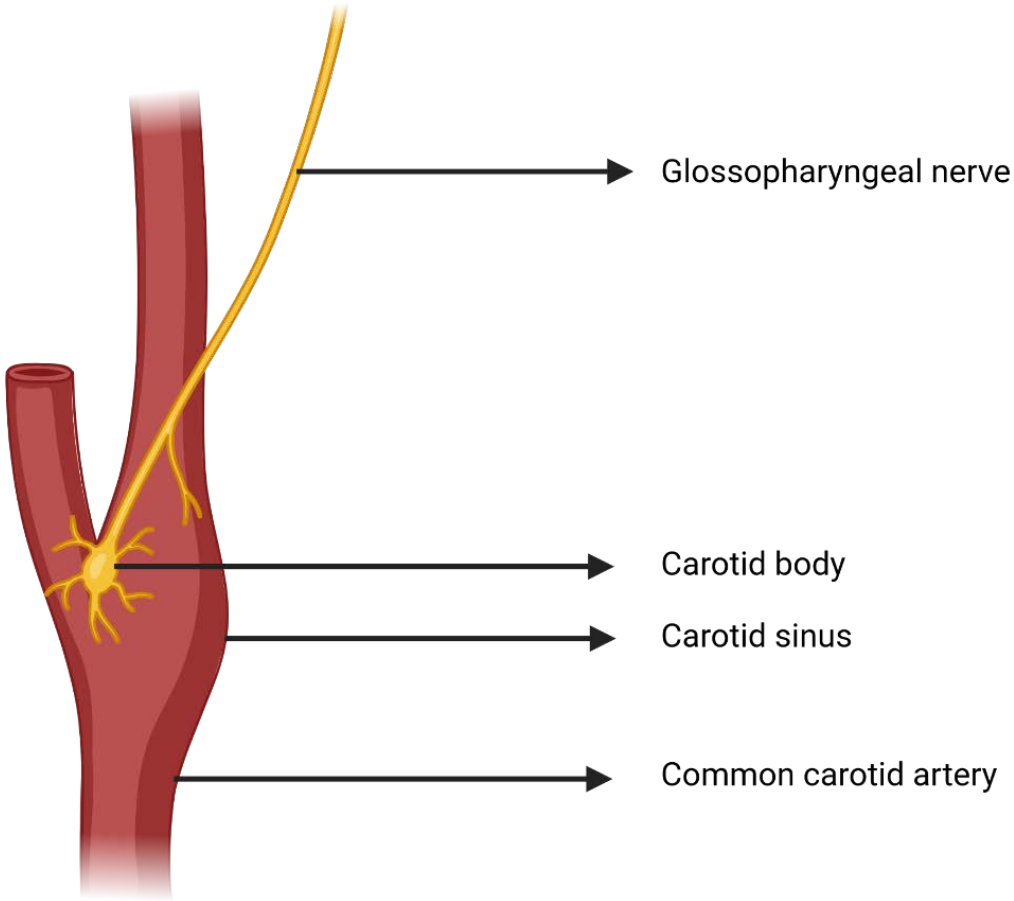

Figure 5 Carotid body chemoreceptor

Diagram displaying carotid artery and the position of the carotid body and its innervation

CBs are 1.5- to 7.0-mm ovoid, polymodal organs located bilaterally in the neck, at the rostral end of the left and right common carotid arteries where they bifurcate into external and internal carotid arteries (Figure 5). The primary blood supply to the CBs arises from the external carotid artery, and then branches into multiple first, second, third, and fourth-order arterioles (McDonald et al., 1983). The mammalian CB consists of clusters of parenchymal chemoreceptor glomus (type I) cells and sustentacular cells (also called type II cells) (Figure 6) innervated through the carotid sinus nerve by sensory afferent nerve terminals whose chemo-afferent cell

bodies lie in the petrosal ganglion (Gonzalez et al., 1994; Prabhakar et al., 2004). Plenty of thin-walled, fenestrated capillaries (~8–20 μm) penetrate type I cell clusters, thereby allowing for rapid communication between blood contents and the chemoreceptor cells (Nurse et al., 2013). Carotid bodies are supplied by the afferent nerve fibres from the glossopharyngeal (carotid sinus nerve), vagus nerve and also receive a rich efferent sympathetic supply of the nearby superior cervical ganglion and a parasympathetic efferent supply (Marshall, 1994; Paton et al., 2013).

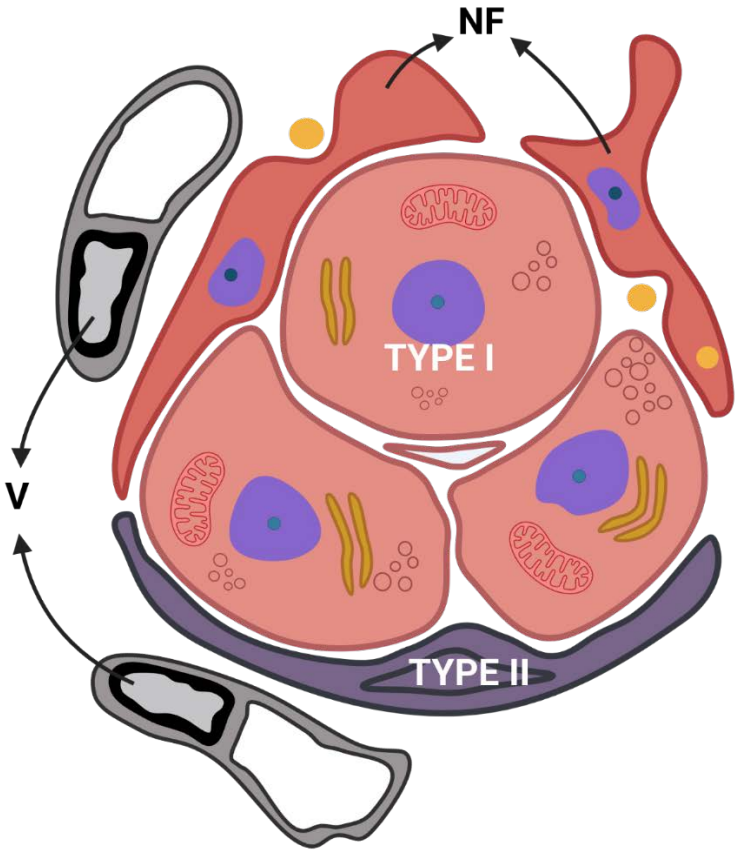

Figure 6 Schematic representation of a CB with type 1 and type II cells

The figure denotes the carotid body with neighbouring blood vessels (V) and afferent nerve fibers (NF).

1.3.2 *The type I cells in the carotid body*

Type 1 cells (glomus cells) are of neuronal origin, as strongly suggested by numerous immunological neural and glial cell markers and growth factors (Kondo et al., 1982). The neuron-like type-1 cells are the most abundant cell types in the CB glomeruli, which are enveloped by processes of glia-like, sustentacular type-II cells (Campanucci et al., 2006).

Glomus cells are arranged in groups and physiologically complex, as they express a wide variety of ligand- and voltage-gated ion channels and K^+ channels. They contain secretory granules filled with a wide variety of neurotransmitters, such as dopamine, noradrenaline, ATP, and acetylcholine (Nurse, 2005; O'Regan et al., 1982). Ionic currents recorded from these cells have shown the presence of outward K^+ channels and inward Na^+ and Ca^{2+} channels. Quantitatively, the proportion of the various subtypes of K^+, Na^+, and Ca^{2+} channels expressed in glomus cells dramatically varies among the mammalian species studied (López-Barneo et al., 2001).

Due to voltage-gated membrane channels, glomus cells are electrically excitable and can generate action potentials. This property is evident in rabbit glomus cells, with relatively large voltage-dependent Na^+ currents (Urena et al., 1989). Depolarization of the glomus cell membrane induces a reversible neurosecretory response, which is dependent on extracellular Ca^{2+} influx (Montoro et al., 1996; Urena et al., 1994). Therefore, glomus cells function as presynaptic-like elements that make contact with the postsynaptic sensory nerve fibers (Marshall, 1994; O'Regan et al., 1982). There is substantial evidence that suggests that the glomus cells are the source of initial sensory transduction. Isolated Type I cells can mount a vigorous, physiological response to hypoxia (López-Barneo et al., 2008). It is believed that hypoxia releases neurotransmitters from glomus cells and transmits the hypoxic signal to the

nerve ending, which then causes an increase in sensory discharge (Gonzalez et al., 1994; O'Regan, 1977; Prabhakar et al., 2004).

As dopamine is highly concentrated in Type 1 cells, the CB is considered the most dopaminergic structure in the body. Dopamine release depends on extracellular calcium, and it is blocked by the Ca^{2+} channel antagonists in glomus cells (Benot et al., 1990). ATP and acetylcholine appear to be the major active neurotransmitters at the glomus cell-afferent fibre synapse (Nurse, 2005). There are several other neuropeptides and amines in the CB whose functional significance is still not known (López-Barneo et al., 2008). Glomus cells also have high neurotrophic factors, which appear to exert a local autocrine and paracrine action (Nurse et al., 1997). Among these factors, the glia cell line-derived neurotrophic factor (GDNF) has brought particular attention because it is highly expressed in adult glomus cells (Nosrat et al., 1996; Villadiego et al., 2005).

1.3.3 *The Type II cell*

Around 15-20 % of CB parenchyma cells are Type-II cells, which *in vivo* exhibit long processes surrounding type-I cells. A single type II cell is closely associated with a group of approximately 3 to 5 glomus cells and is therefore found in relatively small numbers within a CB (De Kock, 1954; De Kock et al., 1966). Type-II cells are non-excitable and lack most of the voltage-gated channels characteristic of type-I cells (Duchen et al., 1988; Urena et al., 1989). Historically, type-II cells were considered to play a supportive role that belongs to the peripheral glia. However, a more recent study has shown that the CB is a functionally active germinal center. It has been suggested that sustentacular type-II cells are dormant stem cells that can proliferate and differentiate into new glomus cells in response to physiological hypoxia (Pardal et al., 2007).

It is well established that the Type II cells are essential functional elements of neuronal systems, expressing Ca^{2+} signaling responses to neurotransmitter stimulation (Verkhratsky et al., 1998). While it has been confirmed that the type II cell is relatively unexcited by membrane depolarization, it was shown that P2Y2 (ATP sensitive) receptors are localized on the type II cell plasma membrane, and it is suggested that the type II cell may therefore be a site of action for stimulus activated ATP release from type I cells, for instance, during hypoxia (Xu et al., 2003).

1.3.4 *Sensing hypoxia in the carotid body*

Initially, it was believed that CBs could only sense oxygen during hypoxia (Del Rio, 2015). However, later, it has been shown that the carotid chemoreceptors are stimulated not only by a fall in resting level of the arterial partial pressure of oxygen (Po_2) but also a rise in the partial pressure of carbon dioxide (Pco_2) and fall in pH and thereby induce hyperventilation and a marked increase in sympathetic nerve activation (Kara et al., 2003).

Alterations in how the CBs respond to hypoxia can substantially affect autonomic and respiratory control (Del Rio, 2015). The sensitivity to acute changes of arterial O_2 tension makes the CB essential for adaptive hyperventilation reflex in response to the decreased partial pressure of oxygen (Po_2) or hypoxemia. The glomus cells are the chemoreceptive elements in the CB, and they contain O_2-sensitive potassium ion (K^+) channels, which close in hypoxic conditions (López-Barneo et al., 2008; López-Barneo et al., 2001).

Voltage-dependent K^+ channels were first reported in rabbit CB cells (Lopez-Barneo et al., 1988). The K^+ channel inhibition leads to glomus cell depolarization and subsequently Ca^{2+} (calicium ion) channel opening, transmembrane Ca^{2+} influx, and neurotransmitter release (López-Barneo et al., 2008). Hypoxic inhibition of the K^+ currents and inhibition of single K^+ channel function (Ganfornina et al., 1991; Lopez-Barneo et al., 1988), external Ca^{2+}-dependent

increase of cytosolic Ca^{2+} in hypoxia (Buckler et al., 1994; Urena et al., 1994), and catecholamine release from hypoxic glomus cells (Montoro et al., 1996; Urena et al., 1994) are the key steps throughout the chemotransduction method. The dose-dependent cellular responses to hypoxia almost exactly match the characteristic hyperbolic association between arterial O_2 tension and the afferent discharge of the CB sinus nerve or the increase in ventilation seen in vivo (López-Barneo et al., 2008; Montoro et al., 1996). The widely accepted "membrane model" of CB O_2 sensing has schematically described in Figure 7 (López-Barneo et al., 2008).

The released catecholamine from hypoxic glomus cells activates the afferent fibers that send signals to the central nervous system (Lopez-Barneo et al., 1988; López-Barneo et al., 2001). Consequently, stimulation of the CB drives systemic sympathetic tone through direct signaling to the nucleus tractus solitarius (NTS) and rostral ventrolateral medulla (RVLM), resulting in increased BP and ventilation (Marshall, 1994).

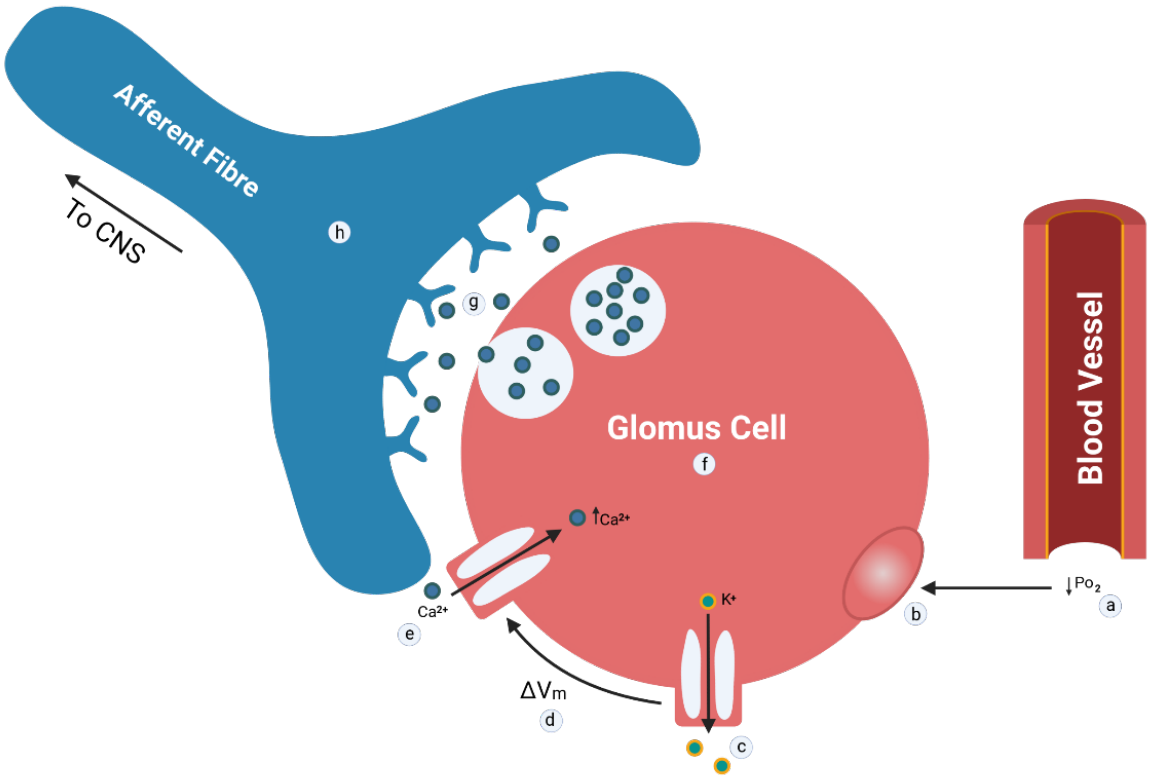

Figure 7 Membrane model of glomus cell oxygen sensing by CB chemoreceptors

The main steps in chemosensory transduction are as follows: a) Decrease of O_2 tension (Po_2), b) O_2 sensing, c) potassium channels closure, d) cell depolarization, e) calcium channels opening, f) rise in cytosolic calcium concentration, [Ca^{2+}], g) neurotransmitter release and h) activation of afferent nerve fibers, which send the information to the CNS

1.3.5 *Carotid body function in Heart Failure*

The CB is primarily known for its involvement in regulation of breathing, but there is growing evidence that CB dysfunction is involved in the pathophysiology of many human diseases such as HF and HTN. CB chemoreflex function is known to be maladaptive in certain disease states (Schmidt et al., 2005; Schultz et al., 2007c). In particular, patients with HF

(Niewinski, 2014) and animal models of HF (Schultz et al., 2013) exhibit enhanced CB chemosensitivity that contributes to elevated sympathetic outflow and ventilation under normoxic and hypoxic conditions. This maladaptation leads to tonic over-activation of sympathetic neural outflow, especially to the heart and kidney, and further exacerbates the progression of HF (Esler, 2010).

Fundamental to understanding the defective role of CB in HF is the finding that there is an increased baseline afferent discharge in the CB of HF animals under normoxic conditions to levels that would otherwise represent severe hypoxemia in normal animals (Schultz et al., 2015). In pacing induced HF rabbits and myocardial infarct-induced HF rats, the basal CB afferent discharge driven by the type I cells is markedly elevated at rest under normoxia conditions (Del Rio et al., 2013b; Sun et al., 1999a).

Hyperventilation induced by CB overactivity in HF contributes to breathing instability, oscillatory breathing (OB), and increased central apnoea incidence that further negatively effect autonomic and metabolic homeostasis (Brack et al., 2012). The CB receives efferent innervation primarily from the sympathetic fibers originating from the superior cervical ganglion and parasympathetic fibers (Kumar et al., 2011; Neil et al., 1971). Stimulation of CB by hypoxia or hypercapnia generates a ventilatory response expressed as increases in tidal volume and breathing frequency (Mortara et al., 1997; Ponikowski et al., 1999). The cardiovascular response includes an increase in BP. Reflex cardiorespiratory responses are characterized by enhanced sympathetic discharge to the vascular beds and the heart and hyperventilation.These reciprocal interactions between the cardiovascular and respiratory control systems via brain networks and sensory systems mediates this “cardiorespiratory coupling” (Barman et al., 2017; Dick et al., 2014; Guyenet, 2011).

The CB receives afferent innervation from the carotid sinus nerve, and its activity increases during hypoxia, causing compensatory reflex hyperventilation (Campanucci et al., 2007). The carotid sinus nerve originates from the glossopharyngeal (IXth cranial) nerve, to terminate centrally in the NTS. The NTS of the brainstem comprises respiratory neurons, and it is considered the principal integrative center of cardiorespiratory information, carried by the glossopharyngeal and vagus (Xth cranial) nerves (Kumar et al., 2011).

Studies have also reported that the CB could serve as a target organ to improve the outcome of sympathetically mediated diseases such as HF. This concept is confirmed by studies showing that inhibition of CB chemoreflex activity by hyperoxia (excess supply of oxygen) (Ponikowski et al., 1999; Xing et al., 2014) and CB denervation in animals models of HF (Marcus et al., 2014d) reduce sympathetic tonic discharge as well as breathing instability. It has been reported that selective ablation of CB chemoreceptors decreased the activation of RVLM pre-sympathetic neurons, restored normal sympathetic outflow and significantly reduced the frequency of oscillatory breathing patterns in HF (Marcus et al., 2014c). However, there is no potential research that shows the effect of CB denervation on coronary circulation. In my thesis, I will discuss the effect of CB stimulation using low doses of intracarotid KCN injection and silence the CB using supplemental oxygen and its effect on CoBF in both control and HF sheep.

1.3.6 *Factors affecting activation of the carotid body in HF*

1.3.6.1 *Humoral and local tissue factors*

In HF, oxidative stress has been shown to play a key role in CB activation. Both circulating and locally generated Ang II peptide are elevated in HF and contribute to the enhanced CB chemoreflex discharge in this disease condition (Li et al., 2006). Ang II stimulates NADPH oxidase (NOX) to increases the production of superoxide ($O_2^{\bullet-}$) anion, which in turn enhances the glomus cell excitability and central autonomic neurons via the angiotensin II type

1 receptor (AT1R) (Li et al., 2007). In HF, this pathway is upregulated (Li et al., 2007). Ang II-O_2•− directly inhibits the oxygen-sensitive potassium channel (IKv) partly to increase the sensitivity of the CB chemoreceptors (Figure 8) (Schultz et al., 2015).

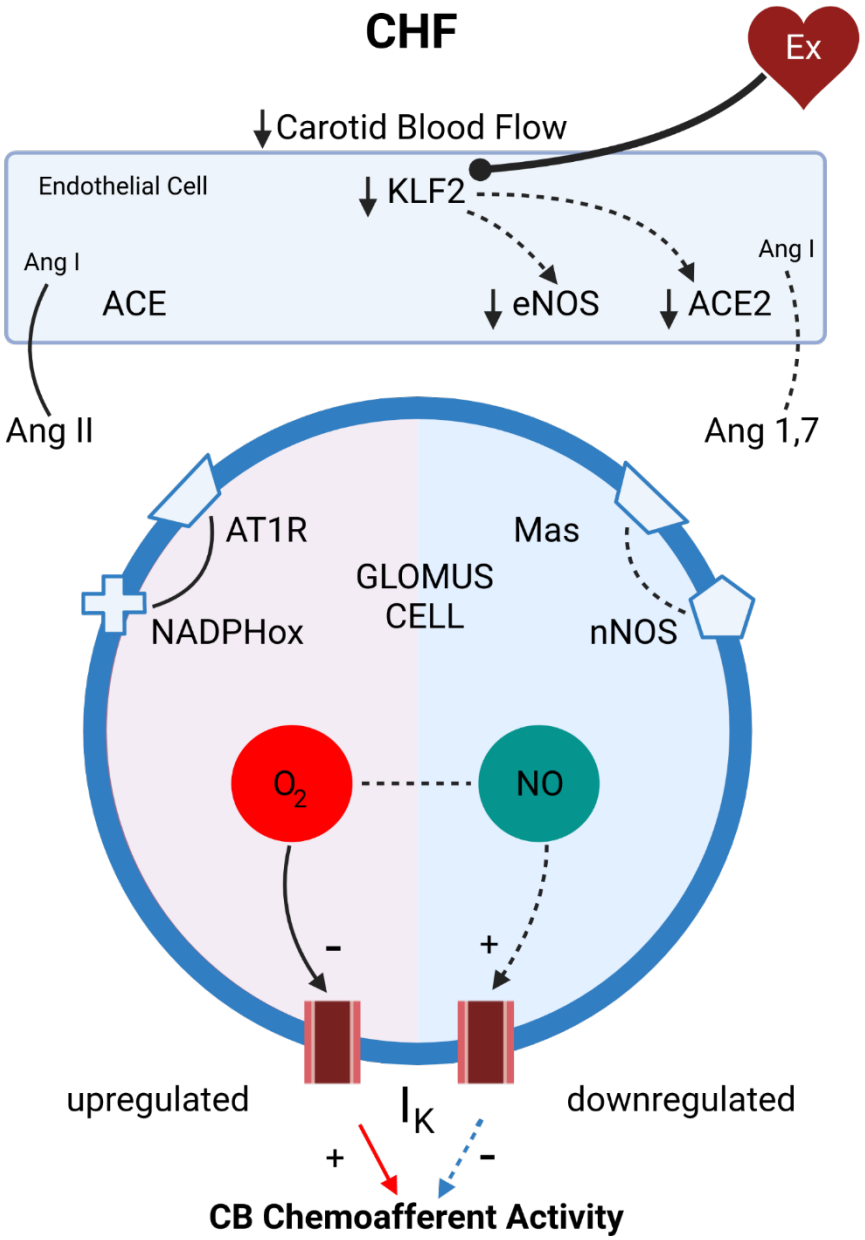

Figure 8 Representative model of known cellular pathways that lead to increased CB chemoafferent sensitivity in HF

Details and abbreviations as discussed in the text. Ex: regular exercise

The Ang II-O_2• pathway is also very likely to alter the sensitivity of other ion channels in CB glomus cells to increase excitability in HF. This hypothesis has not been tested adequately. These changes in the function of the channel are likely to include sensitization of Ca^{2+} voltage-gated channels that mediate glomus cell depolarization and release of neurotransmitters and suppression of K^+ channels responsible for maintenance of the resting membrane potential in glomus cells. The RAAS is activated in HF due to renal hypoperfusion and could serve as an essential source for Ang II effects on the CB. Moreover, other angiotensin metabolites [Ang-(1-7)] may play a role in modulating CB function in HF. [Ang-(1-7)] counteracts the neural actions of Ang II and enhances the production of neural nitric oxide synthase (nNOS) and nitric oxide (NO) by activating catecholaminergic neurons (Yang et al., 2010). Taken together, these studies indicate that high levels of Ang II may play a role in the elevated activity of the CB in HF.

1.3.6.2 *Haemodynamic factors*

A central feature of HF is the reduction in CO due to impairment in cardiac function. Although there is little effect on CB chemoreceptor activity due to acute changes in systemic haemodynamics, chronic changes in blood flow could affect CB sensitivity, presumably due to reductions in oxygen delivery (Schultz et al., 2015). For instance, research suggests that a chronic reduction in blood flow to the CB causes an increase in AT1R expression and decreases nNOS expression in the CB in rabbits (Ding et al., 2011). These effects enhance CB afferent activity, similar to changes observed in HF rabbits (Ding et al., 2011). However, the relationship between diminished carotid blood flow and an altered signaling pathways has not been identified.

Kruppel-like factor 2 (KLF2) is a transcription factor that is important in the transduction of shear stress on endothelial function (Dekker et al., 2005). KLF2 represses ACE transcription, induces endothelial cell transcription of endothelisl nitric oxide synthase (eNOS) (Dekker et al.,

2005), and stimulates the expression of transcription factors controlling anti-oxidant and oxidant expression. A previous study has shown that KLF2 expression is reduced in the CB in HF (Haack et al., 2014), and adenoviral gene transfer of KLF2 to the CB normalizes the hypoxic ventilatory response and reduces periodic breathing incidence in HF (Schultz et al., 2012). These results indicate that KLF2 plays a fundamental role in the altered function of the CB that occurs with a reduction in CB blood flow in HF.

1.3.6.3 *Ventilatory factors*

CB hyperactivity in HF causes progression in breathing instability, characterized as Cheyne-Stokes respiration and enhanced central apnoeas, that further adversely affect autonomic and metabolic homeostasis in patients with HF (Brack et al., 2012; Fung et al., 2014). This breathing instability may cause intermittent hypoxia and contribute to the enhancement of CB response in HF (Del Rio et al., 2013a; Schultz et al., 2015). The sympathetic reflex activity is highly entrained in the respiratory pattern of animals with HF, which was abolished after ablating the CB (Zoccal et al., 2011). In this manner, oscillatory breathing in HF can drive enhanced sympathetic discharge because of the increased sympathetic-respiratory coupling (SRC) caused by the CB chemoreceptors (Schultz et al., 2015). Under normal physiological conditions, CB chemoreflex activates sympathetic outflow to resistance vessels to avert the direct vasodilatory effects of hypoxia and thus maintain adequate blood flow to vital organs, such as the heart and brain. However, the effect of impaired CB function and tonic over-activation of sympathetic neural outflow to CoBF in HF condition is unclear.

1.4 Regulation of coronary blood flow

The heart is solely responsible for providing its own blood supply through the coronary circulation which provides the myocardium with oxygen and other substrates to ensure normal functioning of the heart. The regulation of CoBF is determined through multiple mechanisms such as coronary perfusion pressure, extravascular compressive forces (tissue pressure), myogenic, local metabolic, endothelial as well as neural and hormonal influences. These mechanisms control coronary flow and act to maintain an overall balance between the distribution of myocardial oxygen supply and metabolic oxygen demand (Figure 9) (Ardehali et al., 1990; Duncker et al., 2008; Feigl, 1983b; Tune, 2014).

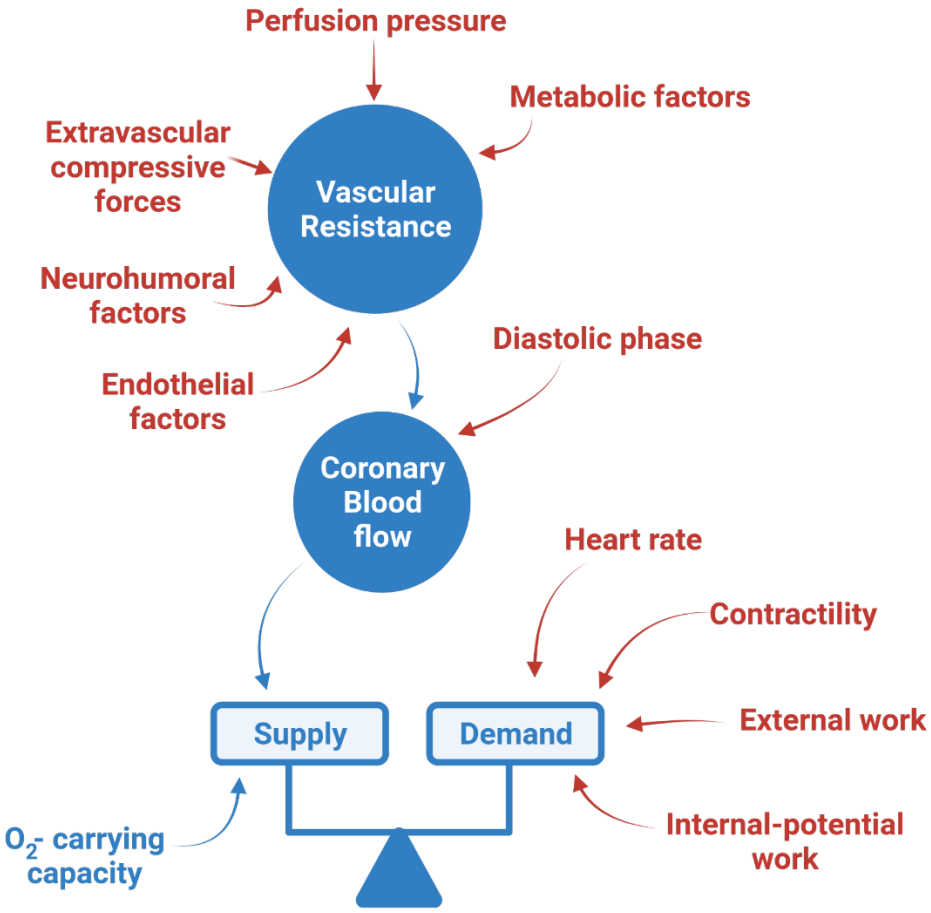

Figure 9 Schematic diagram of the determinants of myocardial oxygen supply and demand

The human heart normally has two coronary arteries, the right and the left, both arising from the aorta just above the aortic valve (coronary ostia) within the sinuses of Valsalva (Belt, 1933). The aortic valve has three cusps. 1). the non-coronary cusp, which has no ostia, 2). The left coronary cusp, has the ostia of the left main coronary artery (LMCA), and 3). The right coronary cusp, which contains the right coronary artery ostia (Turner et al., 1996). The left main coronary artery (LMCA) arises from the left posterior sinus of Valsalva. LMCA is the progenitor to the left anterior descending (LAD) and circumflex coronary (LCx) arteries (Tune, 2014).

Typically, the circumflex artery courses horizontally to the left, in the anterior atrioventricular sulcus, giving rise to obtuse marginal branches along its length. This main coronary artery and its associated marginals are responsible for delivering blood to the left atrium and the lateral wall of the LV (Belt, 1933; Tune, 2014). LAD runs downwards from base to apex along the anterior surface of the heart in the interventricular groove. The LAD gives rise to numerous septal and diagonals branches along its length that supply the anterior surface of the LV, the anterior part of the left bundle branch, the middle part of the right bundle branch, and the anterior septal myocardium (Tune, 2014).

The right coronary artery (RCA) originates from the anterior part of the aorta behind the anterior cusp of the aortic valve (Belt, 1933). The RCA travels horizontally around the atrioventricular groove, similar to the circumflex artery though in the opposite direction. The RCA gives rise to numerous acute marginal branches along its length, responsible for delivering blood to the right atrium and right ventricular free wall (Belt, 1933; Gregg et al., 1963; Gregg, 1946).

1.4.1 *Coronary blood flow and myocardial metabolism*

The heart is a highly metabolic tissue. It is essential that mechanisms exist to ensure that changes in myocardial metabolic demand are balanced by concordant and proportional changes in myocardial oxygen supply (Tune et al., 2004; Tune et al., 2002). Under normal physiologic conditions, myocardial oxygen consumption (MVO_2) is the product of CoBF and the arterial-venous difference in oxygen content (Shapiro, 1972). It is apparent that increases in MVO_2 must be primarily balanced by increases in CoBF (Braunwald, 1971; Feigl, 1983b). The proximity of this normal relationship to the physiologic maximum of 100% oxygen extraction demonstrates how predominantly dependent the LV is on CoBF changes to ensure sufficient oxygen delivery and thus the maintenance of normal cardiac function and output.

Although there is general agreement that locally derived vasodilators play a dominant role in regulating microvascular resistance, the precise mechanisms responsible for the tight coupling of CoBF with myocardial metabolism remain poorly understood (Deussen et al., 2012; Tune, 2014). It is known that neural (sympathetic) influences play both an indirect and direct role in the regulation of CoBF. These effects occur through activation of vascular adrenergic receptors and through an increase in MVO_2 via increases in HR and cardiac contractility, respectively.

1.4.2 *Neural control*

The coronary vasculature is richly innervated with sympathetic and parasympathetic neurons (Bayliss, 1923). Electron microscopic studies showed that these nerve fibers are found inside the coronary vascular wall (Hirsch, 1961) and that, compared to larger coronary arteries, small arteries and arterioles contain more nerve terminals (Lever et al., 1965). Studies have shown that major sympathetic trunks appear in the epicardium alongside the coronary arteries, with transmural penetration to innervate the rest of the myocardium. Alternatively, major parasympathetic ventricular pathways remain epicardial until the AV groove is crossed, where vagal fibers enter the myocardium to become located mainly in the ventricular subendocardium (Ito et al., 1994; Zipes et al., 2006).

Adrenergic receptor distribution varies throughout the coronary artery, with β1-adrenoceptors mainly expressed in larger arteries (Amenta et al., 1991; Young et al., 1991) and β2-adrenoceptors primarily located in arterioles <100 μm in diameter (Hein et al., 2004; Sun et al., 2002). Data from a study supports a relatively equal distribution of β1 versus β2 adrenoceptors in smaller coronary arteries and a β1 versus β2 expression ratio of ~2:1 in larger vessels (Murphree et al., 1988). Another study has shown the functional contribution of both β1 and β2-adrenoceptors to coronary vasodilation in dog hearts (Trivella et al., 1990). In the coronary circulation, the primary location for α-adrenoceptors tends to be more upstream, with

many reports supporting a non-uniform distribution of α1-adrenoceptors in larger arteries α2-adrenoceptors in smaller arteries and large arterioles (Heusch et al., 1984; Heusch et al., 1983).

The direct impact of sympathetic neural activation on CoBF regulation is significantly complicated by the distinct conflicting responses induced by sympathetic activation. First, changes in contractility, HR, and MVO_2 caused by β-adrenoceptor activate local metabolic processes, presumably via feedback control mechanisms involving an error signal, such as decreased tissue Po_2. Second, coronary β-adrenoceptor activation contributes to direct vasodilation, and third, vasoconstriction is caused by stimulation of coronary α-adrenoceptors (Duncker et al., 2008; Feigl, 1998). Pharmacologic inhibition studies demonstrated that inhibition of β-adrenoceptors will block not only direct coronary responses but also diminish metabolic vasodilation secondary to reductions in HR and contractility (Miyashiro et al., 1993). Moreover, studies in both conscious and anaesthetized dogs have shown that electrical stimulation of cardiac sympathetic nerve results in coronary vasodilation (Denison JR et al., 1958; Feigl, 1967; Granata et al., 1965).

Early studies on the parasympathetic control of the coronary circulation were inconclusive because of the confounding influences of vagal mediated reductions in HR and MVO_2 (Feigl, 1983b; Feigl, 1969). A later study demonstrated parasympathetic coronary vasodilation wherein efferent vagal stimulation increased CoBF ~30% and diminished late diastolic coronary resistance ~60% in dogs with HRs held constant by cardiac pacing (Feigl, 1969). This vasodilator effect is essentially abolished by muscarinic receptor blocker with atropine and is normally mediated by acetylcholine-induced nitric oxide production by coronary endothelium (Broten et al., 1992; Shen et al., 1994).

However, parasympathetic dilation is species-dependent and based on normal endothelial function (Hodgson et al., 1989). Although data indicate that the withdrawal of

parasympathetic activity may facilitate β-adrenoceptor dilation in swine during exercise, the effects of the parasympathetic nervous system on the control of CoBF are relatively modest under most physiologic conditions (Duncker et al., 1998). However, there is evidence to support a role for parasympathetic coronary vasodilation in the carotid chemoreceptor reflex (Hackett et al., 1972; Hashimoto et al., 1964; Murray et al., 1984). For instance, stimulation of chemoreceptors activates the reflex vagal cholinergic vasodilator pathway to the coronary artery in the anaesthetized dogs. However, whether the sympathetic nerves play a role in this vasodilation has been debated. My thesis will examine this by recording direct burst signals from the left cardiothoracic nerves by implanting electrodes inside the nerve.

1.5 Renal function in Heart Failure

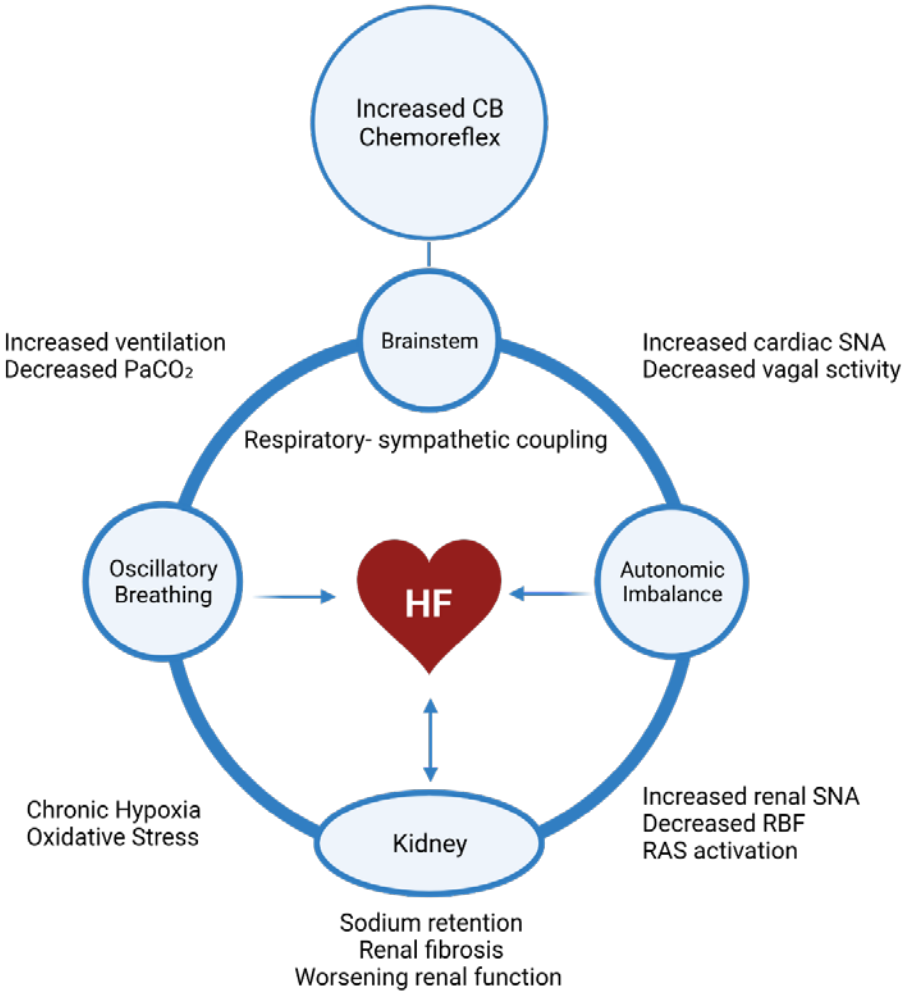

Figure 10 Role of CB Chemoreceptors in Cardiac and Renal Dysfunction in HF

Renal dysfunction is common in patients with HF and is associated with a poor prognosis (Bock et al., 2010). Under normal circumstances, activation of the CB chemoreflex results in a decrease in renal blood flow (RBF) and glomerular filtration rate mediated by renal sympathetic nerves (Karim et al., 1987). Tonic elevations in renal SNA in HF mediate sustained declines in RBF and changes in angiotensin signalling that can intensify renal ischaemia and injury (Clayton et al., 2011). HF rodent studies have shown that resting RBF is markedly decreased, and the reduction in RBF to CB chemoreflex activation is significantly augmented in CH animals (Marcus et al., 2014a; Marcus et al., 2014b). In HF animals, carotid sinus nerve ablation

reduced resting renal SNA, increased RBF, and decreased markers of renal injury and fibrosis (Marcus et al., 2014a), as well as reduced breathing disorder and improved cardiac function (figure 10) (Marcus et al., 2014b).

In addition to the effect of the CB chemoreflex on resting renal SNA, oscillatory breathing and enhanced respiratory-sympathetic coupling will superimpose additional surges in renal SNA to produce repeated bouts of renal vasoconstriction and impaired blood flow. These findings indicate that tonic activation of CB chemoreflex in HF can contribute to renal pathology through its effect on sympathetic outflow to the kidneys (Marcus et al., 2014b). Renal dysfunction in HF is especially ominous because, through volume retention and increased cardiac preload, it may precipitate a further deterioration in cardiac function, causing a downward spiral of declining cardiac and renal function, known as cardiorenal syndrome.

The etiology of cardiorenal syndrome is diverse, but it is exaggerated by excessive cardiac and renal sympathetic activation causing increases in sodium and water retention, activation of the RAA system, renal ischaemia, and neuro-hormonal impairment of cardiac function (Bock et al., 2010). Tonic activation of CB chemoreflex in HF may contribute to cardiorenal syndrome by increasing sympathetic activation of the heart (Del Rio et al., 2013a; Marcus et al., 2014b; Xing et al., 2014) and kidneys (Marcus et al., 2014b; Sun et al., 1999a).

1.6 Hypertension and carotid body

Primary HTN, also known as essential HTN, accounts for the vast majority of hypertensive cases, with an estimated 95% prevalence (Carretero et al., 2000). HTN is a major risk factor for coronary artery disease, stroke, and kidney failure (Cubrilo-Turek, 2003). In HTN, pharmacotherapy aims to improve BP management and minimize cardiovascular risk. However, only about 30% of patients with HTN have good BP control, and 50% of them quit taking their medication after a year (Burt et al., 1995; Costa, 1996; Sackett et al., 1975). Neurogenic HTN is another form of essential HTN characterized by high BP with sympathetic overdrive, lack of parasympathetically mediated cardiac variability, and excessive Ang II activity (Esler, 2010). Increased vasoconstrictor sympathetic tone has been observed in both animal models of HTN and patients with HTN (Esler et al., 2001; Smith et al., 2004), suggesting that it may play a role in the development and maintenance of HTN.

It is well documented that the CB chemoreceptors contribute significantly to the activity of the sympathetic nervous system and its enhanced activity in patients with HTN (Dibona, 2004; Oliveira-Sales et al., 2011; Pijacka et al., 2016a). Similar to HF studies, the CB has been identified as a potential therapeutic target for treating HTN (McBryde et al., 2017; Paton et al., 2013). Studies show that hypertonicity and hyperreflexia originating from the CB chemoreceptors drive chronic increases in SNA, leading to increased total vascular resistance and BP (Pijacka et al., 2016b). Also, reduced cardiac parasympathetic nerve activity and enhanced noradrenaline release has been reported in spontaneously hypertensive rats (Friberg et al., 1988; Lundin et al., 1984). Increased CB activity causes changes in the respiratory–sympathetic coupling and increased muscle vasoconstrictor activity, which could lead to the development of HTN (Siński et al., 2012; Trzebski et al., 1982).

The ventilatory destabilization in association with increased respiratory-sympathetic coupling mediated by CB hyperreactivity may aggravate autonomic imbalance and its effect on the deterioration of cardiac and renal function. Studies in animal models have demonstrated that surgical chemoreceptor deactivation and CB denervation decreases BP and prevents development of HTN (Abdala et al., 2012; Chang et al., 2020). Therefore, owing to the sheer number of evidence, I believed CBs are involved in the pathogenesis of HTN and which can be an effective and safe target for treating HTN.

Studies have been suggested that the CB hypoperfusion in HTN is a potential contributor to the CB hyperactivity (Ding et al., 2011; Koeners et al., 2016; Lahiri et al., 1980). CB hypoperfusion may also occur following hypertension-induced wall remodelling (Habeck, 1991). These studies have mentioned a reduction in common carotid blood flow, which can be comparable to hypoperfusion and associated CB hyperactivity in HF animals where the CO was reduced (Del Rio et al., 2017; Ding et al., 2011). In my study, I have used renovascular hypertensive model of sheep (the 2-kidney, 1-clip model, 2K1C). In renovascular HTN, renal artery stenosis decreases renal artery perfusion pressure, increasing renin relaease and thereby increasing levels of plasma Ang II (Braam et al., 1995; Guyenet, 2006; Johansson et al., 1999; Navar et al., 1998; Ploth, 1983).

In addition to the central and peripheral actions of Ang II, increased plasma Ang II levels are thought to contribute to increased sympathetic outflow in 2K1C rats by CB-mediated actions (Pijacka et al., 2016a). A recent study has shown that the 2K1C rat model exhibit enhanced resting ventilation that depends on CB inputs (Melo et al., 2020). Despite the contribution of CB inputs for these ventilatory changes, there is no research into whether improvement of respiratory instability improves BP in hypertensive 2K1C models. Therefore, to investigate this possibility, I will examine whether the improvement of respiratory instability using high nasal flow (HNF) can improve BP in this ovine hypertensive model. HNF therapy has been widely

used for patients in respiratory distress (Dysart et al., 2009) and evidence suggests that purging nasopharyngeal dead space improves gas fractions in the lung (Dewan et al., 1994). I have used HNF in the conscious large animal model as a potential alternative to continuous positive airway pressure (CPAP) devices.

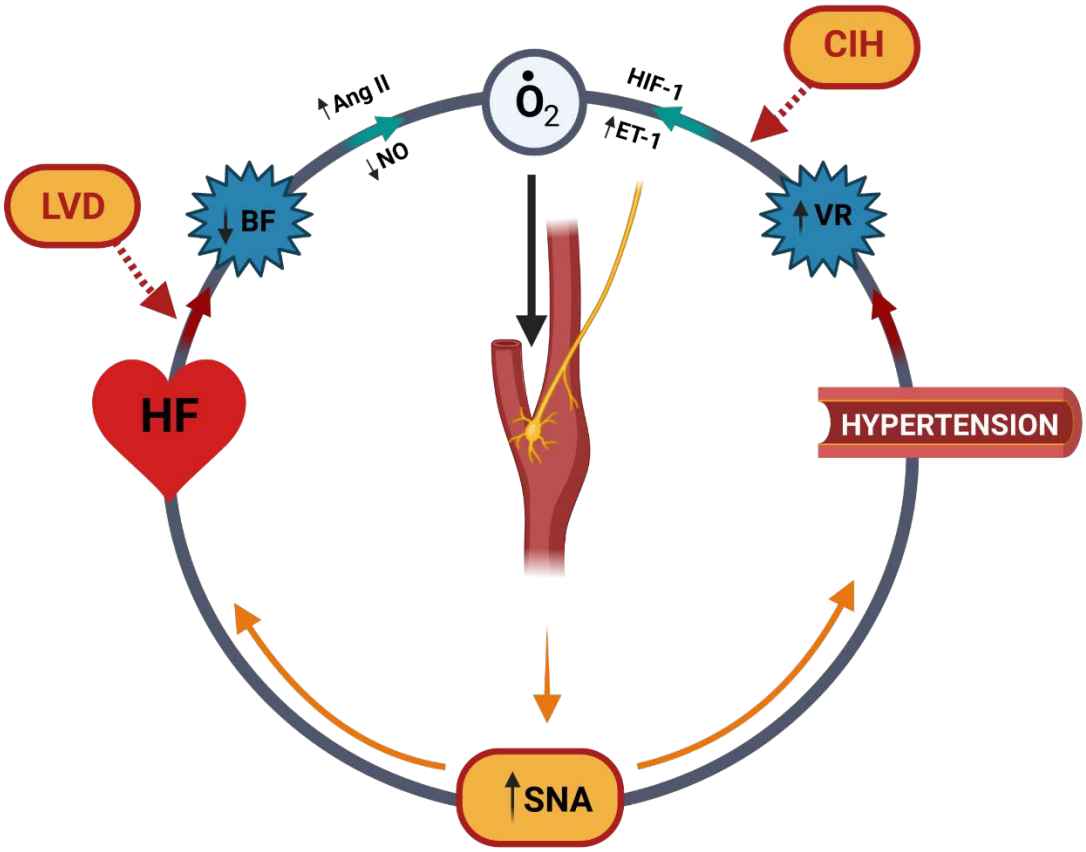

Figure 11 The cycle of CB chemoreflex activation in HF and HTN

The cycle of CB chemoreflex activation in hypertension and HF. (Left) - Left ventricular dysfunction (LVD) induces a severe reduction in CB blood flow (BF), which causes altered signaling pathways and oxidative stress in the CBs, enhancing CB chemoreceptor activity and SNA reflex activation. In HF, increased SNA accelerates cardiac deterioration, lowers BF, and raises CB excitability. (Right) - Chronic intermittent hypoxia (CIH) elicits altered signaling pathways and oxidative stress in the CBs that enhance chemoreceptor activity and reflex activation of SNA. The increased SNA worsens HTN and raises CB vascular resistance (VR), decreasing BF and increasing CB excitability

Due to the biological complexity of the cardiovascular system, it is essential to use an animal model to investigate the underlying mechanisms of cardiovascular disease and explore novel therapeutic targets. The majority of experimental work has been done on rodent models of heart diseases, predominantly rats and mice. Considering the similarities to the human heart, sheep serve as an excellent pre-clinical model for cardiovascular research (Milani-Nejad et al., 2014). There are many sheep models of cardiac disease that have been reported (Lukács et al., 2012; Milani-Nejad et al., 2014). In terms of clinical translation value, major determinants of myocardial work and energy consumption, such as HR, LV wall tension, and vascular wall-to-lumen ratio, are very similar to humans (Lelovas et al., 2014; Markovitz et al., 1989; Milani-Nejad et al., 2014). In my thesis I will be using a stable HF model in conscious sheep with microembolization of the coronary arteries and a 2-kidney, 1-clip model of renovascular HTN sheep (Abukar et al., 2019; Chang et al., 2020; Schmitto et al., 2008).

While it is well recognized that CB activation triggers reflex coronary vasodilation in normal animals, whether the cardiac sympathetic nerve plays a part is debatable. Also in cardiovascular diseases, there is an enhanced activation of cardiac SNA which is partly driven by the CB chemoreflex. However, the role of the CB chemoreceptors in regulating CoBF in diseased states remains unclear. Therefore,

The primary aims of my thesis were

1. To determine the effect of CB stimulation on directly recorded cardiac SNA and CoBF in conscious control and HF sheep.
2. To determine whether CB activation alters CoBF in the control and HF sheep model.
3. To examine the MAP, RBF, and RVC response during continuous HNF administration in conscious normotensive and hypertensive sheep.

Specifically the following hypotheses were tested in this thesis.

1. Stimulation of CB chemoreceptors using intracarotid KCN would increase directly recorded cardiac SNA in the conscious animal. The activation of CB chemoreceptors would result in coronary vasodilation primarily mediated by the increase in cardiac SNA.
2. CB activation would increase MAP, which would cause a greater increase in blood flow to the heart in conscious HF sheep than control. The inhibition of the sympathetic activation to the heart using a β-blocker would attenuate the increase in CoBF.
3. HNF would decrease MAP in both groups of animals and increase RBF and RVC due to a substantial reduction in peripheral vascular resistance associated with decreased MAP.

Chapter 2: General Methods

2.1 Animal preparation

Experiments were conducted on conscious, adult female Romney sheep weighing 50-80 kg, housed in individual crates and acclimatized to laboratory conditions (18ºC, 50% relative humidity, and 12 hour light-dark cycle) and human contact before any experiments. All experiments and surgical procedures are approved by the Animal Ethics Committee of the University of Auckland. The sheep were fed 2 kg/day (Country harvest pellets), water *ad libitum* and supplemental hay or chaff as needed.

2.2 Surgical procedure

In the first group I examined the response of cardiac sympathetic nerve activity (CSNA) to CB stimulation (group-A, n=6). The second group of animals was instrumented for measurement of CoBF and other cardiovascular variables in response to CB stimulation (group-B, n=6) (Chapter 3). In the next stage, a group of HF (n=6) sheep were used to determine the effect of CB stimulation on cardiovascular and haemodynamic variables. For animals assigned to the HF arm of the study, they underwent the microembolization HF induction procedure. Then both groups underwent instrumentation surgery (Chapter 4). Another group of control (n=6) and HF (n=6) sheep were used to determine the effect of supplemental oxygen (hyperoxia) on CoBF in control and HF conditions (Chapter 5). Finally, a group of hypertensive (n=5) and control (n=5) sheep were prepared to determine the effect of HNF on RBF and other haemodynamic variables (Chapter 6).

Prior to all surgical procedures the sheep were starved for 24 hours. Sheep underwent aseptic surgical procedures under general anaesthesia given by an experienced animal handler. Anaesthesia was induced with intravenous propofol (5 mg/kg, i.v.; AstraZeneca, U.K.), and following intubation maintained with 1.5–2.0% isoflurane/oxygen (O_2) (Lunan Better

Pharmaceutical, China). Bupivacaine-Claris solution (2.5mg/mL; Multichem NZ Ltd, New Zealand) injection was given on the intercostal space (1-5 intercostal space, 3ml each) as a nerve blocker, thus preventing post-surgical pain. Ketoprofen (2 mg/kg, i.m.; Merial, Boehringer Ingelheim, NZ) and long-acting Oxytetracycline (20 mg/kg i.m.; Oxytetra, Phenix, NZ) were used for premedication analgesic and antibiotic respectively for all sheep.

2.2.1 *Heart Failure Induction*

For animals assigned to the HF arm of the study, once anaesthetized and intubated, the sheep were placed in a supine cradled position and four limb electrodes were inserted into the left and right sides of the sternum and in the hind-limbs near the knee joint, subcutaneously, to record ECG. Recordings were obtained from lead I, II, III, aVL, aVR and aVF prior to the infusion of the microspheres and for a further 15-20 mins after injection until the animals wake up from the surgery. The recordings were made on a dual bio amp electrocardiograph switch box with power lab and LabChart (AD Instruments, NZ). A change in the ST segment (elevation or depression) and T wave (inversion) on one or more limb leads was taken as indication of successful embolization (Figure 13).

The left or right femoral artery was accessed percutaneously with an 8F (CORDIS®, USA) sheath. The left main coronary artery was then cannulated using an 8F AL2 (CORDIS®, USA) guide catheter under fluoroscopic guidance. MI was induced by infusion of polystyrene latex microspheres (45 microns; 1.3 ml, Polysciences, Warrington, PA, USA) into the left coronary artery, which then developed into HF over time. Three sequential embolizations were performed over 3 weeks to ensure maximum LV coverage. Prior to each embolization procedure, β-blocker (metoprolol up to 20 mg/kg, IV, Mylan, USA) and Xylocaine (2mg/kg, IV, Aspen, NSW, Australia) were injected intravenously in order to prevent ventricular arrhythmias (Abukar et al., 2019) (Figure 12).

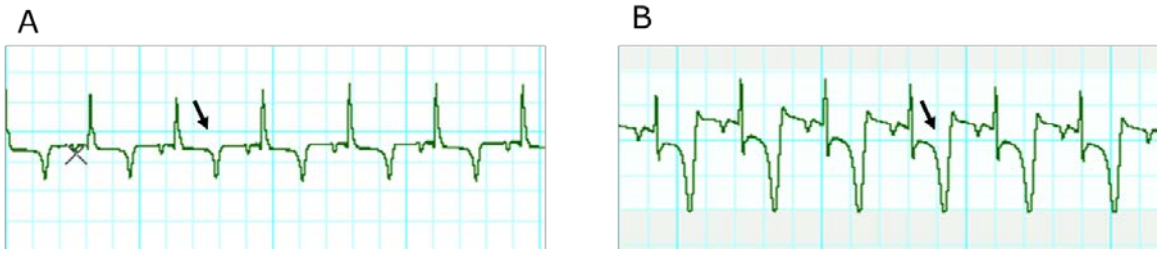

Figure 13a: Representative electrocardiogram traces from one sheep demonstrating changes on T-wave and ST-segments after microembolizations. Lead II trace highlighting the changes in the ECG, with (A) highlighting magnified lead II activity before microembolization and (B) after microembolization. Arrows highlight the ST-segment of the ECG, showing a depression after microembolization.

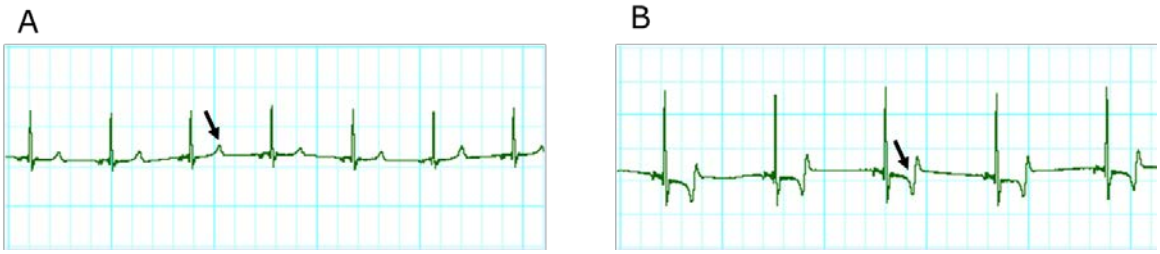

Figure 13b: Representative electrocardiogram traces from one sheep demonstrating changes on T-wave and ST-segments after microembolizations. Lead III trace highlighting the changes in the ECG, with (A) highlighting magnified lead III activity before microembolization and (B) after microembolization. Arrows highlight the ST-segment of the ECG, showing a depression after microembolization.

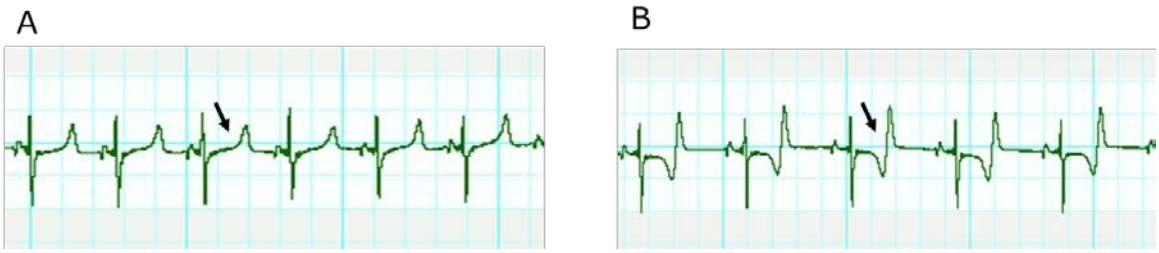

Figure 13c: Representative electrocardiogram traces from one sheep demonstrating changes on T-wave and ST-segments after microembolizations. Lead aVF trace highlighting the changes in the ECG, with (A) highlighting magnified lead aVF activity before microembolization and (B) after microembolization. Arrows highlight the ST-segment of the ECG, showing a depression after microembolization.

Figure 12 ECG changes before and after Embolization of the coronary artery, at the first time point produced changes in ST-segment or T wave.

Changes prominent in the lead II (13a), III (13b) and aVF (13c)

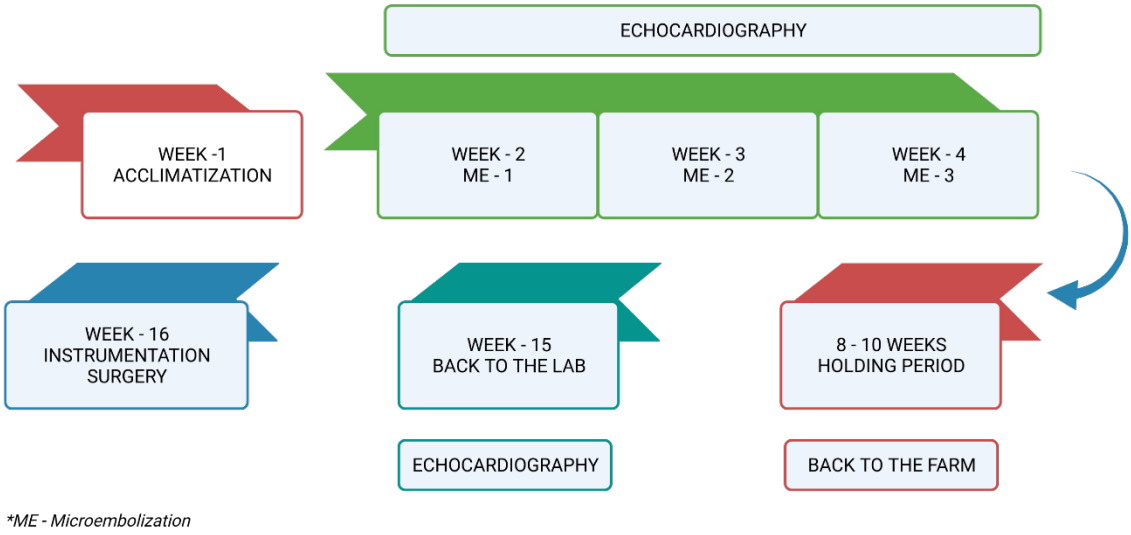

Figure 13 A schematic that highlights the timeline for the microembolization procedure for each HF animal

Once the sheep were acclimatized to laboratory condition and human contact, a group of sheep underwent three sequential embolizations (MEs) over three weeks until the animals started to develop stable clinical signs of heart failure. ME is the procedure to inject microspheres into the left coronary artery. The development of HF was assessed by measuring ejection fraction using transthoracic echocardiography. If the ejection fraction of the animal dropped below 40% after the second ME procedure, the third ME was not undertaken. HF was allowed to develop over eight to ten weeks. Therefore, sheep were sent to the farm for a holding period (8-10 weeks). The sheep was back in the lab after the 14th week of ME. Reassessed the ejection fraction using echocardiography, and the instrumentation surgery was carried out the following week. ME-1 = first microembolization; ME-2 = second microembolization; ME-3 = third microembolization.

2.2.2 *Unilateral renal artery clipping*

HTN was surgically-induced via unilateral constriction of the renal artery (i.e., two-kidney, one-clip model; 2K1C). Briefly, retroperitoneal incisions were made on one side of the flank to expose and isolate the renal artery. The incision was made on the contralateral side to which the renal artery flow probe was placed. A custom-made metal clip was then placed around it tightly to obstruct the blood flow to ≈40% of original flow. Sheep were left to develop HTN over 3 weeks, as we described previously (Tromp et al., 2018).

2.3 Echocardiography

The development of HF was assessed by measurement of EF and fractional shortening (FS) by using short-axis M-wave echocardiography (Hewlett Packard Sonos 1000) on conscious sheep standing on their crate. The 2-Dimensional Echocardiogram was performed before embolizations and 48 hours after each embolization. In the conscious standing sheep, the EF was typically around 70-80%. Echocardiography was performed after each embolization and I see a decrease in EF after each embolization. If the EF of the animal dropped below 40% after first or second embolizations, the next embolization was not undertaken. One week after the final embolization, the sheep were sent to the farm for the holding period (8-10 weeks), and the HF was allowed to develop over eight to ten weeks.

2.4 Timeline of surgical procedures

The microembolized sheep underwent another transthoracic LV echocardiography when they came back to the lab after the holding time (8-10 weeks after the embolization). The development of HF was assessed by measurement of EF and FS by using short axis M-wave echocardiography on conscious sheep standing on their crate. Once sheep were deemed to have sufficient LV dysfunction (EF < 40%), instrumentation surgery (thoracotomy) was performed.

I have focused on EF and FS in my sheep to assess the degree of LV dysfunction. A previous study from our lab has measured the plasma level of BNP and norepinephrine, which relates to the severity of HF (Abukar et al., 2019). In addition to the sheep used for experimentation in this study, in the total number of embolized sheep, two sheep died on the table due to anaesthetic complications and unexpected bleeding during the surgery. One sheep died on the farm, and six sheep developed dyspnoea following the embolizations and were euthanatized. So while we started with a larger number of animals, the end target of animals is lower.

The animals were instrumented to measure MAP, CoBF, CO, and HR. The animals were also instrumented with dEMG, and cardiac SNA electrodes as described in chapter 3, before undergoing the experimental protocol (Figure 14). Before each experiment, the sheep were given time to recover from surgery (2-3 days), and the recovery was determined by assessing basal HR, surgical site pain, and body temperature.

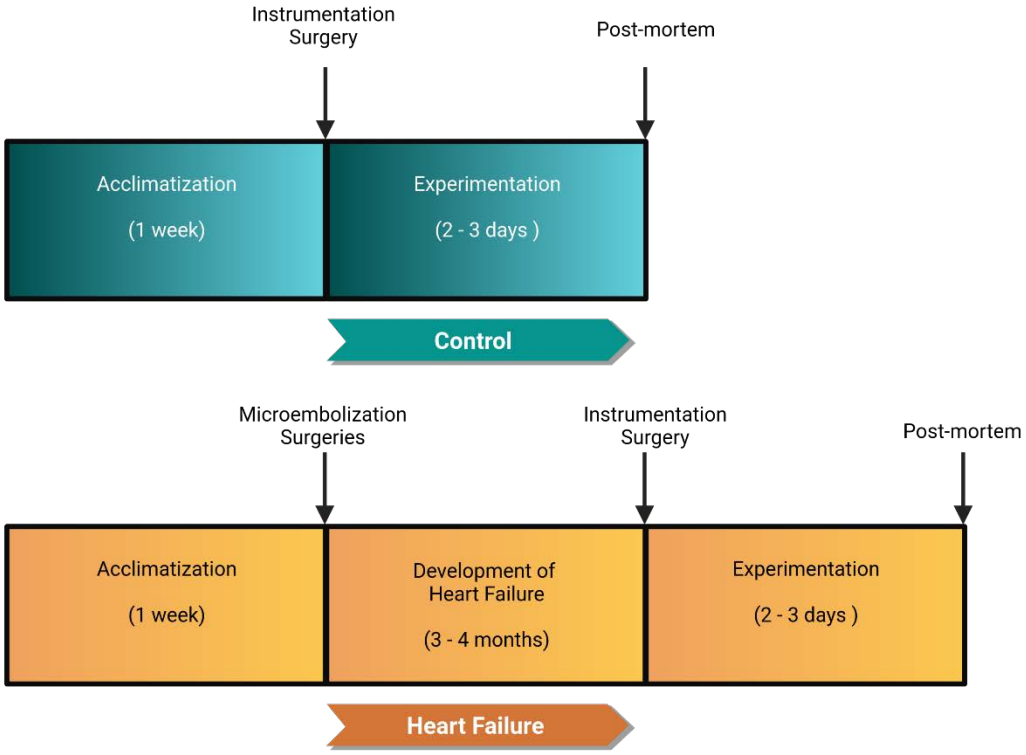

Figure 14 Timeline of surgical procedures and experimentation

2.4.1 *Instrumentation surgery*

In each experimental chapter the animals underwent an instrumentation surgery where a different combination of probes and electrodes were instrumented. Following intubation a thoracotomy was performed. Cardiac sympathetic nerve electrodes were implanted in the left cardiothoracic nerves. Briefly, an incision was made above the left fourth rib, the periosteum was incised and the rib removed. The opened thorax was held open with a rib retractor and the lung was retracted with wet gauze packs. The thoracic cardiac sympathetic nerve(s) was then identified with the use of a binocular microscope and the fascia over the nerve was removed. Electrodes consisted of stainless steel entomological pins (0.05 mm diameter) etched to a fine point, glued into the end of Teflon-coated 25-strand silver-coated copper wire (AS 633-7SSF, Cooner Wire, CA, USA). Up to six electrodes were implanted into the nerve, ensuring that the

tip was positioned in the centre of the cardiac sympathetic nerve. Electrodes were fixed in place with cyanoacrylate glue, and the implantation site was covered with a layer of Kwik-Sil (WPI, Sarasota, USA) surgical silicone adhesive (Watson et al., 2007; Watson et al., 2004).

The pericardium was then incised, a small area of proximal left circumflex (LCX) artery was dissected free, and a transonic flow probe (6PS, Transonic Systems, USA) was positioned around the vessel to measure the CoBF. The proximal segment of the LCX artery is usually covered by the left atrial appendage. A cotton swab was used to gently hold the left atrium backward until the flow probe was placed around the artery, and a transparent flange on the flow probe was sewn to the ventricular tissue.

A size 28 (28PAU, Transonic Systems, USA) CO transonic flow probe was also positioned around the ascending aorta to measure the CO. The thoracic aorta is covered with the pulmonary arterial trunk and loose areolar connective tissue. The connective tissues were dissected out carefully and placed a flow probe around the ascending aorta.

A bipolar active fixation endocardial lead (DexLead Solia S53, Dextronic, CA, USA) was used as an epicardial atrial lead, attached to the left atrial surface, by engaging and screwing the lead's helix into the atrial myocardium. The lead was then tied to atrial tissue and glued (Kwik-Sil, WPI, Sarasota, USA) in securely. Two strips of seven-stranded Cooner Wires (AS 633-7SSF, Cooner Wire, CA, USA) were implanted into the diaphragm and secured with silicone gel (Kwik-Sil, WPI, Sarasota, USA). Finally, a third Cooner wire was looped through the skin and used as an earth. Following this, the wound was closed with surgical suture (monofilament polypropylene 2-0 suture) and negative pressure restored to the thoracic cavity by inflating the lungs.

To eliminate the contribution of altered metabolic demand on coronary flow, the heart was paced at a constant rate during CB chemoreflex stimulation during baseline and after

atropine and propranolol infusion. In each sheep, a stimulator (Grass SD9 stimulator; Grass Instruments, U.S.A)) was used to keep the HR constant. The left atrium was paced at a rate 10-15 bpm higher than the resting HR of each sheep with a width of 0.1 msec, duration of 2 msec at 3-4 volts. For the propranolol and atropine results, comparisons were made with pacing done at the same level of HR in both control and drug conditions.

In normotensive and hypertensive group, instrumentation surgery undertook after 4-weeks of HTN development. An incision was made over the flank contralateral to the clipped kidney to place an ultrasonic flow probe (6PS, Transonic Systems, USA) around the renal artery to measure the RBF.

For all the animals, and during the same surgery, an incision was made in the neck to expose the common carotid artery and the jugular vein. A cannula was inserted into the common carotid artery (with the tip of the cannula lying 1 cm proximal to the carotid sinus region) and jugular vein for the drug and saline infusion. In addition, a sterile solid-state pressure catheter (Mikro-Tip, Millar, U.S.A.) was inserted in the same carotid artery but towards the heart for the measurement of arterial BP. Finally, middle exposed Cooner wire looped through the skin was used as a ground electrode. A schematic representation of the location of implanted instruments is shown in Figure 15.

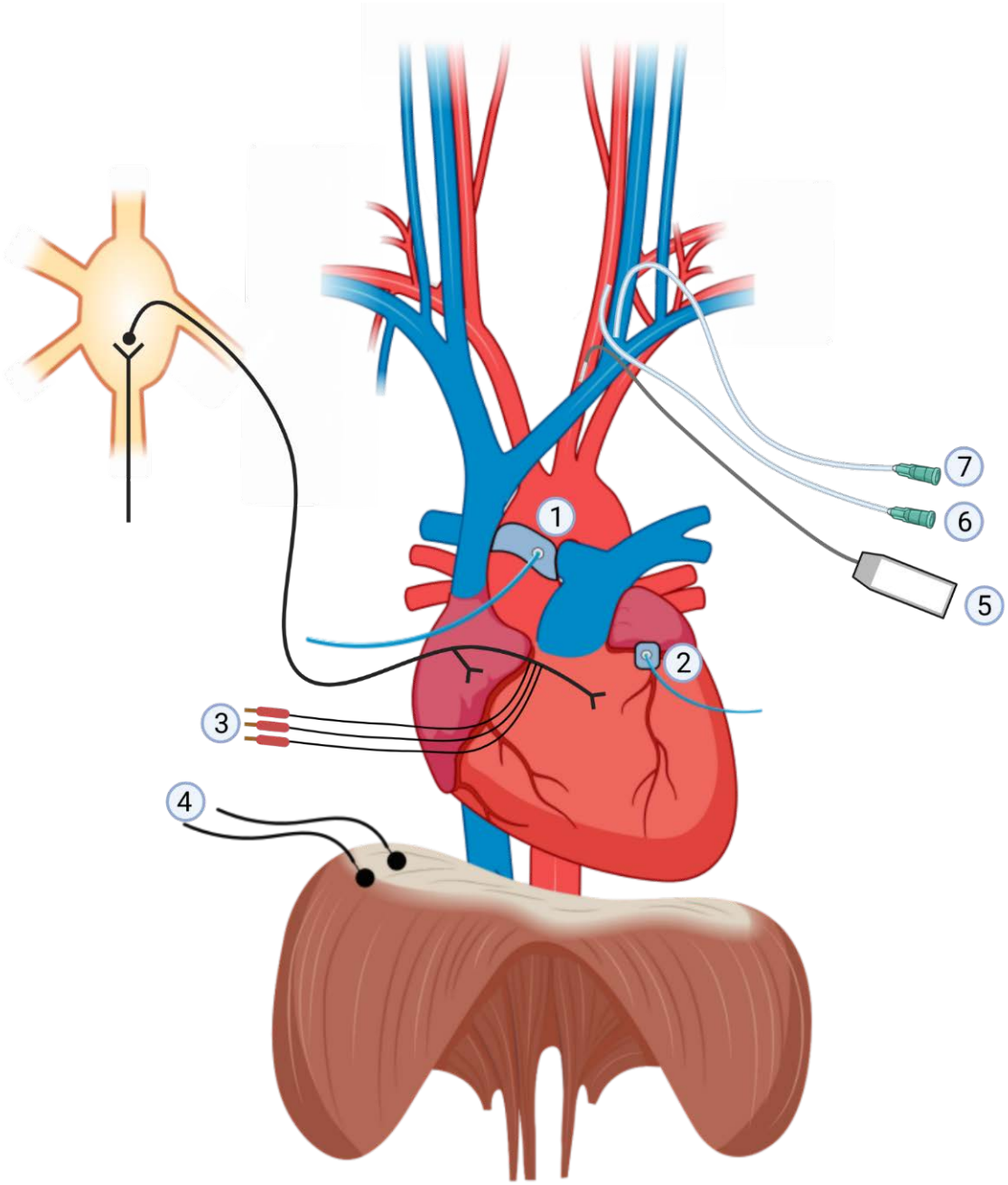

Figure 15 Schematic diagram demonstrating the location of implanted instruments.

1) Aortic flow probe, 2) Coronary blood flow probe 3) Cardiac SNA electrodes (5-6 numbers usually) 4) dEMG electrodes, 5) Pressure catheter inside the common carotid artery 6) Cannula facing up-carotid, 7) Intravenous cannula inside the jugular vein

2.5 Plasma brain natriuretic peptide, epinephrine, norepinephrine and cardiac collagen measurement

A previous study from our lab has measured plasma brain natriuretic peptide, epinephrine, norepinephrine, and cardiac collagen to assess the severity of HF (Abukar et al., 2019). Plasma was separated with a centrifuge at 4°C at 3,000 rpm, within 5 min of blood collection, and snap-frozen at −80°C (Abukar et al., 2019). All samples for brain natriuretic peptide (BNP), epinephrine, and norepinephrine from individual animals were measured using routine assays which have been as described previously (Justice et al., 2015; Lewis et al., 2017). Finally, a portion of the LV free wall was collected from each animal at the end of the experiments to measure the collagen deposition, as described (Abukar et al., 2019).

2.6 Data acquisition

2.6.1 *Sympathetic Nerve and Haemodynamic Recordings*

Cardiac SNA was recorded in conscious standing sheep at least 48 hours after electrode implantation to reduce post-surgical stress. Cardiac SNA was recorded differentially between pairs of electrodes as previously described (Ramchandra et al., 2009; Watson et al., 2007). The signal was amplified (20,000 times) and filtered (band pass 400 to 1000 Hz). MAP was obtained by connecting the carotid artery pressure catheter to a pressure control unit (Millar, pressure control unit, USA); the pressure catheter was connected to the transducer to check the zero point and the value was noted before the surgery.

Sympathetic nerve activity (sampling rate 5000 Hz), CoBF (1000 Hz), CO (1000 Hz) and AP (100 Hz), RBF (1000 Hz) were recorded and the analog output was fed into a computer data sampling system (CED Model 1401, Cambridge Electronics Design, UK) and processed

by a signal analysis program (Spike 2, Cambridge Electronics Design, UK). HR was measured from the phasic AP signal. The diaphragmatic electromyography (dEMG) electrodes were amplified and band-pass filtered (0.3–3.0 kHz).

2.6.2 *Haemodynamic Measurements and Analysis*

Data were analysed on a beat-to-beat basis using custom-written routines in the analysis program Spike 2. For each heartbeat (diastolic pressure to diastolic pressure), the program determined diastolic, systolic, MAP, HR, CoBF, RBF, CO and the area of the rectified and integrated (time constant = 20 msec) SNA and dEMG signals.

For cardiac SNA, the smallest burst was identified in the entire recording from a spreadsheet of data, and its correct position in the cardiac cycle and absence of artifacts were confirmed visually. The rectified and integrated area between the corresponding diastolic pressures of this burst was noted, and this area was taken as the minimum area for the definition of a burst. When the rectified and integrated area between any heartbeats was greater than the minimum area, this was determined to constitute a burst. For each sheep, the accuracy of burst determination was checked by eye for the data collected over the control period and at all subsequent periods. The burst incidence was calculated as the number of bursts per 100 heartbeats. The burst frequency was calculated as the number of bursts per minute (Ramchandra et al., 2018). Total cardiac SNA was taken as the product of the burst area and the burst incidence. The average burst size was determined as the total cardiac SNA divided by the cardiac SNA incidence.

The respiratory rate after KCN infusion was calculated manually by visual inspection of the raw dEMG signal. The rectified and integrated dEMG signal with a low-pass time constant of 20ms was computed using a script on Spike2. The data from the Spike 2 program was then exported into Microsoft Excel for the following analysis. Data were expressed as change in

absolute values with the resting value being that in the 15 sec prior to KCN infusion. Furthermore, CVC (mL/min/mmHg) was calculated by dividing CoBF by the MAP for each heartbeat.

2.7 Statistical Analysis

Results are expressed as mean ± SD. All statistical analysis was done using SPSS version 25 (SPSS, IBM, New York, NY). Paired t-tests were used to compare differences in resting haemodynamic variables in response to intravenous drug infusion (Chapters 3&4), room air vs. 100% oxygen (Chapter 5), and baseline haemodynamic Vs. HNF (chapter 6). For time series data, the dependent variables were MAP, CoBF, CO, CVC, RBF, RVC, dEMG and HR while the independent fixed factors are time, animal and relevant group of sheep. The effects of time, drug and the interaction effect was examined. A significant result was considered if $P < 0.05$.

Chapter 3: Activation of the carotid body increases directly recorded cardiac sympathetic nerve activity and coronary blood flow in conscious sheep

A slightly amended version of this chapter has been published in a peer-reviewed journal.

Mridula Pachen, Yonis Abukar, Julia Shanks, Nigel Lever, and Rohit Ramchandra

American Journal of Physiology-Regulatory, Integrative and Comparative Physiology, Volume 320, Issue 3, March 2021, Pages R203-R212

3.1 Introduction

The heart has one of the highest oxygen consumption per tissue mass of all the organs in the body (Goodwill et al., 2011). Extraction of oxygen in the heart is high (70–80%) compared to the rest of the body. The increase in oxygen demand must principally be met by an increase in CoBF (Duncker et al., 2008; Feigl, 1983a; Tune, 2014). Regulation of CoBF is modulated by multiple mechanisms including coronary perfusion pressure, myogenic mechanisms, local metabolic, endothelial, neural and hormonal influences (Goodwill et al., 2011). While there is good evidence that metabolic oxygen demand plays a dominant role in modulating CoBF (Alella et al., 1955; Berglund et al., 1957; Braunwald et al., 1957; Feinberg et al., 1962; Foltz et al., 1950; Goodwill et al., 2011), there is also an important role for neural modulation of CoBF.

In this context, the coronary blood vessels are innervated by both the sympathetic and the parasympathetic divisions of the autonomic nervous system (Armour et al., 1975; Hirsch, 1961; Mizeres, 1955; Nonidez, 1939). Experimentally, it is difficult to definitively separate out the neural influence on CoBF since changes in HR and contractility can influence metabolic demand. Theoretically, an increase in sympathetic drive can activate α-receptors to produce vasoconstriction and activate β2-receptors to cause direct vasodilation. In addition, sympathetic drive can also indirectly cause vasodilation through increased HR and contractility which increases metabolic demand. Experimentally, studies in both conscious and anaesthetized dogs have shown that activation of either the sympathetic (Denison JR et al., 1958; Feigl, 1967; Granata et al., 1965) or the parasympathetic nerves (Feigl, 1969) results in coronary vasodilation.

Under basal conditions, the heart receives tonic drive from both the sympathetic and parasympathetic nerves. The peripheral chemoreceptor reflex driven by activation of the aortic body and the carotid body (CB) is one reflex which putatively results in co-activation of both

autonomic arms. Previous studies have indicated that activation of the CB results in reflex coronary vasodilation (Hackett et al., 1972; Vatner et al., 1975) but whether the sympathetic nerves play a role in this vasodilation has been debated. Importantly, studies which have examined the effects of CB activation on CoBF have been conducted under anaesthesia which is known to reduce sympathetic drive (Matsukawa et al., 1993; Ninomiya et al., 1971) as well as dampen the chemoreflex (Biscoe et al., 1968; Duffin et al., 1976; Zimpfer et al., 1981). Previous studies in the conscious dog (Murray et al., 1984; Vatner et al., 1975) have inferred that the increase in CoBF during activation of the CB may be mediated by withdrawal of sympathetic drive to the heart. Whether there is a change in directly recorded cardiac SNA during activation of the CB chemoreflex is unknown. Hence, the first aim of this study was to directly record cardiac SNA during activation of the CB in conscious sheep.

I hypothesized that stimulation of CB chemoreceptors using intracarotid KCN would increase directly recorded cardiac SNA in the conscious animal. I also hypothesized that activation of CB chemoreceptors would result in coronary vasodilation that is primarily mediated by the increase in SNA. To separate the β2-adrenergic receptor vasodilatory effects from contractility mediated metabolic changes, I investigated the effects of chemoreflex activation when the heart was electrically paced at a constant rate.

3.2 Methods

Experiments are conducted on conscious, adult female Romney sheep weighing 50-80 kg, housed in individual crates, acclimatized to laboratory conditions (18ºC, 50% relative humidity, and 12 hour light-dark cycle) and human contact before experimentation. All experiments and surgical procedures were approved by the Animal Ethics Committee of the University of Auckland.

3.2.1 *Animal group and anaesthesia details*

For these studies, n=12 adult female sheep (weight: 59±3 kg) were used. Two different groups of animals were used; in the first group I examined the response of cardiac SNA to CB stimulation (group-A, n=6). The second group of animals was instrumented for measurement of CoBF and other cardiovascular variables in response to CB stimulation (group-B, n=6). All sheep underwent aseptic surgical procedures under general anaesthesia administered by an experienced animal technician. Sheep were fasted for 24 hours prior to surgery and anaesthesia was induced with intravenous propofol (5 mg/kg; AstraZeneca, U.K.), and following intubation, maintained with 1.5–2.0% isoflurane/oxygen (Lunan Better Pharmaceutical, China) at 5L/min. Bupivacaine-Claris solution (2.5mg/mL; Multichem NZ Ltd, New Zealand) injection was given into the intercostal space as a nerve block to prevent surgical pain. Ketoprofen (2 mg/kg, IM) and long-acting Oxytetracycline (20 mg/kg, IM) were used for premedication for all sheep. In addition Ketoprofen (2 mg/kg, IM) was provided for two days post-surgery for management of post-surgical pain.

3.2.2 *Cardiac SNA surgery (Group A)*

A thoracotomy was performed to implant electrodes in cardiothoracic sympathetic nerves as described previously (Watson et al., 2007; Watson et al., 2004). Briefly, up to six

electrodes were implanted into the left cardiac sympathetic nerve, ensuring that the tip was positioned in the centre of the sympathetic nerve. Following this, the wound was closed and negative pressure restored to the thoracic cavity.

3.2.3 *CoBF and haemodynamic variables (Group B)*

In a separate group of animals, after thoracotomy, a small area of the proximal left circumflex artery was dissected free and a transonic flow probe (size 6) was positioned around the vessel. A size 28 CO Transonic flow probe was also placed around the ascending aorta. A bipolar active fixation endocardial lead was used as an epicardial atrial lead and attached to the left atrial surface. Two strips of seven-stranded Cooner Wires (AS 633-7SSF, Cooner Wire, CA, USA) were implanted into the diaphragm and secured with silicone gel. Following this, the wound was closed and negative pressure restored to the thoracic cavity.

For animals in both groups, and during the same anaesthesia protocol, an incision was made in the neck to expose the common carotid artery and the jugular vein. A cannula (outer diameter 1.5 mm) was inserted into the left common carotid artery (with the tip of the cannula lying 1 cm proximal to the carotid sinus region) and jugular vein for the drug and saline infusion. In addition, a sterile solid-state pressure catheter (Mikro-Tip, Millar, U.S.A.) was inserted in the same carotid artery but towards the heart for the measurement of arterial pressure.

3.2.4 *Experimental protocols*

3.2.4.1 *Group A – Cardiac SNA:*

I confirmed that the cardiac SNA recordings were indeed SNA using a baroreflex challenge and hexamethonium as previously done (Tromp et al., 2018; Watson et al., 2007). After recording 30 minutes of basal cardiovascular variables, the CB chemosensitivity was assessed using KCN (Sigma-Aldrich, Germany) dissolved in 0.9% sodium chloride solution

(Baxter, U.S.A.) injected as an intra-carotid bolus dose (via the common carotid cannula) at 20 μg/kg followed by 5 ml heparinized saline (25 IU heparin in 1L saline). In addition 5ml of saline was also injected into the carotid artery as a control. To determine the effect of CB activation, the absolute change in cardiac SNA over a 60 second period was measured in response to intracarotid KCN.

3.2.4.2 *Group B: CoBF*

For this group, the haemodynamic responses to CB activation were determined initially during control conditions and when injecting 10, 20, and 30 μg/kg KCN followed by 5 ml heparinized saline. To eliminate the contribution of altered metabolic demand on CoBF, the heart was paced at a constant HR. The left atrium was paced at a constant rate 10-15 bpm higher than the spontaneous sinus rate using the Grass stimulator (Grass SD9 stimulator; Grass Instruments, U.S.A). For the study of propranolol and atropine effects, comparisons were made with pacing done at the same level of HR in both control and drug conditions.

The haemodynamic response to CB activation was determined following cholinergic blockade with intravenous atropine (8 mg bolus followed by 24 mg/h infusion for 30 minutes; LKT Labs, U.S.A.) and β-adrenergic receptor blockade with propranolol (30 mg bolus followed by 0.5 mg/kg/h infusion for 90 minutes). Following drug infusion, the effect of CB activation was repeated with KCN doses in all studies. Each KCN injection was given at least 2 minutes apart and care was taken to avoid any distraction which may have caused changes in basal recording. The KCN effect was short-lasting (<60 sec), and repeatable. There was no noticeable discomfort in the sheep during the KCN injection. At the end of these experiments, sheep were euthanized with an overdose of intravenous sodium pentobarbitone (300 mg/kg; Provet NZ Pty Ltd, New Zealand).

3.2.5 *Sympathetic Nerve and Haemodynamic Recordings*

Cardiac SNA was recorded in conscious sheep at least 48 hours after electrode implantation to reduce post-surgical stress. The SA signal was recorded differentially between pairs of electrodes as previously described (Ramchandra et al., 2009; Watson et al., 2007). MAP was obtained by connecting the carotid artery pressure catheter to a pressure control unit (Millar, pressure control unit, USA). SNA (sampling rate 5000 Hz), CoBF (1000 Hz), CO (1000 Hz) and arterial pressure (100 Hz) were recorded using a CED micro 1401 interface and Spike 2 software (Cambridge Electronic Design, Cambridge, UK). HR was measured from the phasic arterial pressure signal. SV was calculated from CO. The dEMG activity was amplified and band-pass filtered (0.3–3.0 kHz).

3.2.6 *Haemodynamic Measurements and Analysis*

Data were analysed on a beat-to-beat basis using custom-written routines in the analysis program Spike 2. For each heartbeat, the program determined diastolic, systolic, and MAP, heart period, CoBF, CO and the area of the rectified and integrated (time constant = 20 msec) SNA and dEMG signals between diastolic pressures. MAP, CoBF, CO and HR were obtained from the recording and 5 sec averages were obtained at 5 sec intervals and were presented as a time series graph over 75 sec for each animal.

For cardiac SNA, the smallest burst was identified in the entire file, and its correct position in the cardiac cycle and absence of artifacts were confirmed visually. The rectified and integrated area between the corresponding diastolic pressures of this burst was taken as the minimum area for the definition of a burst. The burst frequency was calculated as the number of bursts per minute (Ramchandra et al., 2018). Total cardiac SNA was taken as the product of the burst area and the burst incidence.

The respiratory rate after KCN injection was calculated manually by visual inspection of the raw dEMG signal. The rectified and integrated dEMG signal with a low-pass time constant of 20ms was computed using a script on Spike2. Data were expressed as change in absolute values with the resting value being that in the 15 sec prior to KCN injection. Furthermore, CVC was calculated by dividing CoBF by the MAP for each heartbeat.

3.2.7 *Statistical Analysis*

Results are expressed as mean ± SD. All statistical analysis was done using SPSS version 25 (SPSS, IBM, New York, NY). Paired t-tests were used to compare differences in resting haemodynamic variables in response to intravenous drug infusion. The KCN data were assessed using a two way ANOVA. For time series data, the dependent variables were MAP, HR, CO, dEMG and CoBF while the independent fixed factors were time, animal and drug treatment (KCN dose or receptor blockade). For group A with cardiac SNA recordings, the dependent variable was SNA while the independent fixed factors were time and animal. The effects of time, drug and interaction effects were examined. A difference was considered as statistically significant when $P<0.05$.

3.3 Results

3.3.1 *Control cardiac sympathetic nerve activity responses to CB activation*

A representative raw data trace from a single animal demonstrating changes in directly recorded cardiac SNA and dEMG in response to intracarotid KCN (20 μg/kg) injection is shown in Figure 16. Intracarotid KCN injection resulted in an increase in dEMG amplitude and cardiac SNA (all $p < 0.05$). 5-sec averages were obtained at 5-sec intervals, and so the time point 0 equates to -5 sec to 0 seconds. The increase in cardiac SNA occurred within the first 10 seconds of the KCN bolus injection. Performed a one-way ANOVA where a significant effect of time and then a post hoc analysis which showed that time point 10 had a significant increase in all the animals. The significant increase in total cardiac SNA was mediated by an increase in burst frequency, while burst amplitude was not altered (Figures 17 and 18).

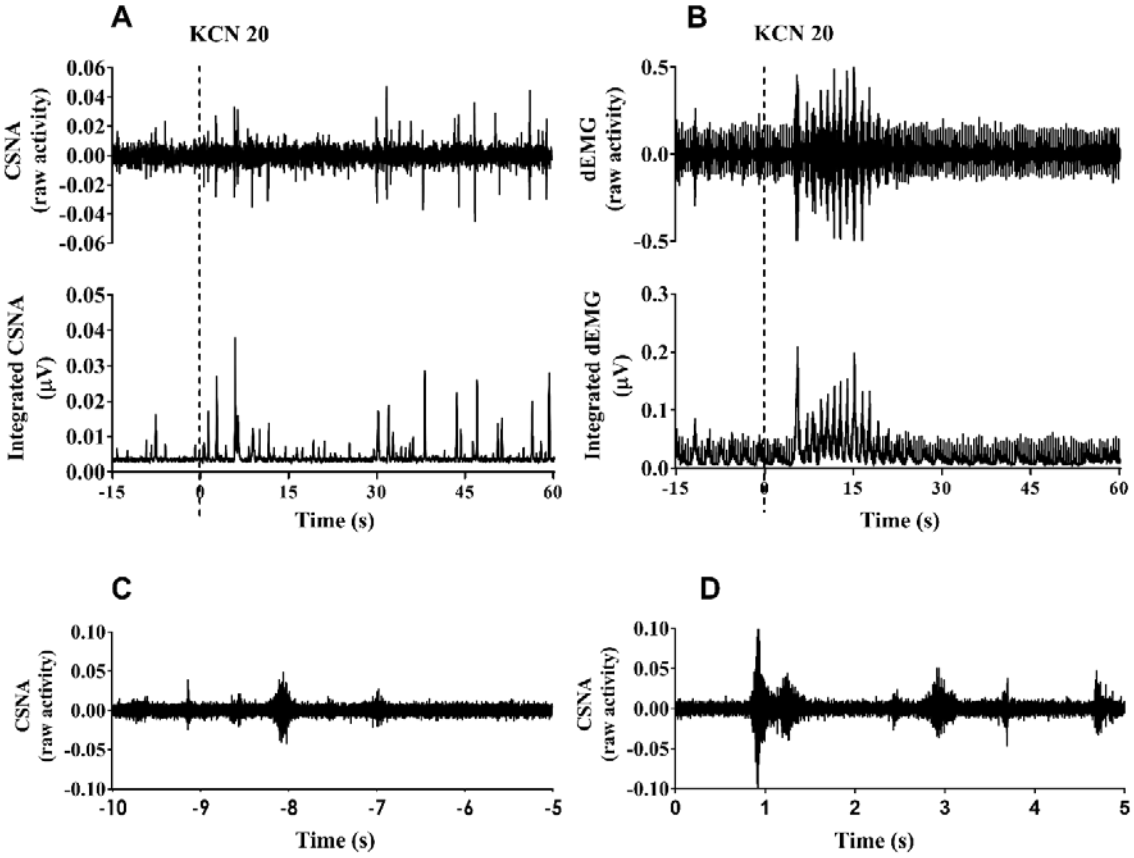

Figure 16 Representative raw signal traces from one control animal

(A) Indicating an increased burst incidence of raw and integrated cardiac SNA signals and (B) Increased raw and integrated dEMG activity in response to intracarotid potassium cyanide (KCN) at a dose of 20 μg/kg. (C) Raw signal of cardiac SNA (5-sec) before KCN injection, (D) 5-sec raw activity just after KCN injection

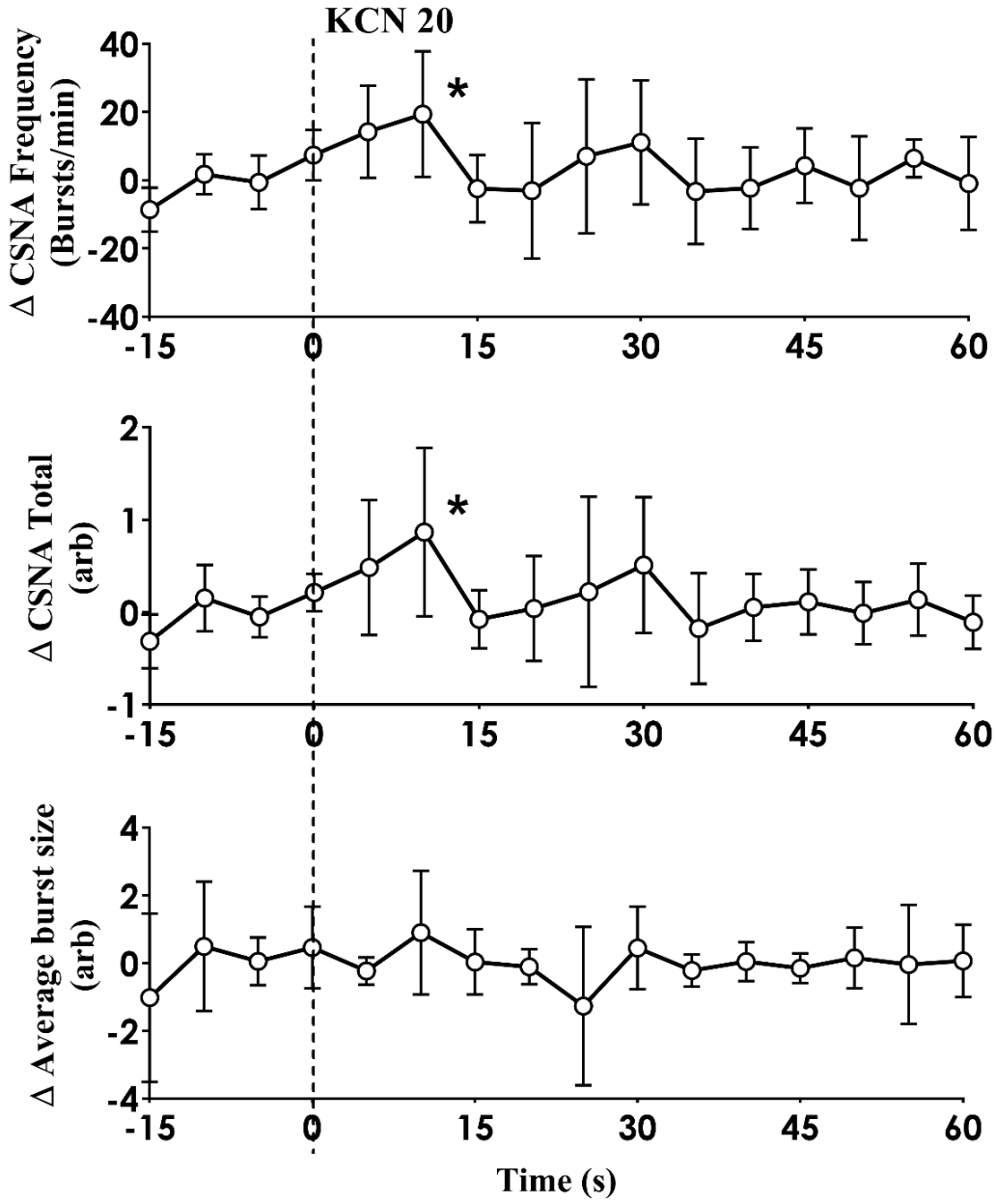

Figure 17 Absolute change in cardiac CSNA.

*Absolute change in burst frequency, total cardiac SNA and average burst size of cardiac SNA (n=6) in response to intracarotid potassium cyanide (KCN; 20 μg/kg) injection in control sheep. Results are mean ± SD. * - p<0.05. N=6 (one-way ANOVA - effect across the 60s period following injections; * - post hoc (Dunnett's test) analysis - time point 10 has a significant increase over baseline).*

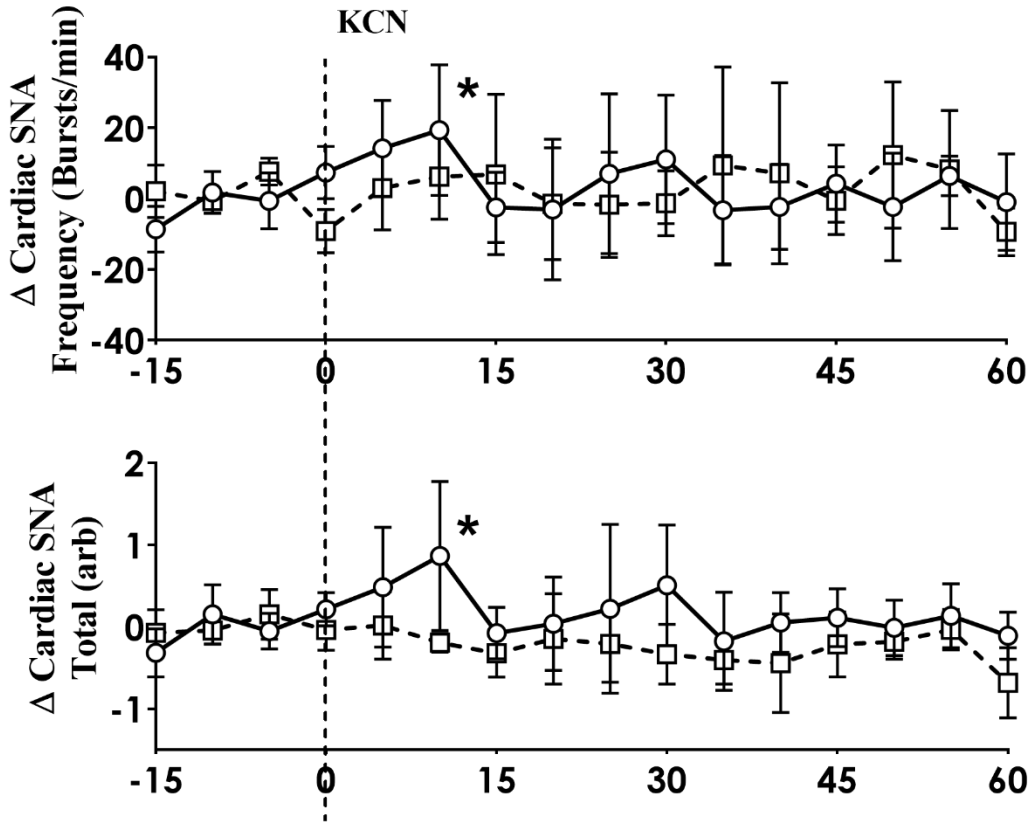

Figure 18 Absolute change in cardiac SNA in response to saline control and KCN

*Absolute change in burst frequency and total cardiac SNA (n=6) in response to intracarotid potassium cyanide (KCN; 20 μg/kg, circles and solid line) and saline control (squares and interrupted line) in control sheep. Results are mean ± SD. * - p<0.05. N=6 (one-way ANOVA - effect across the 60sec period following injections; * - post hoc analysis (Dunnett's test) - time point 10 has a significant increase over baseline).*

3.3.2 *Haemodynamic responses to CB activation*

The control haemodynamic variables in conscious sheep are shown in the first column of Table 2. Figure 19 shows the raw data of MAP, CoBF and CO in a representative sheep during intra-carotid KCN injection. KCN at 10, 20, and 30 μg/kg caused a dose-dependent increase in MAP, CoBF and HR (Figure 20) when the heart was not paced. There was no

significant change in CO in response to activation of the CB. The time course of the increase in CoBF and CVC outlasted the increase in cardiac SNA.

Table 2 Levels of haemodynamic and cardiovascular variables in control animals

*During resting conditions, after atropine and propranolol infusions; Data are represented as mean ± SD. $P \leq 0.05$ (paired t-test). * denotes significantly different from basal values. N=6/group*

	Basal values	After Atropine	After Propranolol
Mean arterial pressure (mmHg)	79±15	88±13*	73±14*
Coronary blood flow (mL/min)	76±37	88±41*	72±35*
Heart Rate (bpm)	105±4	118±7*	99±15
Coronary vascular conductance (mL/min/mmHg)	1±0.7	1±0.6	1±0.6
Cardiac output (L/min)	9±2	8.6±3	9±2
Stroke Volume (mL/beat)	86±27	70±20*	89±27

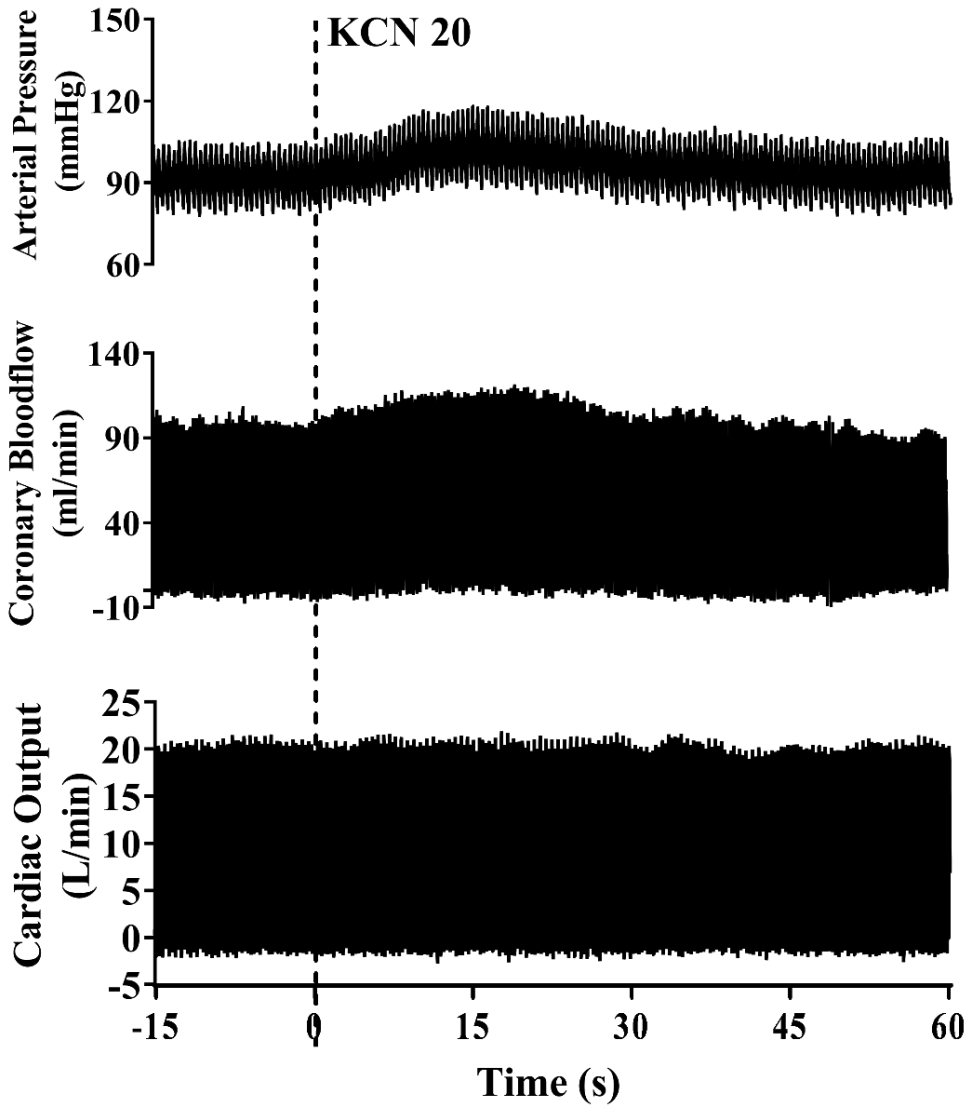

Figure 19 Raw traces from one control animal

Raw traces demonstrating changes in arterial pressure, coronary blood flow, and cardiac output in response to intracarotid potassium cyanide at a dose of 20 μg/kg.

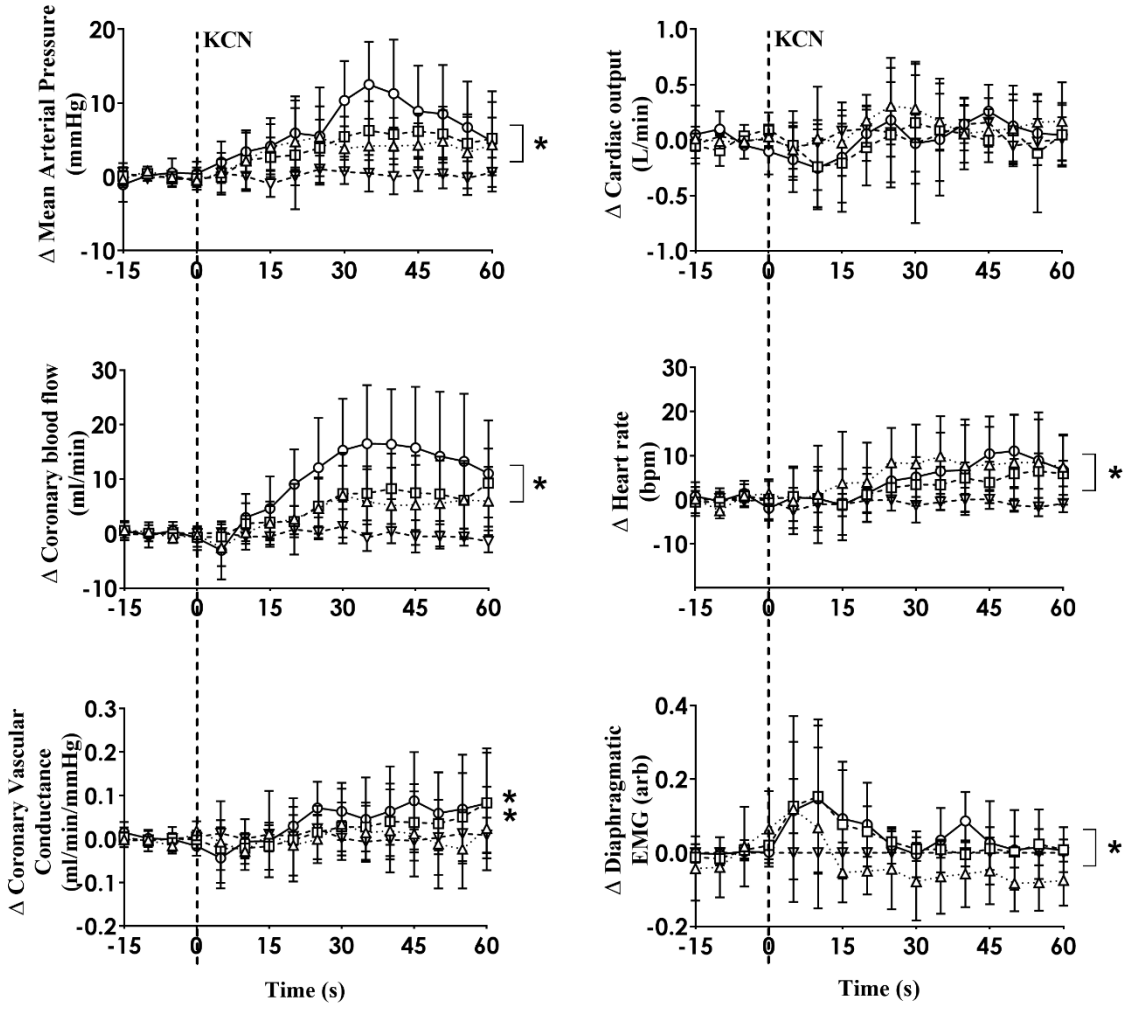

Figure 20 Absolute change in cardiovascular variables in control sheep

*Mean arterial pressure, coronary blood flow, coronary vascular conductance, cardiac output, heart rate and dEMG responses to saline control (inverted triangles and interrupted line) and intracarotid potassium cyanide (KCN; 10 µg/kg (triangles and dotted line), 20 µg/kg (squares and interrupted line), and 30 µg/kg (circles and solid line) injection in control sheep (n=6). Data are mean ± SD. * - p<0.05 (one-way ANOVA, * - significant time effect across the 60sec recording period).*

3.3.3 *Effect of infusion of cholinergic blocker (Atropine sulfate)*

As shown in the second column of Table 2, atropine infusion resulted in significant haemodynamic changes such as increased basal MAP (from 79±6 to 88±5 mmHg; $p<0.05$), CoBF (from 76±14 to 88±15 mL/min; $p<0.05$), and HR (from 105±3to 118±4 bpm; $p<0.05$). CO was unchanged, and SV (from 86±10 to 70±8 mL/beat; $p<0.05$) was decreased after atropine infusion.

Intra-carotid KCN injection when the heart was paced (10-15 bpm above the resting HR) resulted in statistically significant increases in MAP, CoBF, CVC, and dEMG (open circles and solid line; all $p< 0.05$). The peak increase in CoBF and CVC and after that falling back towards baseline compared to the unpaced data where these parameters were raised for the full duration of the 60s recording period. Following intravenous atropine infusion, the MAP (filled squares and interrupted line) response to intracarotid KCN injection was significantly attenuated ($p<0.05$), but no other variables were altered (Figure 21).

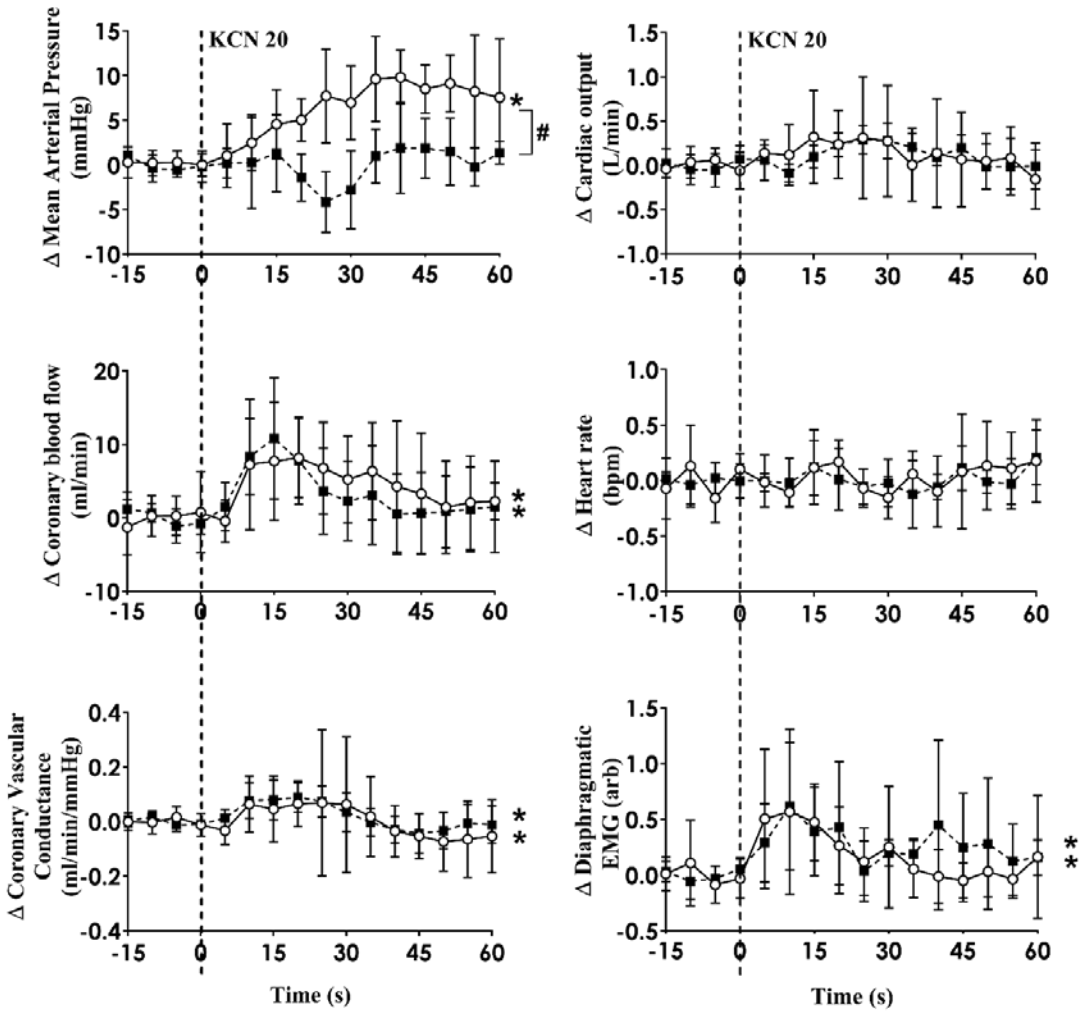

Figure 21 Absolute change in cardiovascular variables to carotid body activation before and after muscarinic receptor blockade.

*CB activation before and after Atropine sulfate (8 mg bolus followed by 24 mg/h infusion for 30 minutes) in conscious control sheep. The heart was paced at a constant rate such that the heart rate was unchanged. The open circles and solid line represent before atropine, and filled squares and interrupted line is after atropine responses. Results are mean ± SD. * - $p<0.05$ denotes a significant effect of time (one-way ANOVA, * - significant time effect across the 60sec recording period; # - two-way ANOVA, significant interaction effect of time x group).*

3.3.4 *Effect of infusion of β-adrenergic blocker (Propranolol)*

Infusion of propranolol significantly decreased basal MAP (from 79±6 to 73±5 mmHg; $p<0.05$) and CoBF (from 76±14 to 72±13 mL/min; $p<0.05$) as shown in the last column of Table 2. KCN injection with HR fixed by pacing resulted in significant increases in MAP, CoBF, CVC, and dEMG (open circles and solid line; all $p<0.05$). The CoBF and CVC response to intracarotid KCN injection were abolished ($p<0.05$) after propranolol infusion during pacing condition (Figure 22). There was no change in any other parameters (Figure 22).

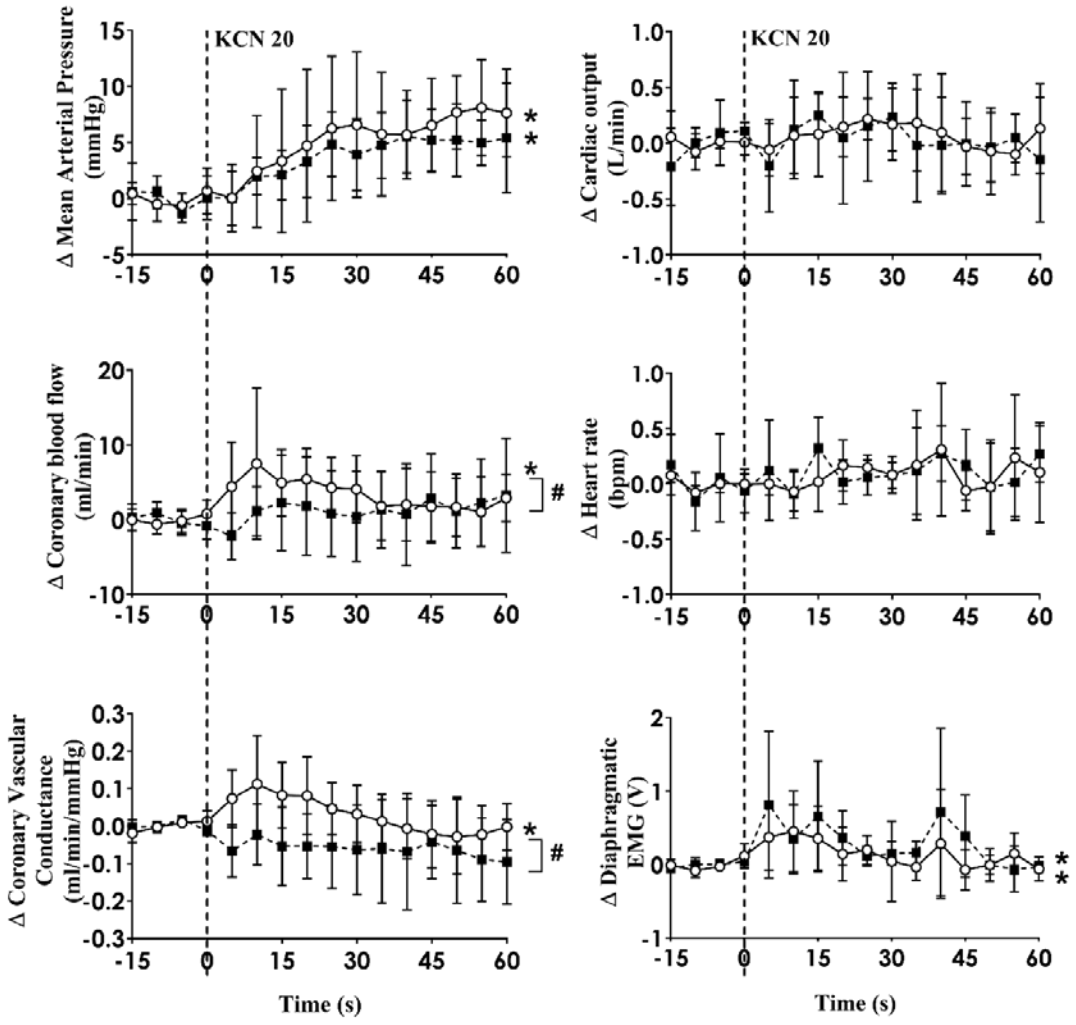

Figure 22 Absolute change in haemodynamic variables to CB activation before and after ß-adrenergic receptor blockade.

*CB activation before and after Propranolol (30 mg bolus followed by 0.5 mg/kg/h infusion for 90 minutes) in conscious sheep. The heart was paced at a constant rate such that the heart rate was unchanged. The open circles and solid line represents the KCN response before propranolol infusion, and filled squares and interrupted line is after propranolol infusion. Results are mean ± SD. * - $p<0.05$ (one-way ANOVA, * - significant time effect across the 60sec recording period; # - two-way ANOVA, significant interaction effect of time x group).*

3.4 Discussion

To the best of our knowledge, this is the first study to examine directly recorded cardiac SNA during activation of the CB in conscious animals. The main findings of this study are: 1) Activation of the CBs using intracarotid KCN increases directly recorded cardiac SNA, MAP, CoBF and CVC. 2) Inhibition of β-receptors using propranolol abolished the CB activation mediated increase in CVC indicating that the increase in cardiac SNA mediates coronary vasodilation in conscious sheep 3) Inhibition of muscarinic mechanisms using atropine abolished the MAP response to CB activation, suggesting that the pressor response depends on cholinergic mechanisms.

3.4.1 *The cardiac SNA response to CB activation*

Numerous research papers have described the significant rise in MAP during CB activation as being mediated by peripheral vasoconstriction (Daly et al., 1962; de Burgh Daly et al., 1959; Fletcher et al., 1992; Guyenet, 2000; Rutherford et al., 1978). This increase in peripheral resistance is mediated in part by an increase in sympathetic nerve activity to the kidney (McBryde et al., 2013; Schultz et al., 2007b). However, given that SNA to various organs is differentially regulated (DiBona et al., 1996; Morrison, 2001), I sought to investigate the response of cardiac SNA. My study shows that similar to renal SNA, cardiac SNA is also elevated after acute CB activation (Figure 17). This increase in cardiac SNA is a potential contributor to the increase in HR observed when the CB is activated (Figure 20). We have previously shown that acute inhibition of the chemoreceptors using hyperoxia reduces cardiac SNA burst frequency and HR in normal animals (Xing et al., 2014) which is consistent with my current finding.

3.4.2 *Effects of sympathetic activation on CoBF response to CB activation*

In addition to the increase in cardiac SNA, activation of the CB also resulted in an increase in CoBF. The increase in cardiac SNA can putatively increase CoBF via multiple mechanisms i) Stimulation of vasodilator β2-adrenoceptors would directly promote vasodilation (Maman et al., 2017; Miyashiro et al., 1993) ii) Activation of the α-receptors results in tachycardia and increased cardiac contractility which would augment myocardial metabolism, so the increase in CoBF may be secondary to increased myocardial metabolism (Denison JR et al., 1958; Feigl, 1967; Granata et al., 1965). iii) In addition to these vasodilatory actions, stimulation of vasoconstrictor α-adrenoceptors would oppose any vasodilation.

In my study, to eliminate the effects of metabolic induced vasodilation, I repeated the KCN study when the heart was paced at a constant rate. An increase in CoBF was still observed suggesting the increase in CoBF persists when myocardial oxygen demand is kept constant (Figure 22). Importantly, CB stimulation following pre-treatment with the β-adrenergic receptor blocker abolished the CoBF and CVC responses to CB activation. Taken together, my data indicate that in the intact sheep, the β2-adrenergic vasodilatory actions supersede the α-adrenergic vasoconstriction during reflex sympathetic activation and are responsible for the coronary vasodilation. My studies contrast with previous studies performed in conscious dogs (Murray et al., 1984; Vatner et al., 1975) that observed an increase in CoBF with CB activation only when ventilation was allowed to increase.

The authors inferred that the coronary vasodilation was mediated by withdrawal of sympathetic drive to the heart. Interestingly in my study, propranolol infusion did not alter ventilation although the coronary vasodilation was abolished. I cannot rule out a difference between species effect in my study and the previous studies. It must be mentioned that recent studies indicate that the ventilatory and sympathetic responses to CB activation may be

differentially mediated so I cannot rule out a change in the sympathetic responses (Prasad et al., 2020). It must also be mentioned that propranolol has been shown to directly inhibit CB activity under certain conditions (hypoglycaemia) (Thompson et al., 2016). This coupled with the fact that propranolol can cross the blood-brain barrier means that I cannot rule out that the inhibition of the coronary vasodilation may be mediated by actions of propranolol at the CB or centrally.

3.4.3 *The role of cardiac vagal drive on the CoBF response to CB activation*

To determine if the coronary vasodilation was mediated by parasympathetic activation, I also tested the responses to KCN after infusion of atropine. Atropine infusion caused a significant increase in basal HR (Table 2), indicating the dose of atropine was sufficient to block vagal drive to the heart. In my study, atropine did not alter the CoBF or CVC responses to CB activation. This contrasts with a previous study that has observed that stimulation of the carotid chemoreflex using nicotine causes coronary vasodilation in conscious control dogs mediated by activation of parasympathetic cholinergic efferent fibers (Shen et al., 1994). Another study in α-chloralose anaesthetized, closed-chest dogs shows that carotid chemoreceptor stimulation by hypoxic-hypercapnic blood, nicotine, or cyanide increased CoBF, which was abolished after infusion of atropine (Ito et al., 1985) which is again in contrast to my current study. The reasons for this discrepancy are not clear; however I cannot rule out a species difference effect. I cannot rule out that the parasympathetic nerves may play a role mediated via other neurotransmitters such as vasoactive intestinal peptide which is shown to mediate coronary vasodilation (Feliciano et al., 1998a, 1998b).

The pressor response to CB activation was attenuated post atropine in the conscious animals similar to a previous study from our group (Chang et al., 2020). Some previous studies have shown that the pressor and HR responses to chemoreflex activation are unchanged or potentiated with atropine pre-treatment (Braga et al., 2008; Franchini et al., 1997). However,

historical studies have also demonstrated attenuation of peripheral vasoconstriction attributable to CB activation following mACh (muscarinic acetylcholine) receptor blockade (Henderson et al., 1978; Jänig et al., 1983). It is possible that my atropine dose may cross the blood-brain barrier and have central effects. Indeed, acetylcholine can modulate various parts of the chemoreflex arc including the CB itself and centrally within the nucleus tractus solitarius (NTS) and rostral ventrolateral medulla (RVLM) (Furuya et al., 2014; Padley et al., 2007; Vieira et al., 2007). In the CB, acetylcholine (ACh) is released from glomus cells during chemoreceptor stimulation and acts as an excitatory neurotransmitter onto apposed sensory nerve terminals (Eyzaguirre et al., 1990; Iturriaga et al., 2007; Kåhlin et al., 2014; Nurse et al., 2013).

3.4.4 *Respiratory response to CB activation*

Activation of the CB resulted in marked increases in tidal volume and respiratory effort in the animals (Figures 16 and 20). While the pressor response to KCN is abolished post-atropine, the ventilatory response was not. Indeed, the ventilatory response as measured by alterations in the dEMG signal were not altered by any of the interventions in my study. A discordance between the sympathetic and ventilatory responses to CB activation has been observed by others before (Prasad et al., 2020).Our findings support the concept that the various effector components of the CB chemoreflex may be differentially regulated by different neuromodulators as has been suggested recently (Zera et al., 2019).

3.4.5 *Perspectives and significance*

In summary, my study indicates that CB activation increases directly recorded cardiac SNA and CoBF in conscious sheep. Blockade of the β-receptors using propranolol abolished the coronary vasodilation indicating that the increase in cardiac SNA mediates β-adrenoceptor coronary vasodilation in the conscious state. My data indicates the CB plays an important role

in modulating blood flow to the heart and future studies need to investigate the impacts of interruption of CB afferent input on CoBF.

Chapter 4: Regulation of coronary blood flow by the carotid body chemoreceptors in ovine heart failure

A slightly amended version of this chapter has been published in a peer-reviewed journal.

Mridula Pachen, Yonis Abukar, Julia Shanks, Nigel Lever, and Rohit Ramchandra

Frontiers in Physiology, Volume 12, May 2021, Article 681135

4.1 Introduction

HF is a severe, debilitating condition with poor survival rates and increasing prevalence (Swedberg et al., 2005). Amongst other features, patients with HF commonly exhibit disordered breathing patterns and autonomic dysfunction (Chua et al., 1997; Chua et al., 1996; Reserve et al.). A characteristic of the autonomic dysfunction is an increase in sympathetic nerve activity to the heart which acutely provides inotropic support and maintains CO (Watson et al., 2006) but over the long-term also promotes disease progression and shortens life expectancy (Kaye et al., 1995). Both the disordered breathing and the autonomic dysfunction are strongly related to a higher mortality risk and poorer prognosis in patients (Cohn et al., 1984; Floras, 1993; Leung et al., 2004; Naughton et al., 1993). Previous studies have suggested that altered neural reflexes, such as the chemoreflex and baroreflex contribute to the elevated levels of sympathetic nerve activity in HF (Ferguson et al., 1992; Narkiewicz et al., 1999; Narkiewicz et al., 1998; Ponikowski et al., 1997).

Recently, the CB has been implicated as playing a major role in mediating the increase in sympathetic nerve activity during cardiovascular disease. The CB is a polymodal chemoreceptor strategically located at the bifurcation of the common carotid artery. Amongst other stimuli, the CB is activated by hypoxia, hypercapnia, and acidosis (Iturriaga et al., 2016). Studies have shown that the sensitivity of the chemoreflex is elevated in patients with HF (Schultz et al., 2007a) and animal models of HF (Del Rio et al., 2013b; Sun et al., 1999a). Interrupting the chemoreflex both acutely using intranasal oxygen (Xing et al., 2014) and chronically using denervation of the CB (Marcus et al., 2014b) has been shown to reduce sympathetic nerve activity to the heart and the kidney.

The primary blood supply to the heart has been less studied in both control and disease conditions. Oxygen extraction is already high in the heart (Binak et al., 1967; Wolff, 2008)

which means that energy demand is the primary regulator of CoBF. However, neural control of the coronary artery resistance has also been shown to play an important role. In this context, my previous study in conscious sheep showed that activation of the CB increased directly recorded cardiac SNA and CoBF (Pachen et al., 2020). Importantly when the effects of sympathetic activation were blocked, the increase in CoBF was abolished indicating activation of the chemoreflex increases cardiac SNA which augments CoBF (Pachen et al., 2020).

There is profound activation of cardiac SNA in animal models of HF (Ramchandra et al., 2009; Ramchandra et al., 2008) and this increase is at least partly mediated by the CB chemoreflex (Xing et al., 2014). However, the role of the CB chemoreceptors in regulating CoBF in HF remains unclear. Therefore, the first aim of my study was to examine if the CoBF response to CB activation is altered in HF. I hypothesized that CB activation would result in an attenuated increase in CoBF in conscious animals with HF. I also hypothesized that inhibition of the sympathetic activation to the heart using a β-blocker would attenuate the increase in CoBF.

4.2 Methods

Experiments were conducted on conscious, adult female Romney sheep weighing 50-80 kg, housed in individual crates and acclimatized to laboratory conditions (18ºC, 50% relative humidity, and 12 hour light-dark cycle) and human contact before experimentation. The sheep were fed 2 kg/day (Country harvest pellets), water *ad libitum* and supplemental hay or chaff as needed. All experiments and surgical procedures were approved by the Animal Ethics Committee of the University of Auckland.

4.2.1 *Heart Failure induction*

To induce HF, animals had microspheres infused into their coronary arteries as described previously (Schmitto et al., 2008). Briefly, sheep were fasted for 24 hours prior to surgery and anaesthesia was induced with intravenous propofol (5 mg/kg, i.v.; AstraZeneca, U.K.), and following intubation maintained with 1.5–2.0% isoflurane/oxygen (O_2; Lunan Better Pharmaceutical, China). The induction of HF is described detailed in section 2.2.1 HF Induction in Chapter 2 General methods.

Microembolized sheep underwent transthoracic LV echocardiography when the sheep back to the lab after the holding time (8-10 weeks after the last embolization). The development of HF was assessed by measurement of EF and FS by using short axis M-wave echocardiography on conscious sheep standing on their crate. Once sheep were deemed to have sufficient LV dysfunction (EF < 40%), instrumentation surgery (thoracotomy) was performed.

LV collagen deposition is determined as an indicator of cardiac damage. There was a significant degree of ischemic damage seen in the hearts of HF sheep. The mean collagen content and heart weight of sheep with HF were significantly higher than in the control sheep (Abukar et al., 2019).

4.2.2 *Surgery and anaesthesia protocol*

For these studies, a group of HF (n=6) and control (n=6) adult female sheep (weight: 65±10 kg) were used. The control group were identical to those in chapter 3. There was no difference in age between the two groups of animals. Both groups of animals underwent the same instrumentation surgeries. General anaesthesia administered by an experienced animal technician. Sheep were fasted for 24 hours prior to surgery and anaesthesia was induced with intravenous propofol (5 mg/kg, i.v.; AstraZeneca, U.K.), and following intubation maintained with 1.5–2.0% isoflurane/oxygen (O_2; Lunan Better Pharmaceutical, China). The ventilator settings were tidal volume ~ 10ml/kg, and respiration rate started at ~15 breaths. These will adjust to maintain an ETCO2 of 35-45mmg. Bupivacaine-Claris solution (2.5mg/Ml, i.m.; Multichem NZ Ltd, New Zealand) injection was given into the second to sixth intercostal spaces as a nerve block to prevent surgical pain. Ketoprofen (2 mg/kg, i.m.; Merial, Boehringer Ingelheim, NZ) and long-acting Oxytetracycline (20 mg/kg i.m.; Oxytetra, Phenix, NZ) were used for premedication for all sheep

4.2.3 *Surgical instrumentation*

After thoracotomy, a small area of the proximal left circumflex artery was dissected free and a size 6 transonic flow probe (6PS, Transonic Systems, USA) was positioned around the vessel to measure coronary flow. A size 28 transonic flow probe (28PS, Transonic Systems, USA) was also placed around the ascending aorta to measure CO. Two strips of seven-stranded Cooner Wires (AS 633-7SSF, Cooner Wire, CA, USA) were implanted into the diaphragm and secured with silicone gel to measure dEMG. A pacing lead was also attached to the left atrium to enable pacing of the heart. Up to six electrodes were implanted into the left cardiac sympathetic nerve, ensuring that the tip was positioned in the centre of the sympathetic nerve. Following this, the incision site was closed and negative pressure restored to the thoracic cavity.

During the same surgery, an incision was made in the neck to expose the common carotid artery and the jugular vein. A cannula was inserted into the common carotid artery (with the tip of the cannula lying 1 cm proximal to the carotid sinus region) and jugular vein for the drug and saline infusion. In addition, a sterile solid-state pressure catheter (Mikro-Tip, Millar, U.S.A.) was inserted in the same carotid artery but towards the heart for the measurement of arterial BP.

4.2.4 *Experimental protocols*

The experiments were performed on conscious sheep at least 48 h after the instrumentation surgery. Experiments were started after recording 30 minutes of baseline cardiovascular variables, the CB chemosensitivity was assessed using KCN (Sigma-Aldrich, Germany) dissolved in 0.9% sodium chloride solution (Baxter, U.S.A.) injected as an intra-carotid bolus dose (via the common carotid cannula) at 10, 20, and 30 μg/kg followed by 5 ml heparinized saline (25 IU heparin in 1L saline). Before each set of KCN injection was carried out, 5ml of saline at room temperature was injected into the carotid artery as a control and the effects on haemodynamic parameters were examined. To eliminate the contribution of altered metabolic demand on CoBF, the heart was paced at a constant rate and repeated all three doses of KCN injection. The left atrium was paced at a constant rate 10-15 bpm higher than the spontaneous sinus rate using the Grass stimulator (Grass SD9 stimulator; Grass Instruments, U.S.A).

The haemodynamic response to CB activation were determined following cholinergic blockade with intravenous atropine (8 mg bolus followed by 24 mg/h infusion for 30 minutes; LKT Labs, U.S.A.) and β-adrenergic receptor blockade with propranolol (30 mg bolus followed by 0.5 mg/kg/h infusion for 90 minutes; Merck, Germany). Atropine and propranolol studies were done on different days with KCN induced responses. Following drug infusion, the effect of CB activation was repeated with the three KCN doses in all studies. For the study of

propranolol and atropine effects, comparisons were made with pacing done at the same level of HR in both control and drug conditions.

Briefly, each sheep had baseline stabilization, saline control, and 3 doses KCN with non-paced and paced, atropine infusion for 30 minutes with saline control and 3 doses KCN in non-paced and paced on day one and propranolol on the next day with similar KCN doses of pre and during propranolol infusion. KCN testing during atropine and propranolol infusion was performed 5 minutes before running out of the drug infusions.

The response of cardiovascular variables to CB activation was determined as absolute changes of MAP and breathing response in response to intra-carotid KCN (10, 20, and 30 μg/kg) injection. Each KCN injection was given at least 2 minutes apart and when HR and BP were stable. Care was taken to avoid any distraction which may have caused changes in baseline recording. To determine the effect of CB activation, the absolute change of each cardiovascular variable in response to intra-carotid KCN over a 60 second period was compared to its respective 15-second average immediately before the injection of KCN bolus. The KCN effect was short-lasting (<60 sec), and repeatable.

Later on, these sheep were used for other experiments, but the KCN testing always occurred approximately 48 hours after the instrumentation surgery without variability in timing between sheep. At the end of the terminal experiment, sheep were euthanized with an overdose of intravenous sodium pentobarbitone (7.5 g; Provet NZ Pty Ltd, New Zealand).

4.2.5 *Haemodynamic Recordings*

MAP was obtained by connecting the carotid artery pressure catheter to a pressure control unit (Millar, pressure control unit, USA); the pressure catheter was connected to the transducer to check the zero point and the value was noted before the surgery. CoBF (1000 Hz),

MAP (100 Hz) and CO (1000 Hz) were recorded on a computer using a CED micro 1401 interface and Spike 2 software (Cambridge Electronic Design, Cambridge, UK). HR was measured from the AP signal. The dEMG electrodes were amplified and band-pass filtered (0.3–3.0 kHz). The analog output was fed into a computer data sampling system (CED Model 1401, Cambridge Electronics Design) and processed by a signal analysis program (Spike 2, Cambridge Electronics Design).

4.2.6 *Haemodynamic Measurements and Analysis*

Data were analysed on a beat to beat basis using custom-written routines in the Spike 2 program. For each heartbeat, the program determined diastolic, systolic, MAP, HR, CoBF, CO and the area of the rectified and integrated (time constant = 20 msec) dEMG signals between diastolic pressures. MAP, CoBF, CO and HR were obtained from the recording and 5 sec averages were obtained at 5 sec intervals and were presented as a time series graph over 75 sec for each animal. The respiratory rate after KCN infusion was calculated manually by visual inspection of the raw dEMG signal. The rectified and integrated dEMG signal with a low-pass time constant of 20ms was computed using a script on Spike2. Data were expressed as change in absolute values with the resting value being that in the 15 sec prior to KCN infusion. Furthermore, CVC (mL/min/mmHg) was calculated by dividing CoBF by the MAP for each heartbeat.

4.2.7 *Statistical Analysis*

Results are expressed as mean ± SD. All statistical analysis was done using SPSS software (SPSS, IBM, New York, NY). For baseline data, an unpaired t-test was used to compare normal vs. HF animals. Unpaired t-tests were used to compare differences in resting haemodynamic variables in response to intravenous drug infusion. The KCN data were assessed using a two-way ANOVA. For time-series data, the dependent variables were MAP, CoBF, CO,

CVC, dEMG, and HR. Simultaneously, the independent fixed factors are time, animal and drug treatment (KCN dose, receptor blockade as relevant). The effects of time, drug, and the interaction effect was examined. A significant result was considered if $P < 0.05$.

4.3 Results

4.3.1 *Resting haemodynamic and cardiovascular variables*

The resting levels of haemodynamic and cardiovascular variables in the control and HF sheep are shown in Table 3. The microembolization procedure resulted in significant decrease in LVEF ($p < 0.001$) and FS ($p < 0.0001$) in HF sheep, after 12–14 weeks. This was associated with a significant decrease in baseline CO compared to control animals. There were no differences in MAP, CoBF and CVC between the groups (Table 3).

Table 3 Resting values for haemodynamic parameters between conscious normal and heart failure sheep.

*Data are represented as mean ± SD. $P \leq 0.05$ (unpaired t-test). * denotes significantly different from basal values. N=6/group.*

	Basal	
	Control	**Heart failure**
Ejection fraction (%)	79±3	39±5*
Fractional shortening (%)	43±2	20±2*
Mean arterial pressure (mmHg)	79±15	78±9
Coronary blood flow (mL/min)	76±37	72±43
Heart Rate (bpm)	101±8	95±10
Coronary vascular conductance (mL/min/mmHg)	1±0.7	0.8±0.5
Cardiac output (L/min)	9.6±1.4	7.6±1.3*
Heart mass (g)	364±20	430±28

4.3.2 *Haemodynamic and breathing responses to CB activation*

A representative raw data trace from a single control and HF animal demonstrating changes in arterial pressure, CoBF, and dEMG in response to intra-carotid KCN (20 μg/kg) are shown in Figure 23. KCN injection resulted in a significant increase in MAP, CoBF, and dEMG in both groups. KCN at 10, 20, and 30 μg/kg caused a dose-dependent increase in MAP, CoBF, CVC, CO, HR, and dEMG (all $p < 0.05$) when the heart was not paced (Figure 24). There was no significant change in MAP, CoBF, and CVC in response to the lowest dose of KCN (10 μg/kg).

While comparing control and HF sheep, intra-carotid KCN infusion at 20 μg/kg led to similar increases in MAP, CoBF, and CVC. There was a significant increase in HR in both groups and a significant increase in CO in the HF group (Figure 25).

To eliminate the effects of the increase in HR and CO which would have activated metabolic vasodilation, the heart was then paced and the effects compared between both groups. Activation of the CB led to an increase in MAP, CoBF, CVC and dEMG in both groups ($p < 0.05$) (Figure 26). Interestingly, the increase in CoBF and CVC was significantly greater in the HF group than the control group ($p<0.05$, interaction term). The increase in CoBF in the control animals occurred within the first 15 seconds of the KCN bolus injection. In contrast, in HF, the CoBF gradually increased after the bolus KCN injection and persisted for a minute. There was no significant difference in the ventilatory response to intra-carotid KCN between the control and HF sheep. Furthermore, there was no change in either HR or CO in either group when the heart was paced (Figure 26).

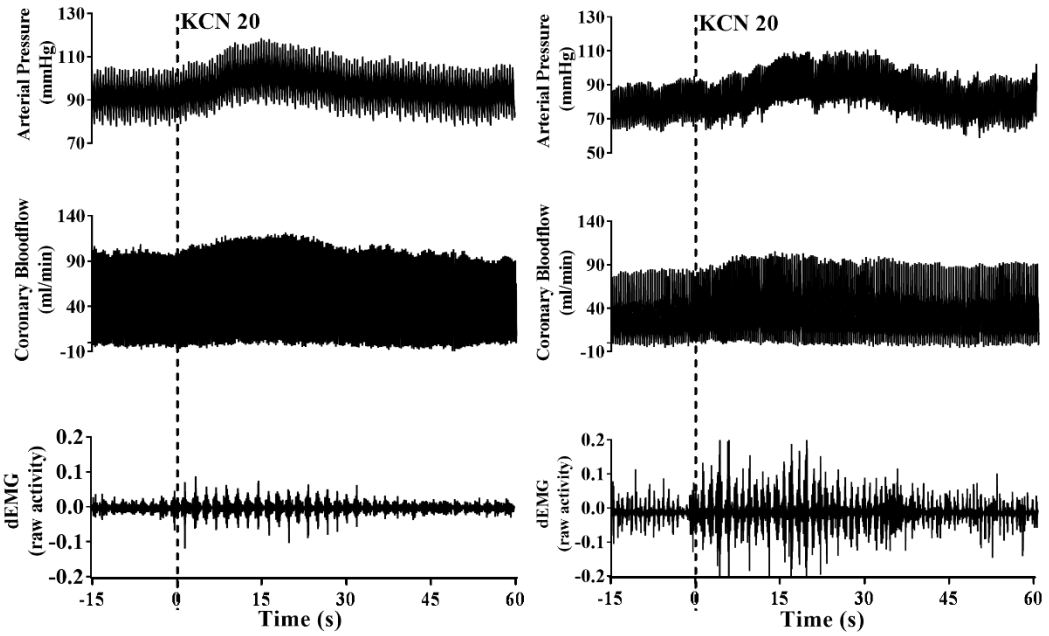

Figure 23 Representative raw traces from one control animal and one heart failure animal.

Raw traces from one control (left) and HF (right) animal demonstrating changes in arterial blood pressure, coronary blood flow, and dEMG in response to intra-carotid potassium cyanide at a dose of 20 μg/kg.

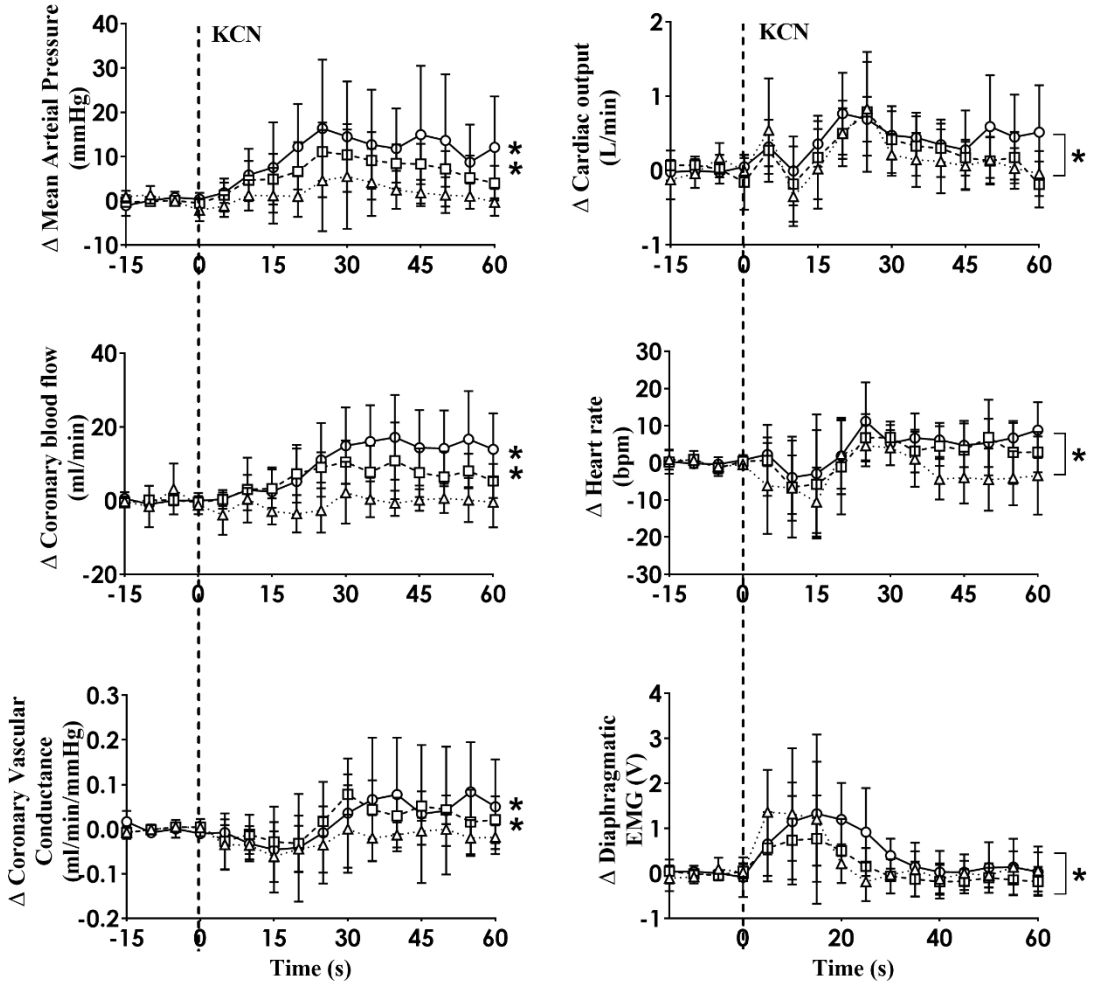

Figure 24 Absolute change in cardiovascular variables in HF group during carotid body activation

*Mean arterial pressure, coronary blood flow, coronary vascular conductance, cardiac output, heart rate and dEMG responses (n=6) to intra-carotid potassium cyanide (KCN; 10 µg/kg (triangles and dotted line), 20 µg/kg (squares and interrupted line), and 30 µg/kg (circles and solid line) injection in sheep with HF. Data are mean ± SD. * - p<0.05 (one-way ANOVA, * - significant time effect across the 60sec recording period,]* - denotes all three doses of KCN showed significant time effect).*

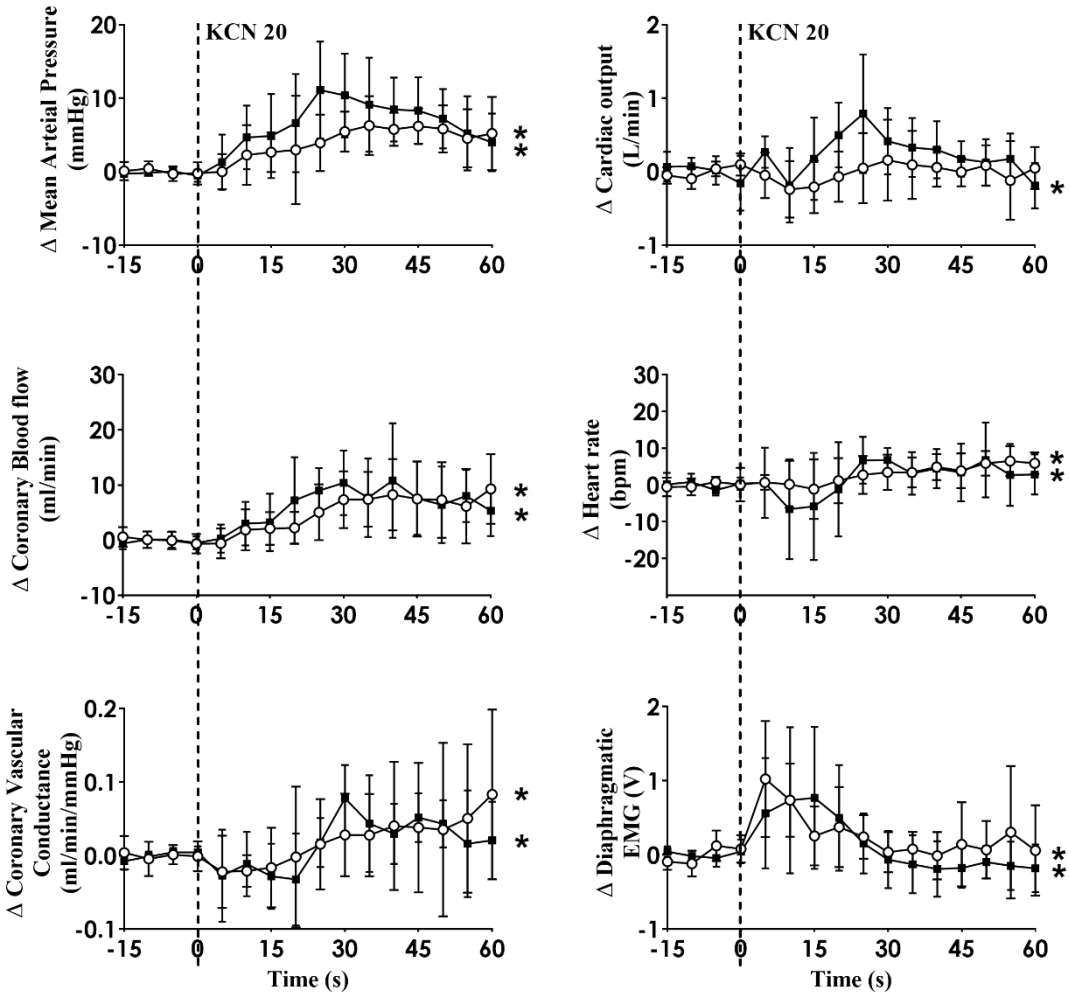

Figure 25 Effect of carotid body activation on breathing and haemodynamic responses in control and HF sheep.

*Absolute change in mean arterial pressure, coronary blood flow, coronary vascular conductance, cardiac output, heart rate, and dEMG in response to intra-carotid potassium cyanide (KCN; 20 μg/kg) injection in control (open circles and solid line), which is the similar group in Chapter 3 and heart failure (filled squares and solid line) sheep (n=6/each group). Results are mean ± SD. * - p<0.05 (one-way ANOVA, * - significant time effect across the 60sec recording period).*

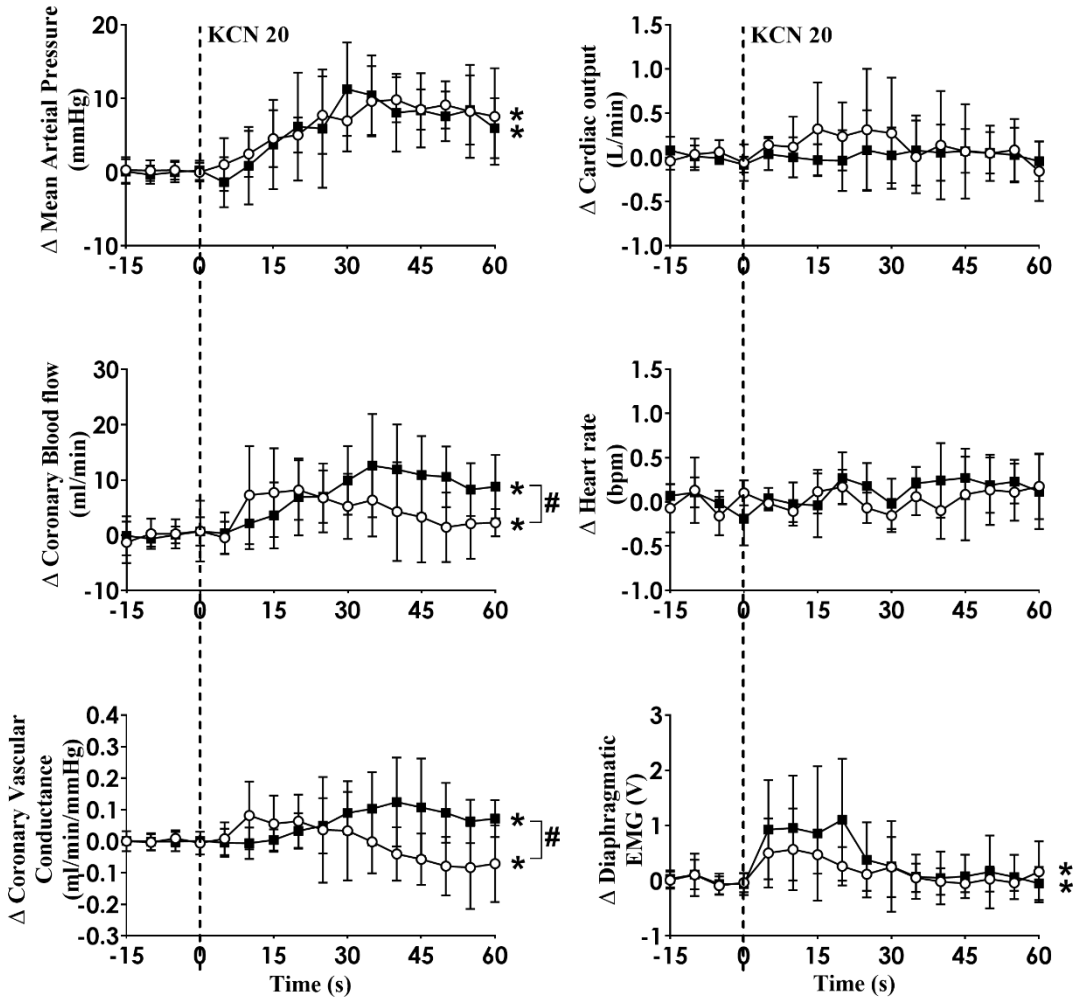

Figure 26 Absolute change in cardiovascular variables in control and HF sheep when the heart was paced.

*Absolute change in mean arterial pressure, coronary blood flow, coronary vascular conductance, cardiac output, heart rate, and dEMG in response to intra-carotid potassium cyanide (KCN; 20 μg/kg) injection in control (n=6) and heart failure (n=6) sheep. Heart was paced at a constant rate such that the heart rate was unchanged. The open circles and solid line represent control, and filled squares and solid line represents HF animals. Results are mean ± SD. * - p<0.05 (one-way ANOVA, * - significant time effect across the 60sec recording period; # - two-way ANOVA, significant interaction effect of time x group).*

4.3.3 *Effect of cholinergic (cardiac vagal) blockade on the cardiovascular variables to CB stimulation*

As shown in Table 4, atropine infusion resulted in significant haemodynamic changes in control and HF sheep (Table 4) such as increased basal MAP (control: from 76±15 to 86±14 mmHg; $p<0.05$, HF: from 76±8 to 84±9 mmHg; $p<0.05$) and HR (control: from 107±4 to 124±16 bpm; $p<0.05$, HF: from 84±9 to 111±15 bpm; $p<0.05$). In the control sheep, CoBF (from 79±37 to 88±41 bpm; $p<0.05$) was also increased significantly, and there seemed a strong trend for this to increase in the HF sheep. All the other variables were unchanged after atropine infusion. Following intravenous atropine infusion, the MAP response to intra-carotid KCN injection was significantly attenuated ($p<0.05$), as observed in the control sheep. There were no significant differences in response observed between pre and during atropine infusion in other variables (Figure 27).

Table 4 Effect of intravenous atropine infusion on resting haemodynamic variables in control and HF sheep.

*The left panel indicates the effect of intravenous atropine infusion on resting haemodynamic variables in control sheep. The right panel indicates the effect of intravenous atropine infusion in heart failure sheep. Data are represented as mean ± SD. P ≤ 0.05 (paired t-test). * denotes significantly different from basal values*

	Control		**Heart failure**	
	Basal	After Atropine	Basal	After Atropine
Mean arterial pressure (mmHg)	76±15	86±14*	76±8	84±9*
Coronary blood flow (mL/min)	79±37	88±41*	82±40	95±68
Heart Rate (bpm)	107±5	124±16*	84±9	111±15*
Coronary vascular conductance (mL/min/mmHg)	1±0.7	1±0.6	0.8±0.5	0.9±0.7
Cardiac output (L/min)	9.6±1.4	8.6±2.3	7.6±1.3	7.5±2.5

.

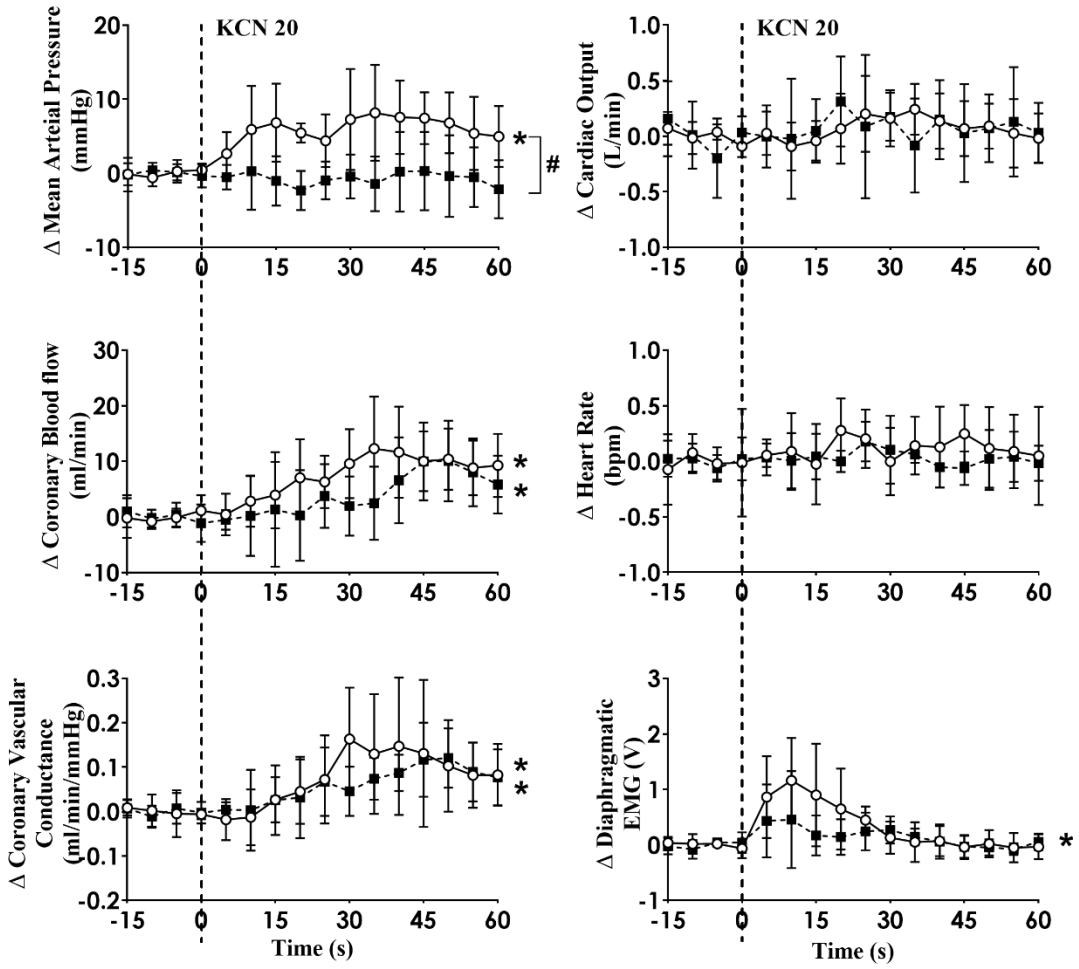

Figure 27 Absolute change in cardiovascular variables to carotid body activation before and after muscarinic receptor blockade in sheep with HF.

*CB activation before and after atropine sulfate (8 mg bolus followed by 24 mg/h infusion for 30 minutes) in conscious sheep with heart failure. The heart was paced at a constant rate such that the heart rate was unchanged. The open circles and solid line represent before atropine, and filled squares and interrupted line is after atropine responses. Results are mean ± SD. * - $p<0.05$ (one-way ANOVA, * - significant time effect across the 60sec recording period; # - two-way ANOVA, significant interaction effect of time x group).*

4.3.4 *Effect of adrenergic (cardiac sympathetic) blockade on the cardiovascular variables to CB stimulation*

Infusion of propranolol significantly decreased basal MAP in both groups (control: from 77±15 to 70±14 mmHg; $p<0.05$, HF: from 86±14 to 79±17 mmHg; $p<0.05$) as shown in the first (control) and second (HF) column of Table 5. There was a significant decrease in HR in the HF group while there was no significant change in HR in the control group (interaction effect, $p<0.05$).

In HF, sheep with HR fixed by pacing, prior to β-blocker, KCN injection resulted in significant increases in MAP, CoBF, CVC and dEMG (open circles and solid line; all $p<0.05$). Similar KCN-induced responses were observed after propranolol infusion with no significant differences between the pre- and during propranolol data during pacing condition (Figure 28).

Table 5 Effect of intravenous propranolol infusion on resting haemodynamic variables in control and HF sheep

*The left panel indicates the effect of intravenous propranolol infusion on resting haemodynamic variables in control sheep. The right panel indicates the effect of intravenous propranolol infusion in heart failure sheep. Data are represented as mean ± SD. $P \leq 0.05$ (paired t-test). * denotes significantly different from basal values.*

	Control		**Heart failure**	
	Basal	After Propranolol	Basal	After Propranolol
Mean arterial pressure (mmHg)	77±15	70±14*	86±14	79±17*
Coronary blood flow (mL/min)	82±32	81±29	75±32	71±27
Heart Rate (bpm)	101±8	96±10	97±8	88±4*
Coronary vascular conductance (mL/min/mmHg)	1±0.7	1±0.6	0.8±0.6	0.7±0.6
Cardiac output (L/min)	9.4±1.5	9.4±1.5	7.2±1.2	8.1±2.0

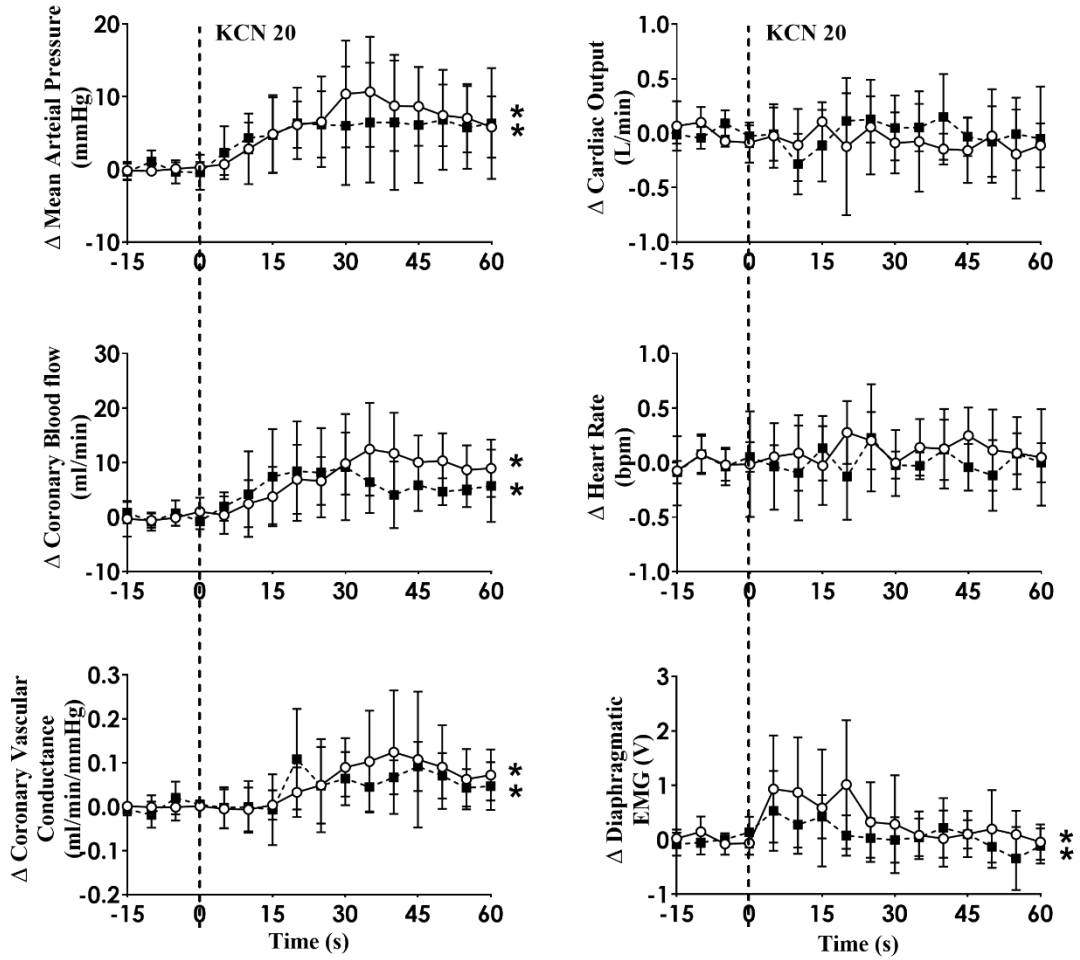

Figure 28Absolute change in haemodynamic variables to CB activation before and after ß-adrenergic receptor blockade in HF sheep.

*CB activation before and after propranolol (30 mg bolus followed by 0.5 mg/kg/h infusion for 90 minutes) in conscious sheep with heart failure. The heart was paced at a constant rate such that the heart rate was unchanged. The open circles and solid line represent the KCN response before propranolol infusion, and filled squares and interrupted line is after propranolol infusion. Results are mean ± SD. * - p<0.05 (one-way ANOVA, * - significant time effect across the 60sec recording period).*

4.4 Discussion

Our study is one of the first to investigate the regulation of CoBF by the carotid bodies in an animal model of HF. The main findings from this study are: 1) Activation of the carotid bodies increases CoBF and CVC in both normal and HF sheep. The increase in both CoBF and CVC is significantly enhanced in the HF group compared to the control group 2) Inhibition of muscarinic mechanisms using atropine abolished the MAP response to CB activation in HF similar to that reported in control animals previously. 3) Unlike the situation in normal control sheep where b-blockade attenuates the CoBF and CVC rises, in HF sheep, these rises persist in the face of b-blockade, suggesting these rises are not medicated by sympathetic activity in the HF state.

4.4.1 *The arterial pressure responses to CB activation in control and HF*

The mammalian CB consists of clusters of parenchymal chemoreceptor glomus (type I) cells which are innervated through the carotid sinus nerve by sensory afferent nerve terminals whose chemo-afferent cell bodies lie in the petrosal ganglion (Gonzalez et al., 1994). The sensitivity of the chemoreflex has been shown to be elevated in patients with HF (Schultz et al., 2007a) and animal models of HF (Del Rio et al., 2013b; Sun et al., 1999a) and interruption of the chemoreflex (Marcus et al., 2014b; Xing et al., 2014) reduces sympathetic nerve activity to the heart and the kidney and also improves autonomic dysfunction and ventilatory instability (Marcus et al., 2014b; Xing et al., 2014). I have previously shown that activation of the CB in the conscious state leads to an increase in MAP. Given the evidence of heightened chemoreflexes in HF, I hypothesized that CB activation would result in greater increases in MAP.

Contrary to my hypothesis, activation of the CB led to similar increases in MAP in the HF group compared to the control group. It is known that sympathetic drive to various organs is elevated in HF (Del Rio et al., 2013b; Grassi et al., 1995; Ramchandra et al., 2018; Sun et al., 1999a; Xing et al., 2014) and this may be one explanation as to why CB activation did not increase MAP to higher levels in HF. While CSNA electrodes were implanted, the signal-to-noise ratio of cardiac SNA were not good enough to decipher changes. As a result, I cannot determine the cardiac SNA response to CB activation in this group of HF sheep. It is possible that inflammation between the implanted electrodes and nerves could be causing the low signal-to-noise ratio of these SNA signals. It is also worth noting that only one CB was activated in my study; it is possible that stimulating both CBs might reveal greater pressor responses in the HF group.

There was no significant difference in the effects of KCN activation on ventilation between the two groups. It is important to note that I examined the inspiratory effort from the dEMG signal and not tidal volume *per se* so I cannot comment on whether tidal volumes may be different between the two groups.

4.4.2 *The CoBF responses to CB activation in control and HF animals*

I have previously shown that in conscious normal sheep, CB activation increases directly recorded cardiac SNA and CoBF (Pachen et al., 2020). I concluded that the β2-adrenergic vasodilatory actions supersede the alpha receptor vasoconstriction during reflex sympathetic activation and are responsible for the coronary vasodilation. This led us to hypothesize that the coronary flow response would be greater in the HF group. When the CoBF responses to CB activation were compared without accounting for metabolic vasodilation, there were no differences between the two groups (Fig 3). When the heart was paced at a steady rate, I could eliminate the effects of metabolic vasodilation and in this scenario, I observed a significantly

enhanced CoBF response during CB activation in the HF sheep. The increase in CoBF and CVC was delayed and remained elevated for a longer time period after CB activation (Fig 4). To the best of our knowledge, this is the first time that the effects of CB activation on CoBF have been examined in a conscious model of HF. My data indicate that activation of the CB leads to a greater increase in CoBF.

4.4.3 *Effect of propranolol on carotid chemoreceptor stimulation*

It is well established that autonomic imbalance with an increase in sympathetic activity and withdrawal of parasympathetic activity is a common finding in HF (Ponikowski et al., 2001; Sun et al., 1999a). In my present study, intravenous propranolol injection decreased HR in sheep with HF more than in the control group (Table 5). This implies that cardiac SNA in the HF animals is maintaining HR to a greater extent compared to control animals.

Intravenous propranolol infusion caused a significant decrease in basal MAP in both groups, suggesting a small but significant role of sympathetic drive to the heart in maintaining BP in these sheep. I hypothesized that the coronary flow response would be mediated by β2-adrenergic vasodilation similar to the normal animals. Contrary to my hypothesis, blockade of beta-receptors did not alter the coronary vasodilation in the HF sheep indicating the vasodilation is mediated by other mechanisms (Fig 6).

4.4.4 *Effect of atropine on carotid chemoreceptor stimulation*

Previous papers have observed that carotid chemoreflex stimulation by nicotine causes coronary vasodilation in conscious control animals mediated by parasympathetic cholinergic efferent fibers (Hackett et al., 1972; Shen et al., 1994) although this is to contrast to my previous study (Pachen et al., 2020). In the present study, the increased CoBF in both control and HF sheep in response to CB stimulation was unchanged following intravenous atropine infusion.

This implies that CB induced coronary vasodilation in HF sheep is not mediated through a cholinergic pathway involving muscarinic acetylcholine receptors. Interestingly, the pressor response to CB activation was attenuated post atropine in the HF group of animals similar to the control animals (Chang et al., 2020; Pachen et al., 2020). The site of action of the atropine is not clear and may include actions on the afferent nerve terminal or given the ability of atropine to cross the blood-brain barrier (Proakis et al., 1979), the rostral ventrolateral medulla (RVLM).

In the group of animals with HF, neither sympathetic blockade nor parasympathetic blockade altered the increase in CoBF seen during CB activation. As such, the mechanism of the increase in CoBF remains unclear. One possibility is that the parasympathetic nerves have been shown to play a coronary vasodilatory role via other neurotransmitters such as vasoactive intestinal peptide (Feliciano et al., 1998b). I cannot rule out that the parasympathetic nerves may still play a role but mediated via neurotransmitters other than acetylcholine.

In summary, my findings indicate that in sheep with HF, CB activation causes an increase in CoBF and CVC which is augmented compared to the response in normal animals. Interestingly, the increase in both CoBF and CVC was not mediated by sympathetic pathways, in contrast to normal animals where the increase in CoBF was inhibited by β-blocker suggesting it is mediated by increased cardiac SNA. My data indicate that in an ovine model of HF, the CB plays an important role in maintaining blood supply to the heart. Further studies are required to explain the possible mechanisms responsible for CB activation induced increases in CoBF in HF.

Chapter 5: Effect of hyperoxia in conscious control and heart failure sheep

5.1 Introduction

In previous chapters (Chapter 3 and chapter 4), CB chemosensitivity was assessed by measuring the ventilatory response, as well as the cardiac SNA, HR and BP response to unilateral intra-carotid KCN injection. These results indicated that stimulation of CBs increases CoBF and CVC in both the control and HF groups, and the response was significantly greater in HF group. My data in terms of the CVC response is in agreement with previous studies that CB chemosensitivity is elevated in animal models and patients with HF (Del Rio et al., 2013b; Schultz et al., 2007a; Sun et al., 1999a). Interestingly, the pressor response to KCN was not altered in the HF group.

In addition to activation of the CB reflex, previous studies have examined the tonic contribution of the CB by either ablation of the carotid sinus nerve or brief hyperoxia / supplemental oxygen (Dejour's effect) to inhibit the peripheral chemoreflex (Duffin, 2007; Ponikowski et al., 1997; Xing et al., 2014). In this context, recent studies have shown that CB ablation or denervation decreases renal SNA in both animal models of HF (Del Rio et al., 2013a; Marcus et al., 2014b) and spontaneously hypertensive rats (Abdala et al., 2012; McBryde et al., 2013). My study in conscious control sheep showed that CB stimulation increased cardiac SNA and increased CoBF (Pachen et al., 2020) suggesting that the CB plays an essential role in modulating blood flow to the heart. However, the tonic contribution of the CB chemoreceptors to either MAP or CoBF in control and HF is unknown.

Therefore, the focus of this chapter was to investigate whether CB inactivation via hyperoxia led to changes in CoBF. I hypothesized that hyperoxia would cause a reduction in CoBF in both the control and HF groups.

5.2 Methods

Experiments were conducted on conscious, adult female Romney sheep weighing 50-80 kg, housed in individual crates and acclimatized to laboratory conditions (18ºC, 50% relative humidity, and 12 hour light-dark cycle) and human contact before experimentation. The sheep were fed 2 kg/day (Country harvest pellets), water *ad libitum* and supplemental hay or chaff as needed. All experiments and surgical procedures were approved by the Animal Ethics Committee of the University of Auckland.

5.2.1 *Experimental protocols and haemodynamic recordings*

12 new conscious adult female sheep (6 control and 6 HF) were given a nasal prong to allow supplementation with intranasal oxygen to suppress CB chemoreceptors (Dejour's effect). It was technically very challenging for conscious sheep to wear nasal prongs and keep them stress-free. To avoid this, the animals were acclimatized to having the nasal prongs on for a long time before trying a complete the hyperoxic protocol. Nasal prongs were tried on the sheep for 1-2 hours for 2 days before the experimentation, which was similar in all sheep. An oxygen cylinder (size $D_{2,}$ BOC) was connected to the other end of the nasal prongs and the oxygen dose manually changed.

After placing the nasal prong (Hudson RCI®, Teleflex 1108), baseline cardiovascular variables such as MAP, CoBF, CVC, CO, HR and dEMG were recorded for at least 30 minutes and the hyperoxia effect was assessed using supplemental oxygen at 1L, 2L, and 4L/min, each for 20 minutes duration. This was followed by a 30-min recovery period. Arterial blood was collected from the common carotid artery cannula while sheep breathed room air and supplemental oxygen (Figure 29) for the arterial blood gas analysis. The blood was collected with a 1ml heparinized syringe (1 mL BD™ Luer Slip Tip Syringe, NJ, USA) (to prevent

clotting) 15 minutes after 4L oxygen started. With a blood gas analysis, partial pressures of oxygen (Po_2) and carbon dioxide (Pco_2) and pH were measured using an arterial blood gas radiometer (ABL800 FLEX blood gas analyser, Australia). CoBF (1000 Hz), CO (1000 Hz) and AP (100 Hz) were recorded as previously described (Chapter 4).

5.2.2 *Statistical Analysis*

Results are expressed as mean ± SD. All statistical analysis was done using SPSS version 25 (SPSS, IBM, New York, NY). Paired t-tests were used to compare between room air and 100% oxygen. Comparison between baseline values in control and HF subjects was performed by unpaired t tests (two tailed). For time series data, the dependent variables were MAP, CoBF, CO, CVC, dEMG and HR while the independent fixed factors are time, animal and supplemental oxygen. The effects of time, supplemental oxygen and the interaction effect was examined. A significant result was considered if $P < 0.05$.

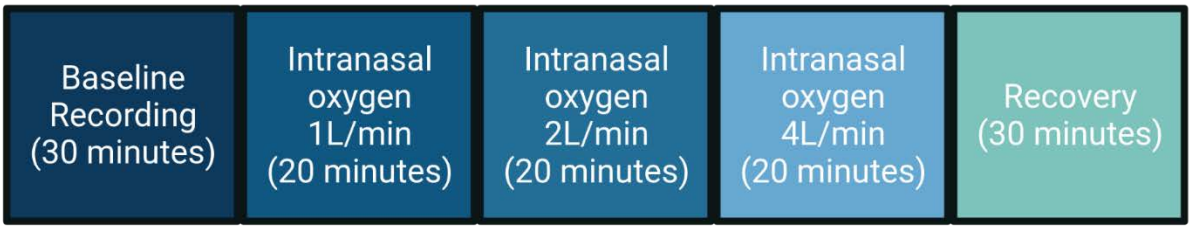

Figure 29 Experimental protocol for hyperoxia on CoBF and haemodynamic variables in control and HF sheep.

5.3 Results

5.3.1 *Resting hemodynamic and cardiovascular variables*

The resting levels of hemodynamic and cardiovascular variables in control and HF sheep are shown in Table 6. There was a significant decrease in LVEF ($p < 0.001$) and FS ($p < 0.0001$) in HF sheep associated with a significant reduction in baseline CO compared to control animals. There were no differences in any other variables between the groups (Table 6).

5.3.2 *Effect of hyperoxic deactivation of CB chemoreceptors on cardiovascular variables*

To determine the effect of hyperoxia, a group of control (n=6) and HF (n=6) were administered with intranasal supplemental oxygen at 1L, 2L, and 4L/min, each for 20 minutes duration. Hyperoxia results in a significant increase in the arterial partial pressure of oxygen (PaO_2) in control and HF sheep, shown in Table 7. There was a significant decrease in MAP ($p<0.001$) and CoBF ($p<0.001$) in the HF group and a substantial reduction in CVC ($p<0.001$) in the control group during intranasal supplemental oxygen (Figure 30). Administration of oxygen reduced CO significantly in the control and HF groups. Moreover, HR and breathing response (dEMG) was significantly lower (Figure 30) in response to the hyperoxia in the HF group, suggesting an inhibition of the CB chemoreceptors by supplementing hyperoxia in conscious sheep.

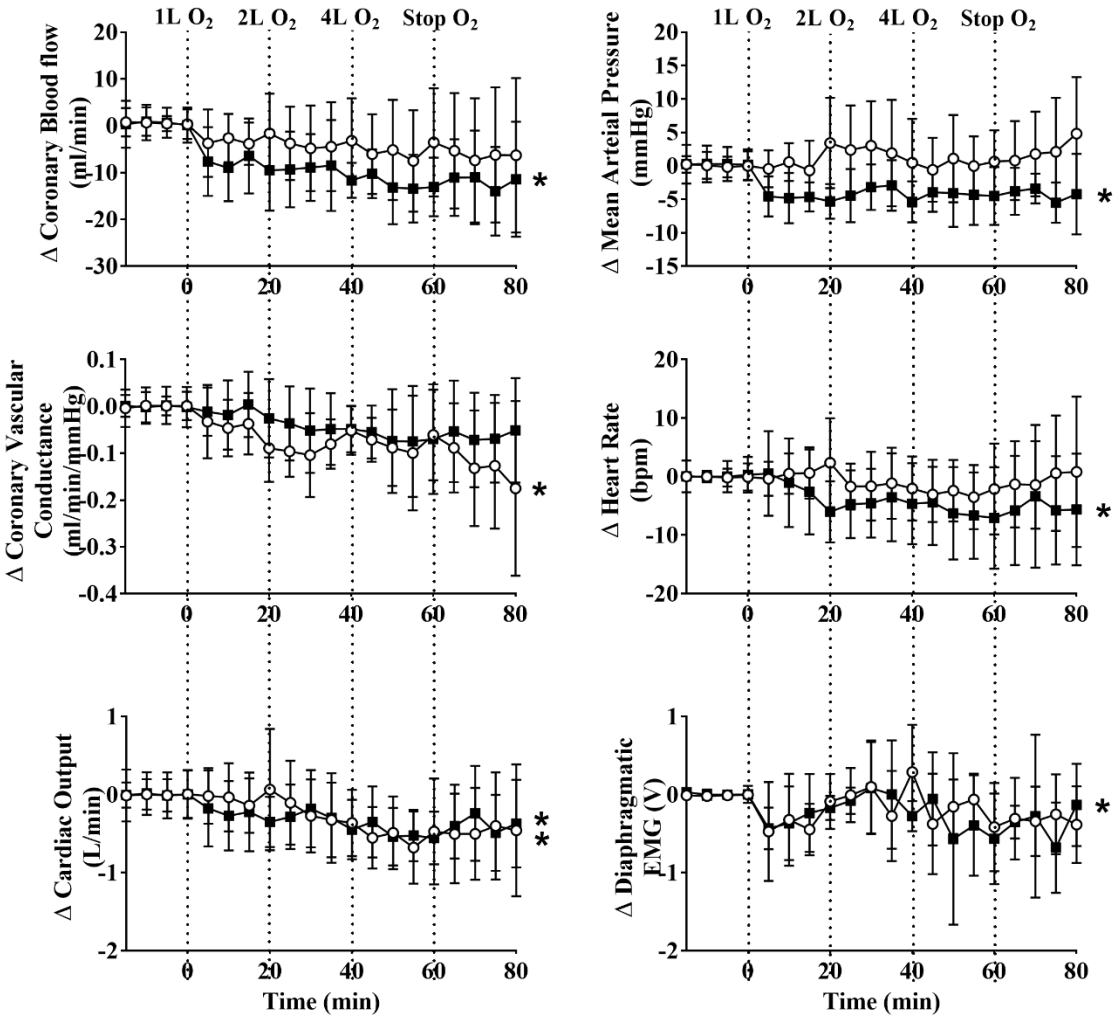

Figure 30 Absolute change in haemodynamic variables to hyperoxia in conscious control and HF sheep.

*The open circles and solid line represent the hyperoxia (1L, 2 L, 4L/minutes, each for 20 minutes duration) effect on control sheep, and filled squares and solid line represent hyperoxia on HF sheep. Results are mean ± SD. * - p<0.05 denotes a significant effect of time (one-way ANOVA, * - significant time effect across the 80mins recording period).*

Table 6 Resting values for haemodynamic parameters between conscious normal and heart failure sheep

*Data are represented as mean ± SD. $P \leq 0.05$ (unpaired t-test). * denotes significantly different from basal values.*

	Basal	
	Control	**Heart failure**
Ejection fraction (%)	79±3	37±5*
Fractional shortening (%)	42±2	18±2*
Mean arterial pressure (mmHg)	85±15	87±9
Coronary blood flow (mL/min)	78±37	72±43
Heart Rate (bpm)	101±8	96±10
Coronary vascular conductance (mL/min/mmHg)	0.9±0.7	0.8±0.5
Cardiac output (L/min)	9±2	7.6±1.3*

Table 7 Arterial blood gas values in conscious control and HF sheep.

*The right panel shows the pH, arterial partial pressure of oxygen (PaO_2), the arterial partial pressure of carbon dioxide ($PaCO_2$) in the conscious HF group during room air, and the hyperoxic state. The left panel shows blood gas values in the control group during room air and hyperoxic state. Data are represented as mean ± SD. $P \leq 0.05$ (paired t-test). * denotes significantly different from room air.*

	Control		**Heart failure**	
	Room air	Hyperoxia	Room air	Hyperoxia
pH	7.5±0.05	7.5±0.01	7.5±0.04	7.4±0.01
PaO_2 (mmHg)	90±5	148±13*	90±7	150±6 *
$PaCO_2$ (mmHg)	38±9	37±2	32±5	33±4

5.4 Discussion

The main finding of this study is that hyperoxia caused a significant reduction in CoBF and HR in the HF group, along with a significant decrease in MAP, CO, and dEMG. There was a fall in CVC which was not significant. CVC and CO were significantly decreased in the control group with a clear for decreased CoBF and dEMG, but this was not statistically significant.

In recent years, there has been mounting evidence demonstrating the potential adverse effects of hyperoxia on the cardiovascular system (Sepehrvand et al., 2016; Smit et al., 2018). Studies in patients using ultrasound (Momen et al., 2009), intracoronary Doppler flow wire and coronary angiography (McNulty et al., 2005) have indicated coronary vasoconstriction during hyperoxia which may help explain the finding of adverse outcomes following hyperoxia. My findings using direct recordings of CoBF support these previous findings using non-invasive indirect measures of CoBF and re-iterate that hyperoxia can decrease CoBF in the HF group.

The coronary vasoconstriction has been postulated to be a direct vasoconstrictor action of the high oxygen levels at the level of the coronary vasculature (Moradkhan et al., 2010). However, it is important to note that the CB is de-activated during hyperoxia (Dejours effect). Studies in patients with HF suggested that brief hyperoxia inhibits the peripheral chemoreflex (Ponikowski et al., 1997; Trzebski, 1992). As such the change in CoBF may be due to inactivation of the CB chemoreflex. My data in this chapter supports the hypothesis that CB inactivation by hyperoxia causes coronary vasoconstriction in HF.

Experimental studies have shown that the sensitivity of the chemoreflex is elevated in both patients with HF (Schultz et al., 2007a) and animal models of HF (Del Rio et al., 2013b; Sun et al., 1999a). When the sheep were exposed to hyperoxia, I found significant decreases in MAP, CoBF, HR, and breathing response in the HF sheep and a potential fall in CoBF in the control group. This suggests that baseline tonic drive from the CB to these variables is low in

control conditions but is heightened in HF as suggested previously (Ponikowski et al., 2001; Schultz et al., 2013). Given these findings, I speculate that the actions of hyperoxia on CoBF may be mediated in part by inactivation of the CB chemoreflex, and augmentation of the chemosensitivity in HF may be a compensatory mechanism to maintain blood supply to the heart.

I argue that in an ovine HF model, the CB has an important role in maintaining blood supply to the heart. It could be possible that the small group size meant that these studies may have been under-powered and therefore more numbers will be needed for these clear trends to be significant. Further studies are required to explain the possible mechanisms responsible for CB activation induced increases in CoBF in HF as indicated in Chapter 4. Experiments in the pacing induced HF model in rabbits has been shown that hyperoxic inhibition of the chemoreflex decreases resting renal SNA and plasma norepinephrine levels (Sun et al., 1999b). In light of my findings, I hypothesize that there may be a negative impact of abolishing CB afferent input on CoBF, resulting in reduced CoBF in the HF state. This hypothesis remains to be tested.

Chapter 6: Effect of high nasal flow in conscious normotensive and hypertensive sheep

6.1 Introduction

Similar to the HF state, the CBs have been identified as a potential therapeutic target for treating HTN (McBryde et al., 2017; Paton et al., 2013). Studies utilizing acute hyperoxia in young hypertensive subjects demonstrate a marked reduction in arterial BP mediated by a significant reduction of peripheral vascular resistance (Izdebska et al., 1998). Similar results have been reported after chemoreflex inhibition in young patients with borderline HTN or a family history of HTN (Tafil-Klawe et al., 1985). Similar to studies in human patients, evidence from animal studies also indicates that the CB chemoreceptors play an important role in driving chronic increases in sympathetic nerve activity, leading to increased total vascular resistance and MAP (Pijacka et al., 2016b). A previous study form our lab in hypertensive sheep showed that CB stimulation increases MAP and reduces RVC (Chang et al., 2020). Importantly, when the carotid sinus nerve was cut, there was a significant decrease in BP further confirming that the CB chemoreceptors maintain BP in HTN. This has led to attempts to inhibit CB activity using pharmacological approaches.

Dyspnea is a major problem in patients with cardiovascular disease (Stevens et al., 2018). To circumvent this, conventional oxygen therapy is a standard first-line strategy where oxygen is delivered through a nasal cannula or nasal mask (O'driscoll et al., 2008). My previous study in conscious sheep with HF indicated that conventional supplemental oxygen therapy leads to substantial reductions in MAP ($p<0.05$), CoBF ($p<0.05$), and intensity of breathing (dEMG) ($p<0.05$) (Chapter 5). I concluded that inhibition of the hyperactive CB chemoreceptors in HF reduces MAP. Whether this action of hyperoxia is a direct action of oxygen on the vasculature or an action via the CBs has been debated previously. Any putative positive effects of inhibition of CB chemoreceptors using hyperoxia could be offset by a direct action of oxygen on the vasculature.

To circumvent this, previous researchers have proposed HNF or continuous positive airway pressure (CPAP) (Pelosi et al., 2010) as an alternative where room air is given such that the effects of high oxygen are negated. Studies in anaesthetized horses have shown that CPAP might be able to increase the partial pressure of oxygen (PaO_2) and therefore improve oxygenation (MacFarlane et al., 2012; Mosing et al., 2011). The problem with CPAP is that it is not well tolerated by patients with HTN (Kario, 2009; Martínez-García et al., 2007). HNF is a new respiratory support therapy that allows for up to 60 litres/min of heated and humidified gas through a wide-bore nasal cannula (Parke et al., 2009). It is commonly used in human patients to treat dyspnea and respiratory failure as an alternative to continuous positive airway pressure (CPAP). Studies in patients have reported that HNF may be beneficial in treating respiratory disease (McGinley et al., 2007) and demonstrated that HNF effects are comparable with nasal continuous airway pressure (Lampland et al., 2009; Saslow et al., 2006). Owing to the small number of studies, no definite conclusions can be drawn regarding any putative beneficial effects of HNF or adverse effects on vascular systems.

Hence, in this study, I examined the response of MAP, RBF, and RVC during continuous HNF in conscious normotensive and hypertensive sheep. I have chosen the 2-kidney, 1-clip model of HTN as I was interested in the response of the non-clipped kidney to HNF. I hypothesized that HNF would decrease MAP in both groups of animals, and the magnitude of decrease would be greater in the hypertensive group. I also hypothesized that HNF would increase RBF and RVC due to a substantial reduction in peripheral vascular resistance associated with decreased MAP.

6.2 Methods

Experiments were conducted on conscious, adult female Romney sheep housed in individual crates and acclimatized to laboratory conditions (18ºC, 50% relative humidity, and 12-hour light-dark cycle) and human contact before experimentation. The sheep were fed 2 kg/day (Country harvest pellets, Farmland co-operative, Christchurch, NZ), water *ad libitum*, and supplemental hay or chaff as needed. All experiments and surgical procedures were approved by the Animal Ethics Committee of the University of Auckland.

6.2.1 *Surgery and anaesthesia protocol*

For these studies, a group of hypertensive (n=5) and normotensive (n=5) adult female sheep were used. All sheep underwent aseptic surgical procedures under general anaesthesia administered by an experienced animal technician. Anaesthesia was induced for both unilateral renal artery clipping and instrumentation surgery. Sheep were starved for 24 hours prior to surgery, and anaesthesia was induced with intravenous propofol (5 mg/kg, i.v.; AstraZeneca, U.K.), and following intubation maintained with 1.5–2.0% isoflurane/oxygen (O_2; Lunan Better Pharmaceutical, China). Ketoprofen (2 mg/kg, i.m.; Merial, Boehringer Ingelheim, NZ) and long-acting Oxytetracycline (20 mg/kg i.m.; Oxytetra, Phenix, NZ) were used for premedication for all sheep. The timeline of surgical procedures and experimentation in normotensive and hypertensive sheep are shown in Figure 31.

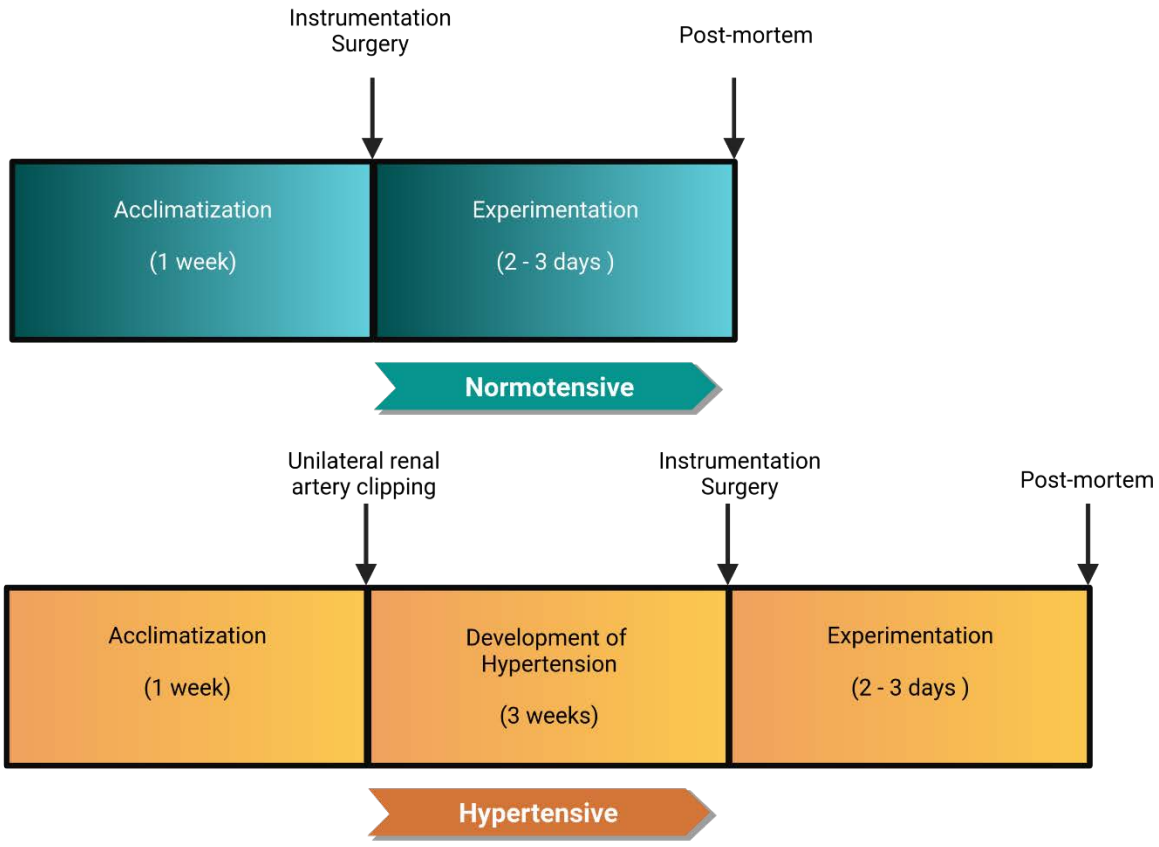

Figure 31 Timeline of surgical procedures and experimentation in normotensive and hypertensive sheep.

6.2.2 *Unilateral Renal Artery Clipping*

HTN was surgically-induced via unilateral constriction of the renal artery (i.e., two-kidney, one-clip model; 2K1C). Briefly, retroperitoneal incisions were made on one side of the flank to expose and isolate the renal artery. The incision was made on the contralateral side to which the renal artery flow probe was placed. A custom-made metal clip was then placed around the renal artery to tightly obstruct the blood flow to ≈40% of original flow. Sheep were left to develop HTN over 3 weeks, as described previously (Tromp et al., 2018).

6.2.3 *Instrumentation surgery*

Under aseptic conditions, normotensive and hypertensive sheep underwent instrumentation surgery. An incision was made over the flank contralateral to the clipped kidney to place an ultrasonic flow probe (6PS, Transonic Systems, USA) around the renal artery to measure RBF. Another incision was made on one side of the neck during the same surgery to expose the common carotid artery. A solid-state pressure catheter (Mikro-Tip, Millar, U.S.A.) was inserted into the common carotid artery. The pressure catheter was inserted towards the heart, with its tip lying within the common carotid artery to measure the BP. Another cannula (outer diameter 1.5 mm) was inserted into the jugular vein for saline infusion.

6.2.4 *Experimental Protocols*

Sheep were given at least 72 hours to recover from the surgical procedures before conducting any experimental protocol. To determine the effect of HNF on cardiac and renal haemodynamic, heated and humidified gas passed through a wide-bore nasal cannula (Optiflow™+ HNF Cannula) that was connected to an AIRVO 2 humidification system (AIRVO™ 2 Fisher & Paykel, Auckland, NZ). All sheep were trained with a nasal cannula for 1-2 hours for 2-3 days prior to the experiments.

The heater plate warms the water, which warms and humidifies the respiratory gas passing through the water chamber, to body temperature and humidity. The respiratory gas leaving the chamber is regulated to a dew-point temperature, normally set to 37 º C (98.6 º F). This water vapour from the water chamber enters the breathing tube through the port on the top of the AIRVO 2 and the respiratory gas was delivered using an Optiflow nasal cannula (Figure 32). After 20-minutes of basal recording, HNF started at 10L/min for 5 minutes, at 20L, 30L, and 40L/min, each for 25 minutes duration. This was followed by a 25-min recovery period.

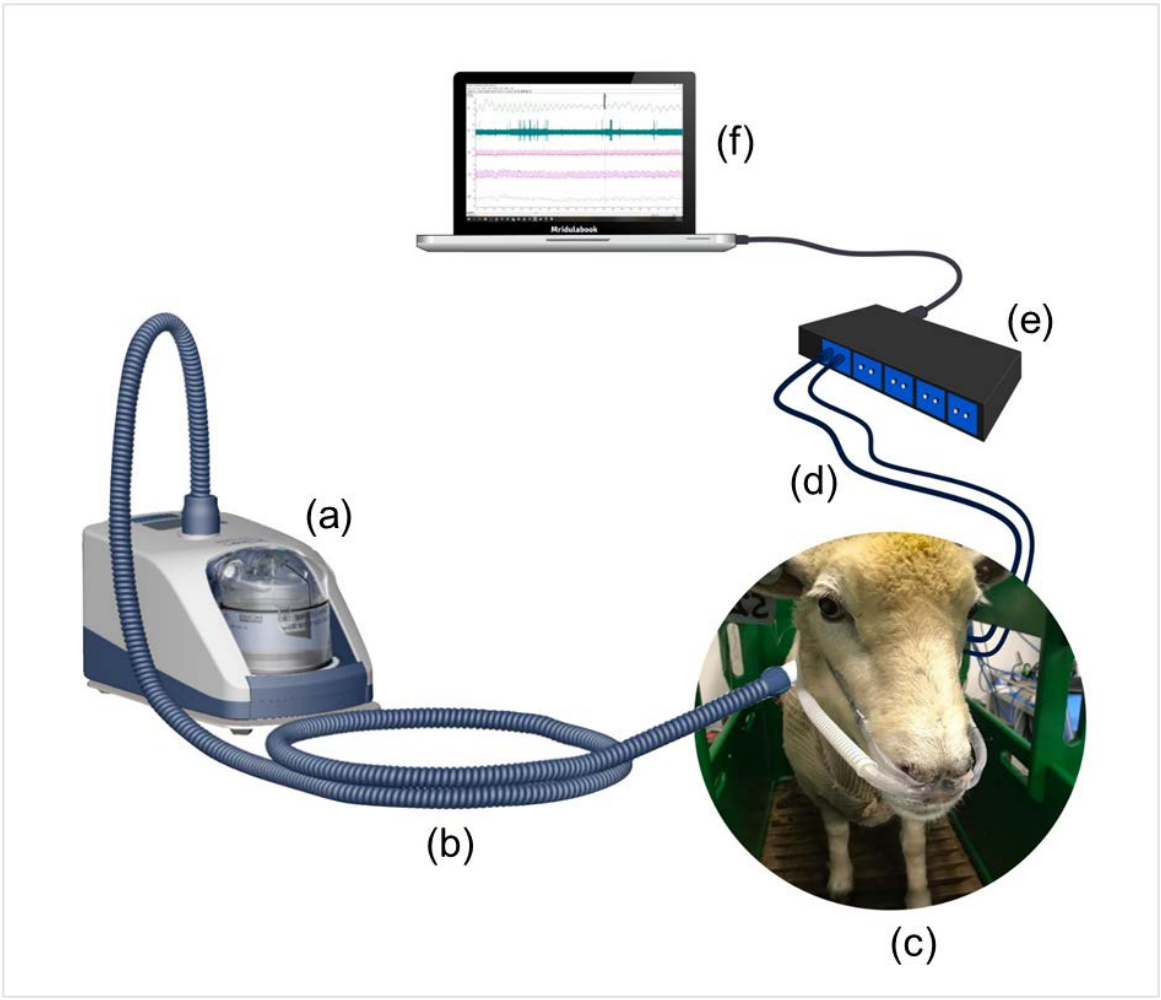

Figure 32 Schematic diagram demonstrating the high nasal flow system set up.

(a) AIRVO 2 humidification system, (b) heated breathing tube, (c) sheep with nasal mask ON, (d) cable connectors, (e) CED micro 1401 interface, (f) computer with spike 2 software.

6.2.5 *Data Acquisition and Analysis*

Haemodynamic and cardiovascular variables were recorded in conscious standing sheep at least 72 hours after the instrumentation surgery to reduce post-surgical stress. BP (100 Hz) and RBF (1000 Hz) were recorded on a computer using a CED micro 1401 interface and Spike 2 software (Cambridge Electronic Design, Cambridge, UK). Data were analysed on a beat-to-beat basis using custom-written routines in the analysis program Spike 2. The program determined diastolic, systolic, MAP, and HR for each heartbeat. RVC (mL/min/mmHg) was calculated by dividing RBF by the MAP. The data from the Spike 2 program was then exported into Microsoft Excel for the following analysis. The analysis has compared the absolute change of each variable in response to HNF over a 1 hour 50 minutes period (includes 25 minutes recovery time) to its respective 20 minutes baseline. 5 minutes averages were taken of the 20 minutes baseline; 90 min HNF administration and 25 min of recovery.

6.2.6 *Statistical Analysis*

Results are expressed as mean ± SD. All statistical analysis was done using SPSS version 25 (SPSS, IBM, New York, NY). ANOVA followed by post hoc (Dunnett's test) analysis were used to compare differences in baseline haemodynamic variables in response to HNF. Comparison between baseline values in normotensive and hypertensive subjects was performed by unpaired t-tests (two-tailed). The effects of time, HNF, and the interaction effect were examined using a two-way ANOVA. For time-series data, the dependent variables were MAP, RBF, RVC, and HR, while the independent fixed factors are time, animal, and HNF. A significant result was considered if $P < 0.05$.

6.3 Results

6.3.1 *Effect of HNF on the cardiovascular variables in normotensive and hypertensive sheep*

Resting haemodynamic variables in conscious normotensive and hypertensive sheep are shown in Table 8. Clipping caused a significant increase in basal MAP in hypertensive sheep compared with normotensive sheep (131±14 vs. 91±13 mm Hg; P <0.001). There was no change in resting RBF, RVC, and HR between normotensive and hypertensive groups (n=5/group). Also, the non-clipped kidney weight in hypertensive sheep was significantly greater than that of either of the two kidneys in the normotensive group (128 ± 23 vs. 93 ± 12 g; P < 0.01).

The haemodynamic variables in response to HNF in conscious normotensive sheep are shown in Table 9, and in conscious hypertensive sheep are shown in Table 10. Figure 33 shows the absolute change in haemodynamic variables in response to the administration of HNF. HNF significantly decreased MAP ($p<0.001$) in the normotensive and hypertensive groups. RVC increased substantially ($p<0.05$) in response to HNF in both groups of conscious sheep (Figure 33). Although there was a slight increase in RBF in both groups when starting the 20L HNF condition, the changes were not significant throughout the HNF administration. There was no change in HR in the hypertensive group, but there was a substantial decrease in HR in the normotensive group ($p<0.01$) (Figure 33).

Table 8 Resting haemodynamic measurements in conscious normotensive and hypertensive sheep.

*Data are represented as mean ± SD. P ≤ 0.05 (unpaired t-test). * denotes significantly different from normotensive group.*

	Normotensive	**Hypertension**
Mean arterial pressure (mmHg)	91±13	131±14*
Renal blood flow (mL/min)	406±158	714±295
Renal vascular conductance (mL/min/mmHg)	4.6±1.8	5.4±2.1
Heart Rate (bpm)	99±16	101±23
Kidney weight (gm)	93±12	128±23*

Table 9 Levels of resting haemodynamic measurements during HNF in normotensive sheep.

*Mean arterial pressure, renal blood flow, renal vascular conductance, and heart rate in conscious normotensive sheep during room air and after each litre of nasal high flow administration. Data are represented as mean ± SD. P ≤ 0.05 (ANOVA followed by post hoc Dunnett's test). * denotes significantly different from the room air*

	Normotensive				
	Room air	10L HNF	20L HNF	30L HNF	40L HNF
Mean arterial pressure (mmHg)	91±13	88±14	86±14*	85±12*	85±9*
Renal blood flow (mL/min)	406±158	406±161	404±159	414±149	418±139
Renal vascular conductance (mL/min/mmHg)	4.6±1.8	4.7±1.9	4.8±1.9	5.0±1.8*	5.0±1.7*
Heart Rate (bpm)	99±16	97±16	93±14*	95±16	93±16*

Table 10 Levels of resting haemodynamic measurements during HNF in hypertensive sheep.

Mean arterial pressure, renal blood flow, renal vascular conductance, and heart rate in conscious hypertensive sheep during room air and after each litre of nasal high flow administration. Data are represented as mean ± SD.

	Hypertension				
	Room air	10L HNF	20L HNF	30L HNF	40L HNF
Mean arterial pressure (mmHg)	131±14	130±13	121±8	118±6	119±10
Renal blood flow (mL/min)	714±295	717±312	719±295	752±335	741±305
Renal vascular conductance (mL/min/mmHg)	5.4±2.1	5.5±2.5	6.1±2.8	6.5±3.1	6.4±3.1
Heart Rate (bpm)	101±23	100±24	97±24	98±27	96±24

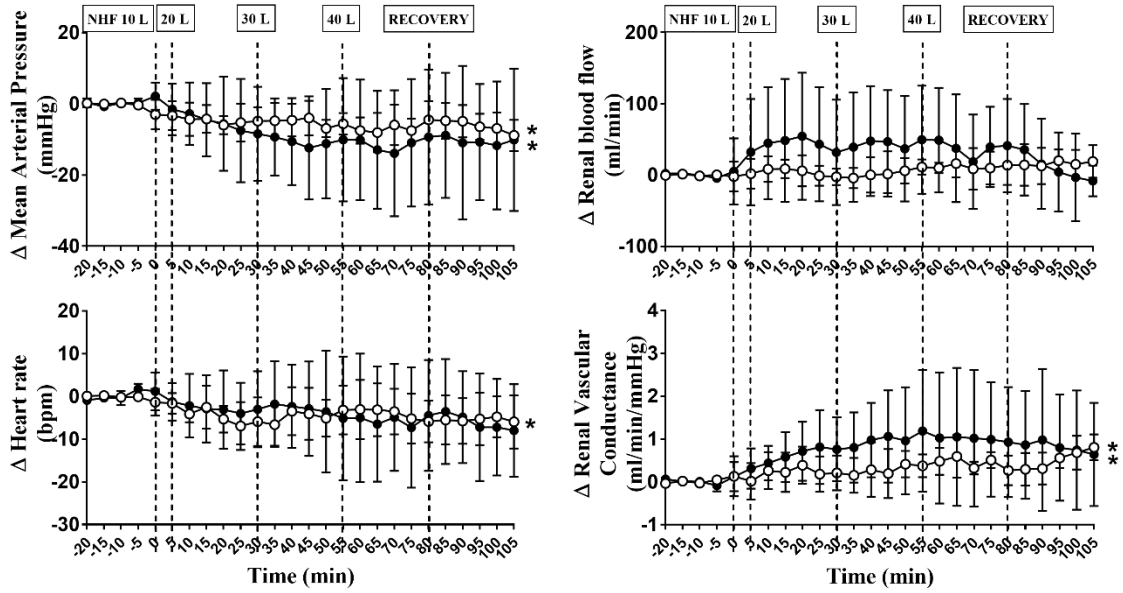

Figure 33 Absolute change in haemodynamic variables in response to HNF.

*HNF (10L, 20L, 30L and 40L/minutes) in conscious normotensive (n=5) and hypertensive sheep (n=5). The open circles and solid lines represent the HNF effect on normotensive sheep, and filled circle and solid line is in hypertensive sheep. Results are mean ± SD. * - p<0.05 denotes a significant effect of time (one-way ANOVA, * - effect within 80 mins after HNF administration).*

6.4 Discussion

This is the first study to report the effects of HNF on MAP and RBF in a large, conscious animal (sheep) model in both the normotensive and hypertensive state. The novel findings are that 1) HNF leads to significant decreases in BP in conscious normotensive and hypertensive sheep. 2) HNF increases RVC in both groups, but the blood flow to the renal artery was unchanged. RBF tends to increase in HTN sheep, which was not statistically significant, possibly due to relatively small group sizes.

Although HNF has become increasingly popular in treating chronic respiratory failure in patients (Lodeserto et al., 2018), the actions of HNF on the peripheral vasculature or BP is not clear. Previous research has indicated that HNF leads to better ventilation as well as oxygenation in pulmonary disease (Chatila et al., 2004). It is also known that HNF can decrease physiological dead space (Dewan et al., 1994). In this chapter, HNF in the normotensive and hypertensive states caused a significant decrease in BP. Interestingly, there was no change in RBF, but RVC was significantly increased. The decrease in BP following HNF in sheep indicates decreasing physiological dead space and improving ventilation can decrease BP in HTN. While I did not measure ventilation or physiological dead space in these animals, I speculate that HNF probably caused a reduction in physiological dead space in the lungs.

Previous studies have shown that an increase in tidal volume in response to lung inflation reduces systemic vascular resistance via a reduction in pre-and post-ganglionic cervical and splanchnic sympathetic nerves (Daly et al., 1967; Daly et al., 1968; James et al., 1969). This previous study concluded that that the lungs are a constant source of afferent impulses that can partially inhibit sympathetic vasomotor tone (Daly et al., 1986; Daly et al., 1967). Fast-conducting, myelinated afferent nerve fibers supply the pulmonary and airway mechanoreceptors. Both are sensitive to the static and dynamic aspects of lung volume and

transmural pressure. Lung inflation has been considered the most common trigger for activating mechanoreceptors (Kubin et al., 2006). The mechanism by which change in pulmonary ventilation modifies the vascular responses to CB stimulation is a vagal reflex from the lungs, triggered by an increase in tidal volume and possibly also in the rate of volume change (Daly et al., 1966; James et al., 1969).

I speculate that the reduction in MAP may be due to an action of pulmonary afferents in these animals. Whether the decrease in BP and the increase in RVC are mediated by a decrease in renal SNA remains to be tested. The decrease in HR after HNF administration in normotensive sheep also suggests that cardiac SNA may be diminished although I have not undertaken direct recordings in this study.

A previous study from our group found that the CB is activated in renovascular HTN and is associated with reduced blood flow to the common carotid artery (Chang et al., 2020). CB activation leads to differential changes in blood flow to different organs, including vasodilation to the common carotid artery but vasoconstriction in the kidney and heart (Pachen et al., 2020). This suggests that activation of the CB can lead to differentiated changes in SNA to different organs and thereby alter blood flow to different organs. Importantly, studies have shown that the CB chemoreceptors are a potential therapeutic target for treating sympathetically mediated diseases such as HF and HTN (McBryde et al., 2017; Paton et al., 2013) as suggested previously.

There is evidence that afferent input from the pulmonary afferents can decrease the sympathoexcitation produced by CB activation (Daly et al., 1986). One possibility is that the HNF can stimulate pulmonary afferents and decrease the hypertonicity from the CB and this may be an additional mechanism behind the decrease in MAP. One way to test this would be to conduct this study in animals with CSN denervation however this had not been done.

Taken together, these findings indicate that HNF produces lung inflation and may lead to inhibition of sympathetic tone which leads to decreased total vascular resistance and BP. However, whether this inhibition of sympathetic nerve activity occurs at the level of the CB or whether there is a central inhibition of the CB chemoreceptors by excitation of pulmonary receptors is unknown and remains to be tested in the future. Finally, only female sheep were used in my study and future studies will need to test whether male sheep also respond in a similar manner.

Chapter 7: General Discussion

The experiments conducted in my thesis have resulted in the following novel findings

1) CB stimulation increases directly recorded cardiac SNA in control animals (Chapter 3).
2) The increase in CoBF and CVC to intracarotid KCN injection was abolished after propranolol infusion, indicating that the increased cardiac SNA mediates coronary vasodilation (Chapter 3).
3) In an ovine model of HF, CB mediated increases in CoBF and CVC are augmented compared to control animals (Chapter 4).
4) The increase in CoBF is not mediated by an increase in cardiac SNA in the HF group (Chapter 4).
5) CB-mediated coronary vasodilation does not occur via a cholinergic pathway in either control of HF animals (Chapter 3 & 4).
6) Hyperoxia causes a reduction in CoBF and HR in the HF group (Chapter 5).
7) HNF causes a decrease in BP and an increase in RVC in normotensive and hypertensive sheep (Chapter 6).

Each of these findings and their relationship to current literature have been discussed in detail in the respective chapters. This chapter discusses the overall functional significance of these results. The possible direction of future studies is also considered.

7.1 Animal Models of heart failure

Due to the biological complexity of the cardiovascular system, it is essential to use an animal model to investigate the underlying mechanisms of HF and to explore novel therapeutic targets. The majority of experimental work has been done on rodent models of HF, predominantly rats and mice. Rat models are relatively inexpensive, and because of the short gestation period, a large sample size can be produced in a relatively short period (Hasenfuss,

1998). Therefore, small animal models have been widely used for the purpose of finding treatments or cures for human diseases.

However, several fundamental cardiac characteristics are different between rats, mice, and humans; refer to (Table 11). The most apparent differences are heart size and HR, rodents have small heart sizes and high HRs; this makes the comparison to human HF difficult (Gandolfi et al., 2011). Moreover, there are considerable differences at cellular and molecular levels, such as differences in myocyte size, ion channels, and pump contractile filament isoform (Ginis et al., 2004; Haghighi et al., 2003; Stoker et al., 1982).

Table 11 Comparison of heart weight, heart rate and systolic pressure between animals used commonly for models of heart disease.

Adapted from (Gandolfi et al., 2011; Ostergaard et al., 2010)

Species	Heart Weight (g)	Heart rate (beat/min)	Systolic Pressure (mm Hg)
Human	360–480	60–90	60–120
Sheep	240–360	70–80	80–120
Pig	400–500	65–75	70–130
Dog	160–420	60–120	120–150
Monkey	37–52	110–140	100–130
Rabbit	9–11	120–300	70–170
Mouse	0.14–0.15	500–600	80–160
Rat	0.88–0.92	250–493	84–184

Preclinical large animal models of HF have been used to discover novel mechanisms underlying the HF syndrome, develop and test new treatments for HF and advance our knowledge about this highly prevalent cardiac disease (Silva et al., 2020). The use of the large animal model of HF also provides important information regarding the safety and efficacy of

new treatments and thus can improve translation of animal research to treat human HF successfully.

However, there are some disadvantages to using large animal models. Notably, large animal models are much more expensive to purchase and maintain in animal facilities. The daily cost of housing the large animals are 30 to 90 times more expensive than small animals such as mice (Milani-Nejad et al., 2014). The experimental design needs longer follow-up times, and that requires proper breeding and housing conditions. Although larger animal models are more costly and difficult to manipulate, their genetic, structural, functional, and even disease similarities to humans make it an ideal model to consider. The main advantages of using large animal models for the *in vivo* heart studies are:

1) They can claim to be the most physiologically and clinically relevant experimental model (Hearse et al., 2000).
2) They allow chronic studies to be undertaken (Hearse et al., 2000).
3) They allow cardiac functions and responses to be assessed in the intact animal (Hearse et al., 2000).
4) They are amenable to all the techniques and measurements made in man and are ethically sound (Hearse et al., 2000).

7.1.1 *Sheep as a large animal model of HF*

Sheep have a left coronary type circulation, in which the majority of the myocardium receives its blood supply via branches of the left coronary artery (Ho, 2000), and their cardiac mass and coronary blood vessels are nearly identical to humans (Lelovas et al., 2014). Sheep do not have a significant coronary collateral network, similar to the situation in pigs and humans (Schaper et al., 1972). The left circumflex artery lies in a groove between the left atrium and the LV which allows (relatively) easy access through a left thoracotomy via the fourth intercostal

space. Therefore, it is safer to place the flow probe around the proximal left circumflex artery without disturbing the left main coronary artery (Crick et al., 1998). The microembolization model of HF can be created in sheep by injecting microspheres into the left coronary artery, which is accessible through the left heart catheterization performed via left femoral arteriotomy under fluoroscopic guidance (Schmitto et al., 2008; Schmitto et al., 2009). Furthermore, at molecular and cellular levels, the sheep heart has the slow β-MHC, the major myosin heavy chain isoform which is similar to humans. Both sheep and human hearts have an identical force-frequency relationship, which means the relaxation-contraction kinetics of sheep cardiomyocytes are also the same as human cardiac cells. All of this evidence suggests that the sheep is one of the most suitable experimental models for cardiovascular research.

In my study, I have used adult female Romney sheep. The reason for using female sheep in my study was, on the farm, usually young male lambs are used for meat, and only a few rams are available for mating each year. Therefore, rams are not readily available. Even when available, rams are very aggressive, and carrying out conscious experiments is very difficult. I have not corrected for the time of the female oestrus cycle in these sheep, and one limitation is that I cannot rule out that there might be a sex difference in the responses examined in the entire thesis.

7.2 CB sensitivity in heart failure

The sensitivity of the CB chemoreflex is augmented in patients with HF (Chugh et al., 1996) and animal models of HF (Del Rio et al., 2013b; Sun et al., 1999a, 1999b). However, the potential role of the CB in the pathophysiological changes in HF has been previously underappreciated since most stable HF patients do not experience overt hypoxia, at least to the degree that would significantly activate the peripheral chemoreflex chronically. While hypoxia has been used to stimulate the CB, experimentally, other stimulants such as KCN and nicotine

have been used (Comroe Jr et al., 1945). My research has used a small, locally applied (intracarotid) dose of KCN, which is a known selective CB stimulant.

Activation of CBs, as a result of a drop in Po_2, initiates a powerful neurogenic reflex response which causes hyperventilation to restore Po_2 (Lahiri, 2000; Lahiri et al., 2006; Lu et al., 2013; Weil, 2011). In my sheep, increased breathing in response to KCN injection indicated robust CB stimulation, albeit on only one side. Moreover, the study has used three different doses of KCN (10, 20, 30 μg/kg), which exhibited greater pressor and breathing responses in every animal. The KCN doses used in my study probably reflects 5% hypoxia given the pressor response to these two different stimuli is similar (Granjeiro et al., 2012). I haven't tried bilateral CB stimulation in my sheep as the cannulation process means blocking blood flow in one carotid artery, and it takes some time to restore blood flow. If I go to the second carotid, there is a potential that there might be surgical recovery issues.

The increase in MAP following CB activation seen in my study is consistent with previous findings (Daly et al., 1962; de Burgh Daly et al., 1959; Fletcher et al., 1992; Guyenet, 2000; Rutherford et al., 1978). Differential control of sympathetic nerve activity has been well established by our lab and others (Morrison, 2001; Ramchandra et al., 2006; Tromp et al., 2018). My data show that CB activation is accompanied by an increase in cardiac SNA (Chapter 3) and an increase in renal SNA (McBryde et al., 2013; Schultz et al., 2007b).

Unlike rodent studies, my study reported an increase in HR after KCN injection. The activation of peripheral chemoreflex resulted in minor changes in HR. One explanation is that the lower HR in sheep compared to rats may make reductions in HR more difficult to observe. Occasionally, I saw a slowing of HR in individual sheep; however, this was not a consistent response either within-subjects or across a group of sheep. Another probability is that in rodents, the KCN infusion given intravenously, resulting in systemic exposure to KCN. In my study, the

catheter location for KCN injection was positioned in the common carotid artery, targeting the carotid artery bifurcation. I speculate that some part of the robust bradycardia observed in rodents may be due to a direct action of the KCN on the heart and/or the aortic bodies. It may be that there are sex differences, and I cannot rule out a difference between sex effects in my study.

One of the major determinants of CoBF is metabolic oxygen demand and it plays an important role in increasing CoBF. Hence, to eliminate the effects of metabolic induced vasodilation, I repeated the KCN study when the heart was paced at a constant rate. An increase in CoBF was still observed suggesting the increase in CoBF persists when myocardial oxygen demand is kept constant. When the CoBF responses to CB activation were compared without accounting for metabolic vasodilation, there were no differences between the two groups. When the heart was paced at a steady rate, I could eliminate the effects of metabolic vasodilation and in this scenario, I observed a significantly enhanced CoBF response during CB activation in the HF sheep. To the best of our knowledge, this is the first time that the effects of CB activation on CoBF have been examined in a conscious model of HF. My data indicate that activation of the CB leads to a greater increase in CoBF in HF.

7.3 The role of cardiac SNA in modulating CoBF during activation of the CB chemoreceptors

In conscious control animals, activation of the CB resulted in an increase in directly recorded cardiac SNA, MAP, CoBF and CVC. The CoBF and CVC responses to CB activation were abolished after pre-treatment with a β-adrenergic receptor blocker, propranolol and I concluded that the β2-adrenergic vasodilatory actions supersede α-adrenergic vasoconstriction in intact sheep.

It must also be mentioned that propranolol has been shown to directly inhibit CB activity under certain conditions such as hypoglycaemia (Thompson et al., 2016), and it can also cross the blood-brain barrier to act centrally (Langley et al., 2015). Hence, I cannot rule out that the inhibition of the coronary vasodilation may be mediated by actions of propranolol at the CB or centrally.

Since I do not have recordings of cardiac SNA in HF animals, I could not determine if there is increased cardiac sympathetic drive to CB activation in this group of animals. Similar to control sheep, only one CB was being stimulated, and it may be that stimulation of both CBs may reveal greater pressor responses in the HF group.

As I have previously shown in normal sheep, CB activation increases cardiac SNA and CoBF; I expected a greater increase in CoBF in the HF group. When the heart paced at a constant rate to eliminate the effects of metabolic vasodilation, the increase in CoBF was significantly higher in HF sheep than the normal sheep. This can be due to an increased cardiac sympathetic activity and hence more vasodilation in this state. However, I have not directly recorded cardiac SNA so cannot conclusively comment on whether CB activation increases cardiac SNA in the HF state more than controls.

In normal sheep, intravenous propranolol infusion caused a significant decrease in basal MAP, suggesting that sympathetic drive to the heart plays a significant role in maintaining BP in these sheep.

7.4 The role of cardiac vagal drive on the CoBF response to CB activation

Generalized sympathetic activation and parasympathetic withdrawal in HF has been associated with changes in inhibitory and excitatory effects on brainstem vasomotor neurons

(Floras John, 1993; Francis et al., 1984; Hirsch et al., 1987; Swedberg et al., 1990). As illustrated in the Introduction section(Figure 3), the arterial baroreflex afferent inputs from the carotid and aortic arch and cardiopulmonary mechanoreceptors are the principal inhibitory influences on sympathetic outflow; discharge from arterial chemoreceptors and muscle metaboreceptors are the major excitatory inputs (Floras John, 1993; Thames et al., 1993).

The vagal limb of the baroreceptor HR reflex responds to afferent feedback from arterial baroreceptors. In normal subjects at rest, the integrated response to these competing factors can be defined as a relatively low sympathetic discharge and a relatively high HR variability. The compensatory vagal and sympatho neural responses to acute BP fluctuations are adequate and fast (Floras John, 1993). HF and its progression disturb this balance. Therefore, the major inputs to arterial baroreceptor afferent discharge become weak, and the sensitivity of atrial, ventricular and arterial mechanoreceptors to stretch reduces, the inhibitory input from arterial and cardiopulmonary receptors will decrease (Ferguson, 1990; Hainsworth, 1991; Hirsch et al., 1987).

In HF, central regulation of parasympathetic outflow is attenuated, and the excitatory inputs may arise from arterial chemoreceptors, skeletal muscle receptors, and the lungs (Ferguson, 1990; Porter et al., 1990). The alteration in the balance between excitatory and inhibitory afferent input comprises a generalized rise in basal sympathetic outflow, parasympathetic withdrawal, diminished reflex parasympathetic and sympathetic control of HR, and impairment of sympathetic reflex regulation of vascular resistance (Ferguson, 1990; Ferguson et al., 1992; Hirsch et al., 1987).

Infusion of atropine was used to test whether the coronary vasodilation to CB activation was induced by activation of the parasympathetic nerves to the heart. Atropine did not affect the CoBF or CVC responses to CB activation in conscious control and HF sheep. This contrasts

with previous studies. One study in conscious dogs showed that stimulation of the carotid chemoreflex using nicotine causes coronary vasodilation in conscious control dogs mediated by activation of parasympathetic cholinergic efferent fibers (Shen et al., 1994). Another study in α-chloralose anaesthetized, closed-chest dogs showed that stimulation of carotid chemoreceptors with hypoxic-hypercapnic blood, nicotine, or cyanide increased CoBF, which was abolished after atropine infusion (Ito et al., 1985). The reasons for this discrepancy are not clear; however I cannot rule out a species difference effect. One possibility is that the parasympathetic nerves may play a role mediated via other neurotransmitters such as vasoactive intestinal peptide which is shown to mediate coronary vasodilation (Feliciano et al., 1998a, 1998b).

Another interesting finding was that the pressor response to CB activation was attenuated post atropine in conscious control and HF sheep, which is consistent with some previous studies (Henderson et al., 1978; Jänig et al., 1983). The site of action of this is not clear. The dose of atropine used in my study may have crossed the blood-brain barrier and have central effects. The site of action of the atropine is not clear and may include the rostral ventrolateral medulla (RVLM) and the NTS (Furuya et al., 2014; Padley et al., 2007; Vieira et al., 2007). Moreover, it has been shown that acetylcholine (ACh) is released from glomus cells during chemoreceptor stimulation (Eyzaguirre et al., 1990; Iturriaga et al., 2007; Kåhlin et al., 2014; Nurse et al., 2013) so atropine may be acting on the CB as well as certain brain regions.

Moreover, neither sympathetic nor parasympathetic blockade had no effect on the increase in CoBF seen during CB activation in the HF group. As a result, the cause of the rise in CoBF is unknown. There is a probability that the parasympathetic nerve has been shown to play a coronary vasodilatory role via other neurotransmitters such as a vasoactive intestinal peptide (Feliciano et al., 1998b), however I cannot rule out the involvement of other neurotransmitters.

7.5 High nasal flow as a novel treatment paradigm

Previous studies have reported that deactivating CB chemoreceptors in hypertensive patients through hyperoxic ventilation can decrease systolic BP acutely via a reduction in total peripheral resistance (Izdebska et al., 2006; Izdebska et al., 1996; Sinski et al., 2014). In animal models of HTN, a short period of hyperoxia decreased tidal volume and respiratory frequency with a decrease in BP and HR (Zapata et al., 2009). Recent studies have also investigated the resection of CBs and their effect on reducing BP in rats, and it is hypothesized that the CBs might be a novel treatment target in HTN (Abdala et al., 2012; McBryde et al., 2013). Both hypertonicity and hyperreflexia originating from these organs drive chronic increases in sympathetic nerve activity leading to increased total vascular resistance and BP (Pijacka et al., 2016b).

There is experimental evidence indicating that the renovascular HTN model in rats is accompanied by increased resting pulmonary ventilation (Melo et al., 2020). The study suggests that the increased resting minute ventilation is due to an increase in tidal volume. Remarkably, the removal of CB normalized the ventilation (Melo et al., 2020) and reduced arterial pressure, which is consistent with previous studies (Abdala et al., 2012; Melo et al., 2019; Pijacka et al., 2016a). These studies suggest that renovascular HTN augments ventilation and that the CB seems to play a primary role in mediating this. While hyperoxia can be used to inhibit CB activity, hyperoxia also has direct actions on the vasculature which can confound interpretations. To circumvent this, my study asked whether decreasing tidal volume using HNF therapy would alter BP in an ovine model. CPAP treatment in patients with resistant HTN and obstructive sleep apnoea patients demonstrated a significant reduction in cardiovascular events (Navarro-Soriano et al., 2021) and a drop in systolic BP (Martínez-García et al., 2007). However, it was reported

that not all of the patients could tolerate CPAP (Kario, 2009; Martínez-García et al., 2007), in which case HNF could be a better option in these cases.

Although HNF has become increasingly popular in treating chronic respiratory failure patients (Lodeserto et al., 2018), HNF is not usually used for treatment of patients with apparent normal respiratory function. In the current study, HNF significantly reduced BP in both normotensive and hypertensive subjects. The RBF remained unchanged, but the RVC increased significantly. However, the mechanism of how HNF produces these effects are not fully understood. As reported in previous studies (Biselli et al., 2018; Möller et al., 2015; Möller et al., 2017), I speculate in this study that the HNF therapy caused a reduction in physiological dead space and thereby increased oxygenation.

The relationship between lung inflation reflex and systemic vascular constrictor response has been discussed in previous studies (Daly et al., 1986; Daly et al., 1967; Daly et al., 1968; James et al., 1969). It has been concluded that lung inflation is a constant source of afferent nerve impulses which cause the partial inhibition of sympathetic vasomotor tone (Daly et al., 1986; Daly et al., 1967). A previous study has confirmed that selective denervation of the lungs abolishes the progressive stepwise reduction in the size of vasoconstrictor response to CB stimulation in response to increasing pulmonary ventilation, indicating that this modification must have been due to a change in the activity of pulmonary receptors (Daly et al., 1986). However, whether there is central inhibition of the CB chemoreceptor vasoconstrictor response by pulmonary receptor excitation is not evident. My findings suggest that HNF produces lung inflation, and the reflex vasodilation resulting from the lung inflation may cause a reduction in sympathetic activity. However, whether the renal artery vasodilation observed in this study is due to decreased sympathetic activity to the kidney remains to be tested.

7.6 Study limitations and Future directions

One of the aims of this thesis was to determine the effect of CB stimulation on the blood supply to the heart and its connection with autonomic neural pathways. The results presented in this thesis are not without limitations due to the research question and species used.

The present study examines, for the first time, the effect of CB activation in directly recorded cardiac SNA and CoBF in a conscious large animal (sheep) model. The technical difficulty while recording the direct cardiac SNA was one of the biggest challenges in this study. In HF, I could not get enough sheep with good quality sympathetic nerve activity, so the nerve activity response to KCN injection will need to be examined in the HF condition in the future. Also in my study, I have used adult female Romney sheep. Hence, I cannot rule out that there might be a sex difference in response to KCN. Furthermore, the resting HR in both groups was > 100 bpm. While ideally the HR would be lower, the quality of the cardiac SNA signal can deteriorate rapidly after surgery. The longer one waits after surgery, the greater the chance that the nerve activity signal to noise ratio will be too low. Hence, the wait period after surgery was minimal unless the sheep showed clear signs of pain and stress.

I have shown that the increase in cardiac SNA mediates increased coronary vasodilation and blood flow in control sheep. It is known that the sympathetic nervous system innervates various parts in the heart, such as sino-atrial node, conduction system, and myocardial tissues (Hoover et al., 2004; Kawashima, 2005). Data from my study indicating increased cardiac SNA and CoBF together with the propranolol data suggest a direct action of SNA on the coronary blood vessels in control sheep. Future studies will need to investigate the impacts of interruption of CB afferent input on CoBF via CB resection or carotid sinus nerve denervation bilaterally. I also showed that in ovine HF, the CB chemoreceptors played an important role in maintaining blood supply to the heart.

Propranolol infusion did not alter the CoBF response to CB activation in HF. However, propranolol can cross the blood-brain barrier and has no specificity for the beta 1 or beta 2 receptors. In the future, one could try ICI-118,551, a selective β2-adrenergic receptor antagonist (Bilski et al., 1983). ICI-118,551 is a more potent β-adrenoceptor antagonist with a greater affinity towards β2-adrenoceptors.

The result of the present study and previous study from our lab (Chang et al., 2020) implies that the coronary and renal vasculature are under differential reflex control by the CBs such that CB activation induces coronary vasodilation, carotid vasodilation and renal vasoconstriction. These findings support the fact that the CB can differentially modulate distinct chemoreflex responses, as has been suggested recently (Zera et al., 2019). Therefore, CB activation may induce targeted sympathetically mediated haemodynamic responses in the periphery by recruiting a particular population of atropine-sensitive sympathetic preganglionic neurons. In contrast, CB-mediated carotid blood flow responses may be mediated by a different population of atropine-insensitive sympathetic preganglionic fibres (Chang et al., 2020). This remains an intriguing hypothesis that needs further testing.

In conscious sheep with HF, CB regulation of CoBF response to KCN was not mediated by a pathway including muscarinic acetylcholine or β-adrenergic receptors. The mechanisms mediating this vasodilation of the coronary vasculature need to be examined in future studies. Furthermore, in HTN, renin-angiotensin overactivity cause an increase production of Ang II and this elevated levels of circulating Ang II (Iwanami et al., 2009; Te Riet et al., 2015; Young et al., 2015). The functions of angiotensin II, such as elevated BP and vasoconstriction, are regulated by type 1 (AT1) receptors for angiotensin II in hypertensive conditions. Activation of AT1 receptors in the kidney is an integral part of BP control (Crowley et al., 2005). AT1 receptors are located abundantly in type 1 cells at CB (Lam et al., 2014) and centrally within the nucleus tractus solitarius and rostral ventrolateral medulla. Attenuation of central (NTS and

RVLM) AT1 receptors has been shown to reduce the pressor and bradycardic responses to CB stimulation in healthy rats (Rocha et al., 2003). Also, in HF, it has been shown that the chemoreflex-mediated pressor response and augmented cardiac SNA are dampened following the blockade of the AT1 receptors in the nucleus tractus solitarius (Wang et al., 2008). Therefore, it would be worthwhile to investigate the function of the AT1 receptors in mediating the CoBF response to CB activation in the HF state.

Finally, the model of HTN (2K1C) used in this study does not reflect the polygenic nature of human HTN. However, they have pathophysiological similarities, including hypersensitive chemoreflex and hyperactivity of the renin-angiotensin and sympathetic nervous systems, and end-organ damage (Coffman, 2011; Guyenet, 2006; Oliveira-Sales et al., 2009; Te Riet et al., 2015). My study suggested lung inflation caused by HNF decreased MAP in the sheep model of renovascular HTN. However, I don't know whether the inhibition of sympathetic drive happened at the CB level or via actions of the pulmonary afferents and this remains to be examined

Apart from CB removal, hyperoxia has also been shown to suppress CB activity and have a marked beneficial effect on baroreflex sensitivity (BRS) and HR variability in patients with HF (Ponikowski et al., 1997). In untreated humans and spontaneously hypertensive rats, hyperoxia can also normalize sympathetic nerve activity to the kidney and muscle (McBryde et al., 2013; Siński et al., 2012). My findings indicate that suppression of CB function may not have all positive effects. Hyperoxia resulted in a negative impact as it attenuated the CoBF response to CB activation in the HF state (Chapter 5). This suggests that in addition to the improvement of autonomic imbalance and BRS, hyperoxia may attenuate the CoBF response, which would lead to coronary vasoconstriction in the HF state.

Our novel model of HNF therapy showed that HNF could cause a marked reduction in BP in normotensive and renovascular hypertensive sheep, implying that sympathoinhibtion during lung inflation decreased arterial pressure in both groups. The kidneys are densely innervated with efferent and afferent renal nerves and they play a major role in BP regulation (Dibona et al., 1997). Central and peripheral mechanisms are responsible for regulating sympathetic activity to the kidney. The neuronal activity in the sympathetic premotor nuclei in the brainstem and hypothalamus, such as the RVLM and the paraventricular nucleus (PVN), determines the degree of renal SNA (Sata et al., 2018). The RVLM is a central brain region containing sympatho-excitatory neurons that can regulate efferent renal nerve activity. Neurons in the RVLM send signals to pre-ganglionic neurons in the spinal cord, which send signals to peripheral organs such as the heart, arteries, and kidneys through postganglionic neurons (Kumagai et al., 2012).

Studies in patients with HTN showed that catheter-based renal sympathetic denervation caused a marked reduction in BP (Krum et al., 2009; Schlaich et al., 2009) which again supports the crucial role of renal SNA in the regulation of BP and pathogenesis of HTN. HNF led to renal vasodilation which suggests that reduced sympathetic drive leads to decreased vascular resistance and lowers BP. However, whether the renal artery vasodilation is due to a reduction in sympathetic nerve activity to the kidney needs to be investigated in the future with the direct recording of renal SNA during HNF therapy.

In conclusion, the ultimate aim of my study was to investigate how CB chemoreceptor alters heart function in disease conditions. I have shown that CB activation increases directly recorded cardiac SNA and CoBF in conscious sheep. The sympathetic pathway is involved in coronary vasodilation in the conscious control state. There may be other possible mechanisms responsible for CB-stimulation-induced increase in CoBF in HF. Overall my studies suggest

that CBs play an essential role in modulating blood flow to the heart, and HNF can be helpful during hypertonic CB conditions without impairing blood flow to vital organs.

Bibliography

Abdala, A. P., et al. (2012). Hypertension is critically dependent on the carotid body input in the spontaneously hypertensive rat. *The Journal of physiology, 590*(17), 4269-4277.

Abukar, Y., et al. (2019). Impaired baroreflex function in an ovine model of chronic heart failure induced by multiple coronary microembolizations. *Frontiers in Physiology, 10*, 1420.

Abukar, Y., et al. (2018). Increased cardiac sympathetic nerve activity in ovine heart failure is reduced by lesion of the area postrema, but not lamina terminalis. *Basic Research in Cardiology, 113*(5), 1-11.

Alella, A., et al. (1955). Interrelation between cardiac oxygen consumption and coronary blood flow. *American Journal of Physiology-Legacy Content, 183*(3), 570-582.

Amenta, F., et al. (1991). Autoradiographic localization of beta-adrenergic receptors in human large coronary arteries. *Circulation research, 68*(6), 1591-1599.

America, H. F. S. o. (2010). Executive summary: HFSA 2010 comprehensive heart failure practice guideline. *Journal of Cardiac Failure, 16*(6), 475-539.

American Heart Association, A. (2011). New York Heart Association (NYHA) Functional Classification in a patient with heart disease. *Accessed on, 2*(3)

Andrade, D. C., et al. (2015). Relevance of the carotid body chemoreflex in the progression of heart failure. *BioMed research international, 2015*

Ardehali, A., et al. (1990). Myocardial oxygen supply and demand. *Chest, 98*(3), 699-705.

Armour, J. A., et al. (1975). Functional anatomy of canine cardiac nerves. *Acta Anat (Basel), 91*(4), 510-528. 10.1159/000144411

Azad, N., et al. (2014). Management of chronic heart failure in the older population. *Journal of geriatric cardiology: JGC, 11*(4), 329.

Barker, W. H., et al. (2006). Changing incidence and survival for heart failure in a well-defined older population, 1970–1974 and 1990–1994. *Circulation, 113*(6), 799-805.

Barman, S. M., et al. (2017). Deciphering the neural control of sympathetic nerve activity: status report and directions for future research. *Frontiers in neuroscience, 11*, 730.

Bayliss, W. M. (1923). *The vaso-motor system* (Vol. 5): Longmans, Green.

Belt, T. (1933). The anatomy and physiology of the coronary circulation. *Canadian Medical Association Journal, 29*(1), 19.

Benot, A., et al. (1990). Feedback inhibition of Ca2+ currents by dopamine in glomus cells of the carotid body. *European Journal of Neuroscience, 2*(9), 809-812.

Berglund, E., et al. (1957). Myocardial Oxygen Consumption and Coronary Blood Flow during Potassium-Induced Cardiac Arrest and during Ventricular Fibrillation1. *Acta Physiologica Scandinavica, 41*(2-3), 261-268.

Bilski, A. J., et al. (1983). The pharmacology of a beta 2-selective adrenoceptor antagonist (ICI 118,551). *Journal of cardiovascular pharmacology, 5*(3), 430-437.

Binak, K., et al. (1967). Oxygen extraction rate of the myocardium at rest and on exercise in various conditions. *British heart journal, 29*(3), 422.

Biscoe, T., et al. (1968). Effects of inhalation anaesthetics on carotid body chemorceptor activity. *British journal of anaesthesia, 40*(1), 2-12.

Biselli, P., et al. (2018). Reductions in dead space ventilation with nasal high flow depend on physiological dead space volume: metabolic hood measurements during sleep in patients with COPD and controls. *European Respiratory Journal, 51*(5)

Bloomfield, A. (2017). Health and Independence Report 2017.

Bock, J. S., et al. (2010). Cardiorenal syndrome: new perspectives. *Circulation, 121*(23), 2592-2600.

Braam, B., et al. (1995). Modulation of tubuloglomerular feedback by angiotensin II type 1 receptors during the development of Goldblatt hypertension. *Hypertension, 25*(6), 1232-1237.

Brack, T., et al. (2012). Cheyne-Stokes respiration in patients with heart failure: prevalence, causes, consequences and treatments. *Respiration, 83*(2), 165-176.

Braga, V. A., et al. (2008). Cardiovascular responses to peripheral chemoreflex activation and comparison of different methods to evaluate baroreflex gain in conscious mice using telemetry. *American Journal of Physiology-Regulatory, Integrative and Comparative Physiology, 295*(4), R1168-R1174.

Braunwald, E. (1971). Control of myocardial oxygen consumption: physiologic and clinical considerations. *The American journal of cardiology, 27*(4), 416-432.

Braunwald, E., et al. (1957). Hemodynamic determinants of coronary flow: effect of changes in aortic pressure and cardiac output on the relationship between myocardial oxygen consumption and coronary flow. *American Journal of Physiology-Legacy Content, 192*(1), 157-163.

Broten, T., et al. (1992). Role of endothelium-derived relaxing factor in parasympathetic coronary vasodilation. *American Journal of Physiology-Heart and Circulatory Physiology, 262*(5), H1579-H1584.

Brunner-La Rocca, H. P., et al. (2001). Effects of intravenous brain natriuretic peptide on regional sympathetic activity in patients with chronic heart failure as compared with healthy control subjects. *Journal of the American College of Cardiology, 37*(5), 1221-1227.

Buckler, K., et al. (1994). Effects of hypoxia on membrane potential and intracellular calcium in rat neonatal carotid body type I cells. *The Journal of physiology, 476*(3), 423-428.

Burt, V. L., et al. (1995). Prevalence of hypertension in the US adult population: results from the Third National Health and Nutrition Examination Survey, 1988-1991. *Hypertension, 25*(3), 305-313.

Butler, R. N. (1997). Population aging and health. *Bmj, 315*(7115), 1082-1084.

Campanucci, V. A., et al. (2007). Autonomic innervation of the carotid body: role in efferent inhibition. *Respiratory physiology & neurobiology, 157*(1), 83-92.

Campanucci, V. A., et al. (2006). Expression of multiple P2X receptors by glossopharyngeal neurons projecting to rat carotid body O2-chemoreceptors: role in nitric oxide-mediated efferent inhibition. *Journal of Neuroscience, 26*(37), 9482-9493.

Carr, J., et al. (2002). Heart failure: ethnic disparities in morbidity and mortality in New Zealand. *New Zealand medical journal, 114*(1146), 15.

Carretero, O. A., et al. (2000). Essential hypertension: part I: definition and etiology. *Circulation, 101*(3), 329-335.

Chaggar, P. S., et al. (2009). Neuroendocrine effects on the heart and targets for therapeutic manipulation in heart failure. *Cardiovascular therapeutics, 27*(3), 187-193.

Chang, J. W.-H., et al. (2020). Role of the Carotid Body in an Ovine Model of Renovascular Hypertension. *Hypertension, 76*(5), 1451-1460.

Chatila, W., et al. (2004). The effects of high-flow vs low-flow oxygen on exercise in advanced obstructive airways disease. *Chest, 126*(4), 1108-1115.

Chatterjee, K. (2005). Neurohormonal activation in congestive heart failure and the role of vasopressin. *The American journal of cardiology, 95*(9), 8-13.

Chua, T., et al. (1997). Clinical characteristics of chronic heart failure patients with an augmented peripheral chemoreflex. *European heart journal, 18*(3), 480-486.

Chua, T. P., et al. (1996). Relation between chemosensitivity and the ventilatory response to exercise in chronic heart failure. *Journal of the American College of Cardiology*, *27*(3), 650-657.

Chugh, S. S., et al. (1996). Peripheral chemoreflex in chronic heart failure: friend and foe. *American heart journal*, *132*(4), 900-904.

Clayton, S. C., et al. (2011). Renal denervation modulates angiotensin receptor expression in the renal cortex of rabbits with chronic heart failure. *American Journal of Physiology-Renal Physiology*, *300*(1), F31-F39.

Coffman, T. M. (2011). Under pressure: the search for the essential mechanisms of hypertension. *Nature medicine*, *17*(11), 1402-1409.

Cohn, J. N., et al. (2000). Cardiac remodeling—concepts and clinical implications: a consensus paper from an international forum on cardiac remodeling. *Journal of the American College of Cardiology*, *35*(3), 569-582.

Cohn, J. N., et al. (1984). Plasma norepinephrine as a guide to prognosis in patients with chronic congestive heart failure. *New England Journal of Medicine*, *311*(13), 819-823.

Comroe Jr, J., et al. (1945). Applied physiology. *Annual review of physiology*, *7*(1), 653-676.

Coote, J. (2013). Myths and realities of the cardiac vagus. *The Journal of physiology*, *591*(17), 4073-4085.

Costa, F. V. (1996). Compliance with antihypertensive treatment. *Clinical and experimental hypertension*, *18*(3-4), 463-472.

Cowie, M. (2001). The prognosis of heart failure: the view from the real world. *European heart journal*, *22*(15), 1247-1248.

Crick, S. J., et al. (1998). Anatomy of the pig heart: comparisons with normal human cardiac structure. *Journal of anatomy*, *193*(1), 105-119.

Crowley, S. D., et al. (2005). Distinct roles for the kidney and systemic tissues in blood pressure regulation by the renin-angiotensin system. *The Journal of clinical investigation*, *115*(4), 1092-1099.

Cubrilo-Turek, M. (2003). Hypertension and coronary heart disease. *Ejifcc*, *14*(2), 67.

Daly, M., et al. (1986). Modification by lung inflation of the vascular responses from the carotid body chemoreceptors and other receptors in dogs. *The Journal of physiology*, *378*(1), 13-30.

Daly, M. D. B., et al. (1967). The reflex effects of alterations in lung volume on systemic vascular resistance in the dog. *The Journal of physiology*, *188*(3), 331-351.

Daly, M. d. B., et al. (1968). An analysis of the reflex systemic vasodilator response elicited by lung inflation in the dog. *The Journal of physiology*, *195*(2), 387-406.

Daly, M. D. B., et al. (1962). An analysis of the primary cardiovascular reflex effects of stimulation of the carotid body chemoreceptors in the dog. *The Journal of physiology*, *162*(3), 555-573.

Daly, M. d. B., et al. (1966). Comparison of the reflex responses elicited by stimulation of the separately perfused carotid and aortic body chemoreceptors in the dog. *The Journal of physiology*, *182*(2), 379-403.

Dampney, R., et al. (2002). Central mechanisms underlying short-and long-term regulation of the cardiovascular system. *Clinical and experimental pharmacology and physiology*, *29*(4), 261-268.

de Burgh Daly, I., et al. (1959). The effects of stimulation of the carotid body chemoreceptors on the pulmonary vascular bed in the dog: thevasosensory controlled perfused living animal'preparation. *The Journal of physiology*, *148*(1), 201.

De Kock, L. (1954). The intra-glomerular tissues of the carotid body. *Cells Tissues Organs*, *21*(2), 101-116.

De Kock, L., et al. (1966). An electron microscope study of the carotid body. *Cells Tissues Organs, 64*(1-3), 163-178.
Dekker, R. J., et al. (2005). Endothelial KLF2 links local arterial shear stress levels to the expression of vascular tone-regulating genes. *The American journal of pathology, 167*(2), 609-618.
Del Rio, R. (2015). The carotid body and its relevance in pathophysiology. *Experimental physiology, 100*(2), 121-123.
Del Rio, R., et al. (2017). Carotid body-mediated chemoreflex drive in the setting of low and high output heart failure. *Scientific reports, 7*(1), 1-10.
Del Rio, R., et al. (2013a). Carotid chemoreceptor ablation improves survival in heart failure: rescuing autonomic control of cardiorespiratory function. *Journal of the American College of Cardiology, 62*(25), 2422-2430.
Del Rio, R., et al. (2013b). Inhibition of hydrogen sulfide restores normal breathing stability and improves autonomic control during experimental heart failure. *Journal of Applied Physiology, 114*(9), 1141-1150.
Denison JR, A. B., et al. (1958). Effects of autonomic nerves and their mediators on the coronary circulation and myocardial contraction. *Circulation Research, 6*(5), 633-643.
Deussen, A., et al. (2012). Mechanisms of metabolic coronary flow regulation. *Journal of molecular and cellular cardiology, 52*(4), 794-801.
Dewan, N. A., et al. (1994). Effect of low flow and high flow oxygen delivery on exercise tolerance and sensation of dyspnea: a study comparing the transtracheal catheter and nasal prongs. *Chest, 105*(4), 1061-1065.
Díaz, H. S., et al. (2020). Episodic stimulation of central chemoreceptor neurons elicits disordered breathing and autonomic dysfunction in volume overload heart failure. *American Journal of Physiology-Lung Cellular and Molecular Physiology, 318*(1), L27-L40.
Dibner-Dunlap, M. E., et al. (1996). Enalaprilat augments arterial and cardiopulmonary baroreflex control of sympathetic nerve activity in patients with heart failure. *Journal of the American College of Cardiology, 27*(2), 358-364.
Dibner-Dunlap, M. E., et al. (1989). Baroreflex control of renal sympathetic nerve activity is preserved in heart failure despite reduced arterial baroreceptor sensitivity. *Circulation research, 65*(6), 1526-1535.
Dibona, G. F. (2004). The sympathetic nervous system and hypertension: recent developments. *Hypertension, 43*(2), 147-150.
DiBona, G. F., et al. (1995a). ANG II receptor blockade and arterial baroreflex regulation of renal nerve activity in cardiac failure. *American Journal of Physiology-Regulatory, Integrative and Comparative Physiology, 269*(5), R1189-R1196.
Dibona, G. F., et al. (1997). Neural control of renal function. *Physiological reviews, 77*(1), 75-197.
DiBona, G. F., et al. (1994). Reflex regulation of renal nerve activity in cardiac failure. *American Journal of Physiology-Regulatory, Integrative and Comparative Physiology, 266*(1), R27-R39.
DiBona, G. F., et al. (1995b). Increased renal nerve activity in cardiac failure: arterial vs. cardiac baroreflex impairment. *American Journal of Physiology-Regulatory, Integrative and Comparative Physiology, 268*(1), R112-R116.
DiBona, G. F., et al. (1996). Differentiated sympathetic neural control of the kidney. *American Journal of Physiology-Regulatory, Integrative and Comparative Physiology, 271*(1), R84-R90.
Dick, T. E., et al. (2014). Cardiorespiratory coupling: common rhythms in cardiac, sympathetic, and respiratory activities *Progress in brain research* (Vol. 209, pp. 191-205): Elsevier.

Ding, Y., et al. (2011). Role of blood flow in carotid body chemoreflex function in heart failure. *The Journal of physiology, 589*(1), 245-258.
Doughty, R., et al. (1995). Hospital admissions and deaths due to congestive heart failure in New Zealand, 1988-91. *The New Zealand medical journal, 108*(1012), 473-475.
Duchen, M., et al. (1988). Biophysical studies of the cellular elements of the rabbit carotid body. *Neuroscience, 26*(1), 291-311.
Duffin, J. (2007). Measuring the ventilatory response to hypoxia. *The Journal of physiology, 584*(1), 285-293.
Duffin, J., et al. (1976). The effect of halothane and thiopentone on ventilatory responses mediated by the peripheral chemoreceptors in man. *British journal of anaesthesia, 48*(10), 975-981.
Duncker, D. J., et al. (2008). Regulation of coronary blood flow during exercise. *Physiological reviews, 88*(3), 1009-1086.
Duncker, D. J., et al. (1998). Autonomic control of vasomotion in the porcine coronary circulation during treadmill exercise: evidence for feed-forward β-adrenergic control. *Circulation research, 82*(12), 1312-1322.
Dysart, K., et al. (2009). Research in high flow therapy: mechanisms of action. *Respiratory medicine, 103*(10), 1400-1405.
Dzau, V. J., et al. (1981). Relation of the renin-angiotensin-aldosterone system to clinical state in congestive heart failure. *Circulation, 63*(3), 645-651.
Egan, B. M., et al. (1993). Improved baroreflex sensitivity in elderly hypertensives on lisinopril is not explained by blood pressure reduction alone. *Journal of hypertension, 11*(10), 1113-1120.
Esler, M. (2010). The 2009 Carl Ludwig Lecture: pathophysiology of the human sympathetic nervous system in cardiovascular diseases: the transition from mechanisms to medical management. *Journal of Applied Physiology, 108*(2), 227-237.
Esler, M., et al. (1988). Assessment of human sympathetic nervous system activity from measurements of norepinephrine turnover. *Hypertension, 11*(1), 3-20.
Esler, M., et al. (1998). Increased sympathetic nervous system activity and its therapeutic reduction in arterial hypertension, portal hypertension and heart failure. *Journal of the autonomic nervous system, 72*(2), 210-219.
Esler, M., et al. (2001). Sympathetic nerve biology in essential hypertension. *Clinical and experimental pharmacology and physiology, 28*(12), 986-989.
Eyzaguirre, C., et al. (1990). Effects of putative neurotransmitters of the carotid body on its own glomus cells. *European Journal of Neuroscience, 2*(1), 77-88.
Feigl, E. (1983a). Coronary physiology. *Physiological reviews, 63*(1), 1-205.
Feigl, E. (1983b). Coronary physiology. *Physiol Rev, 63*(1), 1-205. 10.1152/physrev.1983.63.1.1
Feigl, E. O. (1967). Sympathetic control of coronary circulation. *Circulation Research, 20*(2), 262-271.
Feigl, E. O. (1969). Parasympathetic control of coronary blood flow in dogs. *Circulation Research, 25*(5), 509-519.
Feigl, E. O. (1998). Neural control of coronary blood flow. *Journal of vascular research, 35*(2), 85-92.
Feinberg, H., et al. (1962). Determinants of coronary flow and myocardial oxygen consumption. *American Journal of Physiology-Legacy Content, 202*(1), 45-52.
Feliciano, L., et al. (1998a). Vagal nerve stimulation during muscarinic and beta-adrenergic blockade causes significant coronary artery dilation. *J Auton Nerv Syst, 68*(1-2), 78-88. 10.1016/s0165-1838(97)00109-4

Feliciano, L., et al. (1998b). Vagal nerve stimulation releases vasoactive intestinal peptide which significantly increases coronary artery blood flow. *Cardiovasc Res, 40*(1), 45-55. 10.1016/s0008-6363(98)00122-9

Ferguson, D. (1990). Baroreflex-mediated circulatory control in human heart failure. *Heart Failure, 6*(3)

Ferguson, D. W., et al. (1992). Effects of heart failure on baroreflex control of sympathetic neural activity. *The American journal of cardiology, 69*(5), 523-531.

Fletcher, E. C., et al. (1992). Carotid chemoreceptors, systemic blood pressure, and chronic episodic hypoxia mimicking sleep apnea. *Journal of Applied Physiology, 72*(5), 1978-1984.

Fletcher, L., et al. (2001). Congestive heart failure: Understanding the pathophysiology and management. *Journal of the American Association of Nurse Practitioners, 13*(6), 249-257.

Floras John, S. (1993). Clinical aspects of sympathetic activation and parasympathetic withdrawal in heart failure. *Journal of the American College of Cardiology, 22*(4_Supplement_1), A72-A84. 10.1016/0735-1097(93)90466-E

Floras, J. S. (1993). Clinical aspects of sympathetic activation and parasympathetic withdrawal in heart failure. *Journal of the American College of Cardiology, 22*(4), A72-A84.

Floras, J. S., et al. (2015). The sympathetic/parasympathetic imbalance in heart failure with reduced ejection fraction. *European heart journal, 36*(30), 1974-1982.

Foltz, E., et al. (1950). Factors in variation and regulation of coronary blood flow in intact anesthetized dogs. *American Journal of Physiology-Legacy Content, 162*(3), 521-537.

Franchini, K. G., et al. (1997). Hemodynamics of chemoreflex activation in unanesthetized rats. *Hypertension, 30*(3), 699-703.

Francis, G. S., et al. (1984). The neurohumoral axis in congestive heart failure. *Annals of internal medicine, 101*(3), 370-377.

Friberg, P., et al. (1988). Sympathetic and parasympathetic influence on blood pressure and heart rate variability in Wistar-Kyoto and spontaneously hypertensive rats. *Journal of hypertension. Supplement: official journal of the International Society of Hypertension, 6*(4), S58-60.

Fung, M. L., et al. (2014). Mechanisms of maladaptive responses of peripheral chemoreceptors to intermittent hypoxia in sleep-disordered breathing. *Sheng li xue bao:[Acta physiologica Sinica], 66*(1), 23-29.

Furuya, W. I., et al. (2014). Differential modulation of sympathetic and respiratory activities by cholinergic mechanisms in the nucleus of the solitary tract in rats. *Exp Physiol, 99*(5), 743-758. 10.1113/expphysiol.2013.076794

Gandolfi, F., et al. (2011). Large animal models for cardiac stem cell therapies. *Theriogenology, 75*(8), 1416-1425.

Ganfornina, M. D., et al. (1991). Single K+ channels in membrane patches of arterial chemoreceptor cells are modulated by O2 tension. *Proceedings of the National Academy of Sciences, 88*(7), 2927-2930.

Giannoni, A., et al. (2008). Clinical significance of chemosensitivity in chronic heart failure: influence on neurohormonal derangement, Cheyne–Stokes respiration and arrhythmias. *Clinical Science, 114*(7), 489-497.

Ginis, I., et al. (2004). Differences between human and mouse embryonic stem cells. *Developmental biology, 269*(2), 360-380.

Gonzalez, C., et al. (1994). Carotid body chemoreceptors: from natural stimuli to sensory discharges. *Physiological reviews, 74*(4), 829-898.

Goodwill, A. G., et al. (2011). Regulation of coronary blood flow. *Comprehensive Physiology, 7*(2), 321-382.

Granata, L., et al. (1965). Coronary inflow and oxygen usage following cardiac sympathetic nerve stimulation in unanesthetized dogs. *Circulation Research, 16*(2), 114-120.
Granjeiro, É. M., et al. (2012). Bed nucleus of the stria terminalis and the cardiovascular responses to chemoreflex activation. *Autonomic Neuroscience, 167*(1-2), 21-26.
Grassi, G., et al. (1997). Effects of chronic ACE inhibition on sympathetic nerve traffic and baroreflex control of circulation in heart failure. *Circulation, 96*(4), 1173-1179.
Grassi, G., et al. (1995). Sympathetic activation and loss of reflex sympathetic control in mild congestive heart failure. *Circulation, 92*(11), 3206-3211.
Gregg, D., et al. (1963). Handbook of Physiology Vol. 2. *Circulation (Baltimore, 1966)*
Gregg, D. E. (1946). The coronary circulation. *Physiological reviews, 26*(1), 28-46.
Guyenet, P. G. (2000). Neural structures that mediate sympathoexcitation during hypoxia. *Respiration physiology, 121*(2-3), 147-162.
Guyenet, P. G. (2006). The sympathetic control of blood pressure. *Nature Reviews Neuroscience, 7*(5), 335-346.
Guyenet, P. G. (2011). Regulation of breathing and autonomic outflows by chemoreceptors. *Comprehensive Physiology, 4*(4), 1511-1562.
Haack, K. K., et al. (2014). Simvastatin treatment attenuates increased respiratory variability and apnea/hypopnea index in rats with chronic heart failure. *Hypertension, 63*(5), 1041-1049.
Habeck, J.-O. (1991). Peripheral arterial chemoreceptors and hypertension. *Journal of the autonomic nervous system, 34*(1), 1-7.
Hackett, J. G., et al. (1972). Coronary vascular responses to stimulation of chemoreceptors and baroreceptors: evidence for reflex activation of vagal cholinergic innervation. *Circulation Research, 31*(1), 8-17.
Haghighi, K., et al. (2003). Human phospholamban null results in lethal dilated cardiomyopathy revealing a critical difference between mouse and human. *The Journal of clinical investigation, 111*(6), 869-876.
Hainsworth, R. (1991). Reflexes from the heart. *Physiological reviews, 71*(3), 617-658.
Hartupee, J., et al. (2017). Neurohormonal activation in heart failure with reduced ejection fraction. *Nature Reviews Cardiology, 14*(1), 30-38.
Hasenfuss, G. (1998). Animal models of human cardiovascular disease, heart failure and hypertrophy. *Cardiovascular research, 39*(1), 60-76.
Hashimoto, K., et al. (1964). Carotid chemoreceptor reflex effects on coronary flow and heart rate. *American Journal of Physiology-Legacy Content, 206*(3), 536-540.
Hasking, G. J., et al. (1986). Norepinephrine spillover to plasma in patients with congestive heart failure: evidence of increased overall and cardiorenal sympathetic nervous activity. *Circulation, 73*(4), 615-621.
Hearse, D. J., et al. (2000). Experimental models for the study of cardiovascular function and disease. *Pharmacological Research, 41*(6), 597-603.
Hein, T. W., et al. (2004). Heterogeneous β2-adrenoceptor expression and dilation in coronary arterioles across the left ventricular wall. *Circulation, 110*(17), 2708-2712.
Henderson, C., et al. (1978). Effect of cholinergic antagonists on sympathetic ganglionic transmission of vasomotor reflexes from the carotid baroreceptors and chemoreceptors of the dog. *The Journal of physiology, 277*(1), 379-385.
Heusch, G., et al. (1984). Alpha 1-and alpha 2-adrenoceptor-mediated vasoconstriction of large and small canine coronary arteries in vivo. *Journal of cardiovascular pharmacology, 6*(5), 961-968.
Heusch, G., et al. (1983). Interaction of methoxamine with compensatory vasodilation distal to coronary stenoses. *Arzneimittel-forschung, 33*(12), 1647-1650.

Hirsch, A., et al. (1987). Baroreceptor function in congestive heart failure: effect on neurohumoral activation and regional vascular resistance. *Circulation, 75*(5 Pt 2), IV36-48.

Hirsch, E. (1961). The innervation of the human heart. I The coronary arteries and the myocardium. *Arch Pathol, 71*, 384-407.

Ho, S. Y. (2000). Congenital Heart Malformations in Mammals: An Illustrated Text.

Hodgson, J. M., et al. (1989). Direct vasoconstriction and endothelium-dependent vasodilation. Mechanisms of acetylcholine effects on coronary flow and arterial diameter in patients with nonstenotic coronary arteries. *Circulation, 79*(5), 1043-1051.

Hoover, D. B., et al. (2004). Localization of cholinergic innervation in guinea pig heart by immunohistochemistry for high-affinity choline transporters. *Cardiovascular research, 62*(1), 112-121.

Hunt, S. A. (2005). ACC/AHA 2005 guideline update for the diagnosis and management of chronic heart failure in the adult: a report of the American College of Cardiology/American Heart Association Task Force on Practice Guidelines (Writing Committee to Update the 2001 Guidelines for the Evaluation and Management of Heart Failure). *Journal of the American College of Cardiology, 46*(6), e1-e82.

Insel, P. A. (1996). Adrenergic receptors—evolving concepts and clinical implications. *New England Journal of Medicine, 334*(9), 580-585.

Ito, B., et al. (1985). Carotid chemoreceptor reflex parasympathetic coronary vasodilation in the dog. *American Journal of Physiology-Heart and Circulatory Physiology, 249*(6), H1167-H1175.

Ito, M., et al. (1994). Efferent sympathetic and vagal innervation of the canine right ventricle. *Circulation, 90*(3), 1459-1468.

Iturriaga, R., et al. (2016). Carotid body chemoreceptors, sympathetic neural activation, and cardiometabolic disease. *Biological research, 49*(1), 13.

Iturriaga, R., et al. (2007). Electrical and pharmacological properties of petrosal ganglion neurons that innervate the carotid body. *Respiratory physiology & neurobiology, 157*(1), 130-139.

Iwanami, J., et al. (2009). Inhibition of the renin–angiotensin system and target organ protection. *Hypertension Research, 32*(4), 229-237.

Izdebska, E., et al. (1998). Postexercise decrease in arterial blood pressure, total peripheral resistance and in circulatory responses to brief hyperoxia in subjects with mild essential hypertension. *Journal of human hypertension, 12*(12), 855-860.

Izdebska, E., et al. (2006). MODERATE EXERCISE TRAINING REDUCES ARTERIAL. *Journal of physiology and pharmacology, 57*(11), 93-102.

Izdebska, E., et al. (1996). Hemodynamic responses to brief hyperoxia in healthy and in mild hypertensive human subjects in rest and during dynamic exercise. *Journal of physiology and pharmacology, 47*(2)

Jackson, G., et al. (2000). ABC of heart failure: Pathophysiology. *BMJ: British Medical Journal, 320*(7228), 167.

James, J. E. A., et al. (1969). Cardiovascular responses in apnoeic asphyxia: role of arterial chemoreceptors and the modification of their effects by a pulmonary vagal inflation reflex. *The Journal of physiology, 201*(1), 87-104.

Jänig, W., et al. (1983). Reflex activation of postganglionic vasoconstrictor neurones supplying skeletal muscle by stimulation of arterial chemoreceptors via non-nicotinic synaptic mechanisms in sympathetic ganglia. *Pflügers Archiv, 396*(2), 95-100.

Jessup, M., et al. (2009). 2009 focused update: ACCF/AHA guidelines for the diagnosis and management of heart failure in adults: a report of the American College of Cardiology Foundation/American Heart Association Task Force on Practice Guidelines: developed

in collaboration with the International Society for Heart and Lung Transplantation. *Circulation, 119*(14), 1977-2016.
Jhund, P. S., et al. (2009). CLINICAL PERSPECTIVE. *Circulation, 119*(4), 515-523.
Jhund, P. S., et al. (2016). The neprilysin pathway in heart failure: a review and guide on the use of sacubitril/valsartan. *Heart, 102*(17), 1342-1347.
Johansson, M., et al. (1999). Increased sympathetic nerve activity in renovascular hypertension. *Circulation, 99*(19), 2537-2542.
Justice, T. D., et al. (2015). Effect of antecedent moderate-intensity exercise on the glycemia-increasing effect of a 30-sec maximal sprint: a sex comparison. *Physiological reports, 3*(5), e12386.
Kåhlin, J., et al. (2014). The human carotid body releases acetylcholine, ATP and cytokines during hypoxia. *Experimental physiology, 99*(8), 1089-1098.
Kantor, P. F., et al. (2010). Pathophysiology and management of heart failure in repaired congenital heart disease. *Heart failure clinics, 6*(4), 497-506.
Kara, T., et al. (2003). Chemoreflexes–physiology and clinical implications. *Acta Physiologica, 177*(3), 377-384.
Karim, F., et al. (1987). The effects of stimulating carotid chemoreceptors on renal haemodynamics and function in dogs. *The Journal of physiology, 392*(1), 451-462.
Kario, K. (2009). Obstructive sleep apnea syndrome and hypertension: mechanism of the linkage and 24-h blood pressure control. *Hypertension Research, 32*(7), 537-541.
Kawashima, T. (2005). The autonomic nervous system of the human heart with special reference to its origin, course, and peripheral distribution. *Anatomy and embryology, 209*(6), 425-438.
Kaye, D. M., et al. (1995). Adverse consequences of high sympathetic nervous activity in the failing human heart. *Journal of the American College of Cardiology, 26*(5), 1257-1263.
Kemp, C. D., et al. (2012). The pathophysiology of heart failure. *Cardiovascular Pathology, 21*(5), 365-371.
Kishi, T. (2012). Heart failure as an autonomic nervous system dysfunction. *Journal of cardiology, 59*(2), 117-122.
Klabunde, R. (2011). *Cardiovascular physiology concepts*: Lippincott Williams & Wilkins.
Koeners, M. P., et al. (2016). Hypertension: a problem of organ blood flow supply–demand mismatch. *Future cardiology, 12*(3), 339-349.
Kondo, H., et al. (1982). Immunocytochemical study on the localization of neuron-specific enolase and S-100 protein in the carotid body of rats. *Cell and tissue research, 227*(2), 291-295.
Krum, H., et al. (2009). Catheter-based renal sympathetic denervation for resistant hypertension: a multicentre safety and proof-of-principle cohort study. *The Lancet, 373*(9671), 1275-1281.
Kubin, L., et al. (2006). Central pathways of pulmonary and lower airway vagal afferents. *Journal of Applied Physiology, 101*(2), 618-627.
Kumagai, H., et al. (2012). Importance of rostral ventrolateral medulla neurons in determining efferent sympathetic nerve activity and blood pressure. *Hypertension Research, 35*(2), 132-141.
Kumar, P., et al. (2011). Peripheral chemoreceptors: function and plasticity of the carotid body. *Comprehensive Physiology, 2*(1), 141-219.
Lahiri, S. (2000). Historical perspectives of cellular oxygen sensing and responses to hypoxia. *Journal of Applied Physiology, 88*(4), 1467-1473.
Lahiri, S., et al. (1980). Relative responses of aortic body and carotid body chemoreceptors to hypotension. *Journal of Applied Physiology, 48*(5), 781-788.

Lahiri, S., et al. (2006). Oxygen sensing in the body. *Progress in biophysics and molecular biology, 91*(3), 249-286.
Lam, S. Y., et al. (2014). Upregulation of a local renin–angiotensin system in the rat carotid body during chronic intermittent hypoxia. *Experimental physiology, 99*(1), 220-231.
Lampland, A. L., et al. (2009). Observational study of humidified high-flow nasal cannula compared with nasal continuous positive airway pressure. *The Journal of pediatrics, 154*(2), 177-182. e172.
Langley, A., et al. (2015). Propranolol and central nervous system function: potential implications for paediatric patients with infantile haemangiomas. *British Journal of Dermatology, 172*(1), 13-23.
Lelovas, P. P., et al. (2014). A comparative anatomic and physiologic overview of the porcine heart. *Journal of the American Association for Laboratory Animal Science, 53*(5), 432-438.
Leung, P. S., et al. (2003). Renin–angiotensin system in the carotid body. *The international journal of biochemistry & cell biology, 35*(6), 847-854.
Leung, R. S., et al. (2004). Provocation of ventricular ectopy by Cheyne-Stokes respiration in patients with heart failure. *Sleep, 27*(7), 1337-1343.
Lever, J., et al. (1965). Neuromuscular and intercellular relationships in the coronary arterioles. A morphological and quantitative study by light and electron microscopy. *Journal of anatomy, 99*(Pt 4), 829.
Lewis, L. K., et al. (2017). Development of a BNP1-32 immunoassay that does not cross-react with proBNP. *Clinical chemistry, 63*(6), 1110-1117.
Li, Y.-L., et al. (2007). NADPH oxidase-derived superoxide anion mediates angiotensin II-enhanced carotid body chemoreceptor sensitivity in heart failure rabbits. *Cardiovascular research, 75*(3), 546-554.
Li, Y.-L., et al. (2006). Angiotensin II enhances carotid body chemoreflex control of sympathetic outflow in chronic heart failure rabbits. *Cardiovascular research, 71*(1), 129-138.
Liu, J.-L., et al. (2000). Chronic exercise reduces sympathetic nerve activity in rabbits with pacing-induced heart failure: a role for angiotensin II. *Circulation, 102*(15), 1854-1862.
Liu, J.-L., et al. (1999a). ANG II and baroreflex function in rabbits with CHF and lesions of the area postrema. *American Journal of Physiology-Heart and Circulatory Physiology, 277*(1), H342-H350.
Liu, J.-L., et al. (1999b). Regulation of sympathetic nerve activity in heart failure: a role for nitric oxide and angiotensin II. *Circulation research, 84*(4), 417-423.
Lodeserto, F. J., et al. (2018). High-flow nasal cannula: mechanisms of action and adult and pediatric indications. *Cureus, 10*(11)
Lohse, M. J., et al. (2003). What is the role of β-adrenergic signaling in heart failure? *Circulation research, 93*(10), 896-906.
Lopez-Barneo, J., et al. (1988). Chemotransduction in the carotid body: K+ current modulated by PO2 in type I chemoreceptor cells. *Science, 241*(4865), 580-582.
López-Barneo, J., et al. (2008). Carotid body oxygen sensing. *European Respiratory Journal, 32*(5), 1386-1398.
López-Barneo, J., et al. (2001). Cellular mechanism of oxygen sensing. *Annual review of physiology, 63*(1), 259-287.
Lu, Y., et al. (2013). Responses of glomus cells to hypoxia and acidosis are uncoupled, reciprocal and linked to ASIC3 expression: selectivity of chemosensory transduction. *The Journal of physiology, 591*(4), 919-932.
Lukács, E., et al. (2012). Overview of large animal myocardial infarction models. *Acta physiologica Hungarica, 99*(4), 365-381.

Lundin, S., et al. (1984). Renal sympathetic activity in spontaneously hypertensive rats and normotensive controls, as studied by three different methods. *Acta physiologica Scandinavica, 120*(2), 265-272.

Ma, R., et al. (1997). Central gain of the cardiac sympathetic afferent reflex in dogs with heart failure. *American Journal of Physiology-Heart and Circulatory Physiology, 273*(6), H2664-H2671.

MacFarlane, P. D., et al. (2012). Early experience with continuous positive airway pressure (CPAP) in 5 horses—a case series. *The Canadian Veterinary Journal, 53*(4), 426.

Malliani, A., et al. (1983). Cardiovascular reflexes mediated by sympathetic afferent fibers. *Journal of the autonomic nervous system, 7*(3-4), 295-301.

Maman, S. R., et al. (2017). Beta-1 vs. beta-2 adrenergic control of coronary blood flow during isometric handgrip exercise in humans. *J Appl Physiol (1985), 123*(2), 337-343. 10.1152/japplphysiol.00106.2017

Mann, D. L., et al. (1992). Adrenergic effects on the biology of the adult mammalian cardiocyte. *Circulation, 85*(2), 790-804.

Marcus, N., et al. (2014a). Carotid body denervation reduces renal sympathetic nerve activity and fibrosis, and increases renal blood flow in congestive heart failure (875.14). *The FASEB Journal, 28*, 875.814.

Marcus, N. J., et al. (2014b). Carotid body denervation improves autonomic and cardiac function and attenuates disordered breathing in congestive heart failure. *The Journal of physiology, 592*(2), 391-408.

Marcus, N. J., et al. (2014c). Central role of carotid body chemoreceptors in disordered breathing and cardiorenal dysfunction in chronic heart failure. *Frontiers in physiology, 5*, 438.

Marcus, N. J., et al. (2014d). Carotid body denervation improves autonomic and cardiac function and attenuates disordered breathing in congestive heart failure. *The Journal of physiology, 592*(2), 391-408.

Mark, A. Y. L. (1995). Sympathetic dysregulation in heart failure: mechanisms and therapy. *Clinical cardiology, 18*(S1), I-3-I-8.

Markovitz, L. J., et al. (1989). Large animal model of left ventricular aneurysm. *The Annals of thoracic surgery, 48*(6), 838-845.

Marshall, J. M. (1994). Peripheral chemoreceptors and cardiovascular regulation. *Physiological reviews, 74*(3), 543-594.

Martínez-García, M. A., et al. (2007). Positive effect of CPAP treatment on the control of difficult-to-treat hypertension. *European Respiratory Journal, 29*(5), 951-957.

Matsukawa, K., et al. (1993). Effects of anesthesia on cardiac and renal sympathetic nerve activities and plasma catecholamines. *American Journal of Physiology-Regulatory, Integrative and Comparative Physiology, 265*(4), R792-R797.

McBryde, F. D., et al. (2013). The carotid body as a putative therapeutic target for the treatment of neurogenic hypertension. *Nature communications, 4*(1), 1-11.

McBryde, F. D., et al. (2017). Evaluating the carotid bodies and renal nerves as therapeutic targets for hypertension. *Autonomic Neuroscience, 204*, 126-130.

McCorry, L. K. (2007). Physiology of the autonomic nervous system. *American journal of pharmaceutical education, 71*(4)

McDonald, D. M., et al. (1983). The ultrastructure and connections of blood vessels supplying the rat carotid body and carotid sinus. *Journal of neurocytology, 12*(1), 117-153.

McGinley, B. M., et al. (2007). A nasal cannula can be used to treat obstructive sleep apnea. *American journal of respiratory and critical care medicine, 176*(2), 194-200.

McMurray, J. J., et al. (2012). ESC Guidelines for the diagnosis and treatment of acute and chronic heart failure 2012. *European journal of heart failure, 14*(8), 803-869.

McNulty, P. H., et al. (2005). Effects of supplemental oxygen administration on coronary blood flow in patients undergoing cardiac catheterization. *American Journal of Physiology-Heart and Circulatory Physiology, 288*(3), H1057-H1062.
Melo, M. R., et al. (2020). Renovascular hypertension elevates pulmonary ventilation in rats by carotid body-dependent mechanisms. *American Journal of Physiology-Regulatory, Integrative and Comparative Physiology, 318*(4), R730-R742.
Melo, M. R., et al. (2019). Importance of the commissural nucleus of the solitary tract in renovascular hypertension. *Hypertension Research, 42*(5), 587-597.
Milani-Nejad, N., et al. (2014). Small and large animal models in cardiac contraction research: advantages and disadvantages. *Pharmacology & therapeutics, 141*(3), 235-249.
Miller, L. W. (2003). Limitations of current medical therapies for the treatment of heart failure. *Reviews in cardiovascular medicine, 4*(S2), 21-29.
Ministry of Health, N. (2011). Tatau Kura Tangata: health of older Māori chart book 2011: Ministry of Health Wellington.
Ministry of Health, N. (2013). *Strategic Overview: Cardiovascular Disease in New Zealand*. Wellington: National Health Committee.
Miyashiro, J. K., et al. (1993). Feedforward control of coronary blood flow via coronary beta-receptor stimulation. *Circ Res, 73*(2), 252-263. 10.1161/01.res.73.2.252
Mizeres, N. J. (1955). The anatomy of the autonomic nervous system in the dog. *Am J Anat, 96*(2), 285-318. 10.1002/aja.1000960205
Mohrman, D. E., et al. (2014). *Cardiovascular physiology*: Univerza v Ljubljani, Medicinska fakulteta.
Möller, W., et al. (2015). Nasal high flow clears anatomical dead space in upper airway models. *Journal of Applied Physiology, 118*(12), 1525-1532.
Möller, W., et al. (2017). Nasal high flow reduces dead space. *Journal of Applied Physiology, 122*(1), 191-197.
Momen, A., et al. (2009). Coronary blood flow responses to physiological stress in humans. *American Journal of Physiology-Heart and Circulatory Physiology, 296*(3), H854-H861.
Montoro, R., et al. (1996). Oxygen sensing by ion channels and chemotransduction in single glomus cells. *The Journal of general physiology, 107*(1), 133-143.
Moradkhan, R., et al. (2010). Revisiting the role of oxygen therapy in cardiac patients. *Journal of the American College of Cardiology, 56*(13), 1013-1016.
Morrison, S. F. (2001). Differential control of sympathetic outflow. *American Journal of Physiology-Regulatory, Integrative and Comparative Physiology, 281*(3), R683-R698.
Mortara, A., et al. (1997). Abnormal awake respiratory patterns are common in chronic heart failure and may prevent evaluation of autonomic tone by measures of heart rate variability. *Circulation, 96*(1), 246-252.
Mosing, M., et al. (2011). Use of continuous positive airway pressure (CPAP) in a horse with diaphragmatic hernia. *Pferdeheilkunde, 27*(1), 66-69.
Murakami, H., et al. (1997). Angiotensin II enhances baroreflex control of sympathetic outflow in heart failure. *Hypertension, 29*(2), 564-569.
Murakami, H., et al. (1996). Blockade of AT1 receptors enhances baroreflex control of heart rate in conscious rabbits with heart failure. *American Journal of Physiology-Regulatory, Integrative and Comparative Physiology, 271*(1), R303-R309.
Murphree, S. S., et al. (1988). Delineation of the distribution of beta-adrenergic receptor subtypes in canine myocardium. *Circulation research, 63*(1), 117-125.
Murphy, S. P., et al. (2020). Heart failure with reduced ejection fraction: a review. *Jama, 324*(5), 488-504.

Murray, P. A., et al. (1984). Alpha-adrenergic-mediated reduction in coronary blood flow secondary to carotid chemoreceptor reflex activation in conscious dogs. *Circulation Research, 54*(1), 96-106.

Narkiewicz, K., et al. (1999). Enhanced sympathetic and ventilatory responses to central chemoreflex activation in heart failure. *Circulation, 100*(3), 262-267.

Narkiewicz, K., et al. (1998). Contribution of tonic chemoreflex activation to sympathetic activity and blood pressure in patients with obstructive sleep apnea. *Circulation, 97*(10), 943-945.

Naughton, M., et al. (1993). Role of hyperventilation in the pathogenesis of central sleep apneas in patients with congestive heart failure. *American Review of Respiratory Disease, 148*, 330-330.

Navar, L. G., et al. (1998). Unraveling the mystery of Goldblatt hypertension. *Physiology, 13*(4), 170-176.

Navarro-Soriano, C., et al. (2021). Long-term effect of CPAP treatment on cardiovascular events in patients with resistant hypertension and sleep apnea. Data from the HIPARCO-2 study. *Archivos de bronconeumologia, 57*(3), 165-171.

Neil, E., et al. (1971). Efferent and afferent impulse activity recorded from few-fibre preparations of otherwise intact sinus and aortic nerves. *The Journal of physiology, 215*(1), 33-47.

Niewinski, P. (2014). Pathophysiology and potential clinical applications for testing of peripheral chemosensitivity in heart failure. *Current heart failure reports, 11*(2), 126-133.

Ninomiya, I., et al. (1971). Sympathetic nerve activity to the spleen, kidney, and heart in response to baroceptor input. *American Journal of Physiology-Legacy Content, 221*(5), 1346-1351.

Nonidez, J. F. (1939). Studies on the innervation of the heart. I. Distribution of the cardiac nerves, with special reference to the identification of the sympathetic and parasympathetic postganglionics. *American Journal of Anatomy, 65*(3), 361-413.

Nosrat, C. A., et al. (1996). Cellular expression of GDNF mRNA suggests multiple functions inside and outside the nervous system. *Cell and tissue research, 286*(2), 191-207.

Nurse, C. A. (2005). Neurotransmission and neuromodulation in the chemosensory carotid body. *Autonomic Neuroscience, 120*(1-2), 1-9.

Nurse, C. A., et al. (2013). *Signal processing at mammalian carotid body chemoreceptors.* Paper presented at the Seminars in cell & developmental biology.

Nurse, C. A., et al. (1997). Role of basic FGF and oxygen in control of proliferation, survival, and neuronal differentiation in carotid body chromaffin cells. *Developmental biology, 184*(2), 197-206.

O'Regan, R., et al. (1982). Role of peripheral chemoreceptors and central chemosensitivity in the regulation of respiration and circulation. *Journal of Experimental Biology, 100*(1), 23-40.

O'driscoll, B., et al. (2008). BTS guideline for emergency oxygen use in adult patients. *Thorax, 63*(Suppl 6), vi1-vi68.

O'Regan, R. (1977). Control of carotid body chemoreceptors by autonomic nerves. *Irish journal of medical science, 146*(1), 199-205.

Oliveira-Sales, E., et al. (2011). Sympathetic over activity occurs before the hypertension in the two-kidney one clip model. *Autonomic Neuroscience: Basic and Clinical, 163*(1), 81-82.

Oliveira-Sales, E. B., et al. (2009). Oxidative stress in the sympathetic premotor neurons contributes to sympathetic activation in renovascular hypertension. *American Journal of Hypertension, 22*(5), 484-492.

Ostergaard, G., et al. (2010). Handbook of laboratory animal science, Volume I: Essential Principles and Practices.

Pachen, M., et al. (2020). Activation of the carotid body increases directly recorded cardiac sympathetic nerve activity and coronary blood flow in conscious sheep. *American Journal of Physiology-Regulatory, Integrative and Comparative Physiology*

Packer, M. (1992a). The neurohormonal hypothesis: a theory to explain the mechanism of disease progression in heart failure. *Journal of the American College of Cardiology, 20*(1), 248-254.

Packer, M. (1992b). Pathophysiology of chronic heart failure. *The Lancet, 340*(8811), 88-92.

Padley, J. R., et al. (2007). Central command regulation of circulatory function mediated by descending pontine cholinergic inputs to sympathoexcitatory rostral ventrolateral medulla neurons. *Circ Res, 100*(2), 284-291. 10.1161/01.RES.0000257370.63694.73

Pardal, R., et al. (2007). Glia-like stem cells sustain physiologic neurogenesis in the adult mammalian carotid body. *Cell, 131*(2), 364-377.

Parke, R., et al. (2009). Nasal high-flow therapy delivers low level positive airway pressure. *British journal of anaesthesia, 103*(6), 886-890.

Paton, J. F., et al. (2013). The carotid body as a therapeutic target for the treatment of sympathetically mediated diseases: Am Heart Assoc.

Pelosi, P., et al. (2010). Noninvasive respiratory support in the perioperative period. *Current Opinion in Anesthesiology, 23*(2), 233-238.

Pijacka, W., et al. (2016a). Carotid sinus nerve denervation ameliorates renovascular hypertension in adult Wistar rats.

Pijacka, W., et al. (2016b). Purinergic receptors in the carotid body as a new drug target for controlling hypertension. *Nature medicine, 22*(10), 1151-1159.

Ploth, D. (1983). Angiotensin-dependent renal mechanisms in two-kidney, one-clip renal vascular hypertension. *American Journal of Physiology-Renal Physiology, 245*(2), F131-F141.

Ponikowski, P., et al. (1999). Oscillatory breathing patterns during wakefulness in patients with chronic heart failure: clinical implications and role of augmented peripheral chemosensitivity. *Circulation, 100*(24), 2418-2424.

Ponikowski, P., et al. (2001). Peripheral chemoreceptor hypersensitivity: an ominous sign in patients with chronic heart failure. *Circulation, 104*(5), 544-549.

Ponikowski, P., et al. (1997). Augmented peripheral chemosensitivity as a potential input to baroreflex impairment and autonomic imbalance in chronic heart failure. *Circulation, 96*(8), 2586-2594.

Porter, T., et al. (1990). Autonomic pathophysiology in heart failure patients. Sympathetic-cholinergic interrelations. *The Journal of clinical investigation, 85*(5), 1362-1371.

Prabhakar, N. R., et al. (2004). Peripheral chemoreceptors in health and disease. *Journal of Applied Physiology, 96*(1), 359-366.

Prasad, B., et al. (2020). The need for specificity in quantifying neurocirculatory vs. respiratory effects of eucapnic hypoxia and transient hyperoxia. *The Journal of physiology*

Proakis, A., et al. (1979). Comparative penetration of glycopyrrolate and atropine across the blood-brain and placental barriers in anesthetized dogs. *Survey of Anesthesiology, 23*(3), 166.

Ramchandra, R., et al. (2006). Evidence of differential control of renal and lumbar sympathetic nerve activity in conscious rabbits. *American Journal of Physiology-Regulatory, Integrative and Comparative Physiology, 290*(3), R701-R708.

Ramchandra, R., et al. (2018). Mechanisms underlying the increased cardiac norepinephrine spillover in heart failure. *American Journal of Physiology-Heart and Circulatory Physiology*

Ramchandra, R., et al. (2009). Basis for the preferential activation of cardiac sympathetic nerve activity in heart failure. *Proceedings of the National Academy of Sciences, 106*(3), 924-928.

Ramchandra, R., et al. (2012). Central angiotensin type 1 receptor blockade decreases cardiac but not renal sympathetic nerve activity in heart failure. *Hypertension, 59*(3), 634-641.

Ramchandra, R., et al. (2008). The Responses of Cardiac Sympathetic Nerve Activity to Changes in Circulating Volume Differ in Normal and Heart Failure Sheep. *American Journal of Physiology-Regulatory, Integrative and Comparative Physiology*

Reid, I. (1992). Interactions between ANG II, sympathetic nervous system, and baroreceptor reflexes in regulation of blood pressure. *American Journal of Physiology-Endocrinology And Metabolism, 262*(6), E763-E778.

Reserve, C., et al. Increased Chemoreceptor Sensitivity-A Contributory Cause of Dyspnea in Chronic Heart Failure?

Riddell, T. (2005). Heart failure hospitalisations and deaths in New Zealand: patterns by deprivation and ethnicity. *The New Zealand Medical Journal (Online), 118*(1208)

Rocha, I., et al. (2003). Angiotensin AT1 receptor antagonist losartan and the defence reaction in the anaesthetised rat. Effect on the carotid chemoreflex. *Experimental physiology, 88*(3), 309-314.

Roger, V. L. (2013). Epidemiology of heart failure. *Circulation research, 113*(6), 646-659.

Rogers, C., et al. (2015). Heart failure: pathophysiology, diagnosis, medical treatment guidelines, and nursing management. *Nursing Clinics, 50*(4), 787-799.

Rundqvist, B. (1997). Elam M, Bergmann-Sverrisdottir Y, Eisenhofer G, and Friberg P. *Increased cardiac adrenergic drive precedes generalized sympathetic activation in human heart failure. Circulation, 95*, 169-175.

Rutherford, J. D., et al. (1978). Integrated carotid chemoreceptor and pulmonary inflation reflex control of peripheral vasoactivity in conscious dogs. *Circulation research, 43*(2), 200-208.

Sackett, D., et al. (1975). Randomised clinical trial of strategies for improving medication compliance in primary hypertension. *The Lancet, 305*(7918), 1205-1207.

Saslow, J., et al. (2006). Work of breathing using high-flow nasal cannula in preterm infants. *Journal of Perinatology, 26*(8), 476-480.

Sata, Y., et al. (2018). Role of the sympathetic nervous system and its modulation in renal hypertension. *Frontiers in medicine, 5*, 82.

Savarese, G., et al. (2017). Global public health burden of heart failure. *Cardiac failure review, 3*(1), 7.

Schaper, W., et al. (1972). Comparative aspects of coronary collateral circulation *Comparative Pathophysiology of Circulatory Disturbances* (pp. 267-276): Springer.

Schaufelberger, M., et al. (2004). Decreasing one-year mortality and hospitalization rates for heart failure in Sweden: data from the Swedish Hospital Discharge Registry 1988 to 2000. *European heart journal, 25*(4), 300-307.

Schlaich, M. P., et al. (2009). Renal sympathetic-nerve ablation for uncontrolled hypertension. *New England journal of medicine, 361*(9), 932-934.

Schmidt, H., et al. (2005). Chemo-and ergoreflexes in health, disease and ageing. *International journal of cardiology, 98*(3), 369-378.

Schmitto, J., et al. (2008). Chronic heart failure induced by multiple sequential coronary microembolization in sheep. *The International journal of artificial organs, 31*(4), 348-353.

Schmitto, J. D., et al. (2009). Hemodynamic changes in a model of chronic heart failure induced by multiple sequential coronary microembolization in sheep. *Artificial organs, 33*(11), 947-952.

Schultz, H. D., et al. (2007a). Carotid body function in heart failure. *Respiratory physiology & neurobiology, 157*(1), 171-185.
Schultz, H. D., et al. (2007b). Arterial chemoreceptors and sympathetic nerve activity. *Hypertension, 50*(1), 6-13.
Schultz, H. D., et al. (2007c). Arterial chemoreceptors and sympathetic nerve activity: implications for hypertension and heart failure. *Hypertension, 50*(1), 6-13.
Schultz, H. D., et al. (2012). Heart failure and carotid body chemoreception. *Arterial Chemoreception*, 387-395.
Schultz, H. D., et al. (2013). Role of the carotid body in the pathophysiology of heart failure. *Current hypertension reports, 15*(4), 356-362.
Schultz, H. D., et al. (2015). Mechanisms of carotid body chemoreflex dysfunction during heart failure. *Experimental physiology, 100*(2), 124-129.
Schwartz, P. J., et al. (2011). Sympathetic–parasympathetic interaction in health and disease: abnormalities and relevance in heart failure. *Heart failure reviews, 16*(2), 101-107.
Sciarretta, S., et al. (2009). Role of the renin–angiotensin–aldosterone system and inflammatory processes in the development and progression of diastolic dysfunction. *Clinical Science, 116*(6), 467-477.
Sepehrvand, N., et al. (2016). Oxygen therapy in patients with acute heart failure: friend or foe? *JACC: Heart Failure, 4*(10), 783-790.
Shapiro, E. (1972). Adolf Fick—Forgotten genius of cardiology. *The American journal of cardiology, 30*(6), 662-665.
Shen, W., et al. (1994). Role of EDRF/NO in parasympathetic coronary vasodilation following carotid chemoreflex activation in conscious dogs. *American Journal of Physiology-Heart and Circulatory Physiology, 267*(2), H605-H613.
Shibasaki, M., et al. (2010). Mechanisms and controllers of eccrine sweating in humans. *Frontiers in bioscience (Scholar edition), 2*, 685.
Silva, K. A. S., et al. (2020). Large Animal Models of Heart Failure: A Translational Bridge to Clinical Success. *JACC: Basic to Translational Science, 5*(8), 840-856.
Siński, M., et al. (2012). Tonic activity of carotid body chemoreceptors contributes to the increased sympathetic drive in essential hypertension. *Hypertension Research, 35*(5), 487-491.
Sinski, M., et al. (2014). Deactivation of carotid body chemoreceptors by hyperoxia decreases blood pressure in hypertensive patients. *Hypertension Research, 37*(9), 858-862.
Smit, B., et al. (2018). Hemodynamic effects of acute hyperoxia: systematic review and meta-analysis. *Critical Care, 22*(1), 45.
Smith, P. A., et al. (2004). Relationship between central sympathetic activity and stages of human hypertension. *American Journal of Hypertension, 17*(3), 217-222.
Stats, N. (2016). National population projections: 2016 (base)–2068. *Stats NZ, Wellington,stats. govt. nz/browse_for_stats/population/estimates_and_projections/NationalPopulationProjections*
Stevens, J. P., et al. (2018). Prevalence of dyspnea among hospitalized patients at the time of admission. *Journal of pain and symptom management, 56*(1), 15-22. e12.
Stoker, M. E., et al. (1982). Regional differences in capillary density and myocyte size in the normal human heart. *The Anatomical Record, 202*(2), 187-191.
Strosberg, A. (1993). Structure, function, and regulation of adrenergic receptors. *Protein Science, 2*(8), 1198-1209.
Sun, D., et al. (2002). Norepinephrine elicits β2-receptor–mediated dilation of isolated human coronary arterioles. *Circulation, 106*(5), 550-555.

Sun, S.-Y., et al. (1999a). Enhanced activity of carotid body chemoreceptors in rabbits with heart failure: role of nitric oxide. *Journal of Applied Physiology, 86*(4), 1273-1282.

Sun, S.-Y., et al. (1999b). Enhanced peripheral chemoreflex function in conscious rabbits with pacing-induced heart failure. *Journal of Applied Physiology, 86*(4), 1264-1272.

Suzuki, H., et al. (2004). Altered effects of angiotensin ii type 1 and type 2 receptor blockers on cardiac norepinephrine release and inotropic responses during cardiac sympathetic nerve stimulation in aorto-caval shunt rats. *Circulation Journal, 68*(7), 683-690.

Swedberg, K., et al. (2005). Guidelines for the diagnosis and treatment of chronic heart failure: executive summary (update 2005) The Task Force for the Diagnosis and Treatment of Chronic Heart Failure of the European Society of Cardiology. *European heart journal, 26*(11), 1115-1140.

Swedberg, K., et al. (1990). Hormones regulating cardiovascular function in patients with severe congestive heart failure and their relation to mortality. CONSENSUS Trial Study Group. *Circulation, 82*(5), 1730-1736.

Tafil-Klawe, M., et al. (1985). Augmented chemoreceptor reflex tonic drive in early human hypertension and in normotensive subjects with family background of hypertension. *Acta Physiologica Polonica, 36*(1), 51-58.

Tanai, E., et al. (2015). Pathophysiology of heart failure. *Comprehensive Physiology*

Te Riet, L., et al. (2015). Hypertension: renin–angiotensin–aldosterone system alterations. *Circulation research, 116*(6), 960-975.

Thames, M. D., et al. (1993). Abnormalities of baroreflex control in heart failure. *Journal of the American College of Cardiology, 22*(4S1), A56-A60.

Thompson, E. L., et al. (2016). Adrenaline release evokes hyperpnoea and an increase in ventilatory CO2 sensitivity during hypoglycaemia: a role for the carotid body. *The Journal of physiology, 594*(15), 4439-4452.

Triposkiadis, et al. (2009a). The sympathetic nervous system in heart failure: physiology, pathophysiology, and clinical implications. *Journal of the American College of Cardiology, 54*(19), 1747-1762.

Triposkiadis, F., et al. (2009b). Current drugs and medical treatment algorithms in the management of acute decompensated heart failure. *Expert opinion on investigational drugs, 18*(6), 695-707.

Trivella, M., et al. (1990). Beta-receptor subtypes in the canine coronary circulation. *American Journal of Physiology-Heart and Circulatory Physiology, 259*(5), H1575-H1585.

Tromp, T. R., et al. (2018). Direct recording of cardiac and renal sympathetic nerve activity shows differential control in renovascular hypertension. *Hypertension, 71*(6), 1108-1116.

Trzebski, A. (1992). Arterial chemoreceptor reflex and hypertension. *Hypertension, 19*(6_pt_1), 562-566.

Trzebski, A., et al. (1982). Increased sensitivity of the arterial chemoreceptor drive in young men with mild hypertension. *Cardiovascular research, 16*(3), 163-172.

Tune, J. D. (2014). *Coronary circulation.* Paper presented at the Colloquium Series on Integrated Systems Physiology: From Molecule to Function to Disease.

Tune, J. D., et al. (2004). Matching coronary blood flow to myocardial oxygen consumption. *Journal of Applied Physiology, 97*(1), 404-415.

Tune, J. D., et al. (2002). Control of coronary blood flow during exercise. *Experimental biology and medicine, 227*(4), 238-250.

Turner, K., et al. (1996). The positions of coronary arterial ostia. *Clinical Anatomy: The Official Journal of the American Association of Clinical Anatomists and the British Association of Clinical Anatomists, 9*(6), 376-380.

Urena, J., et al. (1994). Hypoxia induces voltage-dependent Ca2+ entry and quantal dopamine secretion in carotid body glomus cells. *Proceedings of the National Academy of Sciences, 91*(21), 10208-10211.

Urena, J., et al. (1989). Ionic currents in dispersed chemoreceptor cells of the mammalian carotid body. *The Journal of general physiology, 93*(5), 979-999.

Vaseghi, M., et al. (2008). The role of the autonomic nervous system in sudden cardiac death. *Progress in cardiovascular diseases, 50*(6), 404.

Vatner, S. F., et al. (1975). Interaction of the chemoreflex and the pulmonary inflation reflex in the regulation of coronary circulation in conscious dogs. *Circulation Research, 37*(5), 664-673.

Verkhratsky, A., et al. (1998). Glial calcium: homeostasis and signaling function. *Physiological reviews, 78*(1), 99-141.

Vieira, A. A., et al. (2007). Central cholinergic blockade reduces the pressor response to L-glutamate into the rostral ventrolateral medullary pressor area. *Brain Res, 1155*, 100-107. 10.1016/j.brainres.2007.04.023

Villadiego, J., et al. (2005). Selective glial cell line-derived neurotrophic factor production in adult dopaminergic carotid body cells in situ and after intrastriatal transplantation. *Journal of Neuroscience, 25*(16), 4091-4098.

Wallin, B. G., et al. (2007). Sympathetic neural control of integrated cardiovascular function: insights from measurement of human sympathetic nerve activity. *Muscle & nerve, 36*(5), 595-614.

Wang, W.-Z., et al. (2008). Interaction between cardiac sympathetic afferent reflex and chemoreflex is mediated by the NTS AT1 receptors in heart failure. *American Journal of Physiology-Heart and Circulatory Physiology, 295*(3), H1216-H1226.

Wasywich, C. A., et al. (2007). Changing Survival of Patients with Heart Failure in New Zealand over 18 Years. *Journal of Cardiac Failure, 13*(6), S165.

Watson, A., et al. (2006). Mechanisms of sympathetic activation in heart failure. *Clinical and experimental pharmacology and physiology, 33*(12), 1269-1274.

Watson, A. M., et al. (2007). Increased cardiac sympathetic nerve activity in heart failure is not due to desensitization of the arterial baroreflex. *American Journal of Physiology-Heart and Circulatory Physiology, 293*(1), H798-H804.

Watson, A. M., et al. (2004). Stimulation of cardiac sympathetic nerve activity by central angiotensinergic mechanisms in conscious sheep. *American Journal of Physiology-Regulatory, Integrative and Comparative Physiology, 286*(6), R1051-R1056.

Wehrwein, E. A., et al. (2011). Overview of the anatomy, physiology, and pharmacology of the autonomic nervous system. *Comprehensive Physiology, 6*(3), 1239-1278.

Weil, J. V. (2011). Ventilatory control at high altitude. *Comprehensive Physiology*, 703-727.

Wolff, C. B. (2008). Normal cardiac output, oxygen delivery and oxygen extraction *Oxygen transport to tissue XXVIII* (pp. 169-182): Springer.

Xing, D. T., et al. (2014). Tonic arterial chemoreceptor activity contributes to cardiac sympathetic activation in mild ovine heart failure. *Experimental physiology, 99*(8), 1031-1041.

Xu, B., et al. (2015). Brain mechanisms of sympathetic activation in heart failure: Roles of the renin-angiotensin system, nitric oxide and pro-inflammatory cytokines. *Molecular medicine reports, 12*(6), 7823-7829.

Xu, J., et al. (2003). ATP triggers intracellular Ca2+ release in type II cells of the rat carotid body. *The Journal of physiology, 549*(3), 739-747.

Yancy, C. W., et al. (2017). 2017 ACC/AHA/HFSA Focused Update of the 2013 ACCF/AHA Guideline for the Management of Heart Failure.

Yang, R.-F., et al. (2010). Angiotensin-(1–7) increases neuronal potassium current via a nitric oxide-dependent mechanism. *American Journal of Physiology-Cell Physiology, 300*(1), C58-C64.

Yeung, D. F., et al. (2012). Trends in the incidence and outcomes of heart failure in Ontario, Canada: 1997 to 2007. *Cmaj, 184*(14), E765-E773.

Young, C. N., et al. (2015). Angiotensin-II, the brain, and hypertension: an update. *Hypertension, 66*(5), 920-926.

Young, J. B., et al. (2004). Mortality and morbidity reduction with Candesartan in patients with chronic heart failure and left ventricular systolic dysfunction: results of the CHARM low-left ventricular ejection fraction trials. *Circulation, 110*(17), 2618-2626.

Young, M., et al. (1991). α-and β-adrenergic control of large coronary arteries in conscious calves *Adrenergic Mechanisms in Myocardial Ischemia* (pp. 97-109): Springer.

Zapata, P., et al. (2009). Cardiovascular responses to hyperoxic withdrawal of arterial chemosensory drive *Arterial Chemoreceptors* (pp. 290-297): Springer.

Zera, T., et al. (2019). The logic of carotid body connectivity to the brain. *Physiology, 34*(4), 264-282.

Zhang, D. Y., et al. (2014). The sympathetic nervous system and heart failure. *Cardiology clinics, 32*(1), 33-45.

Zhang, W., et al. (1999). Brain renin-angiotensin system and sympathetic hyperactivity in rats after myocardial infarction. *American Journal of Physiology-Heart and Circulatory Physiology, 276*(5), H1608-H1615.

Zimpfer, M., et al. (1981). Effects of anesthesia on the canine carotid chemoreceptor reflex. *Circulation Research, 48*(3), 400-406.

Zipes, D. P. (2008). Heart-brain interactions in cardiac arrhythmias: role of the autonomic nervous system. *Cleveland Clinic journal of medicine, 75*(2), S94.

Zipes, D. P., et al. (2006). Neural modulation of cardiac arrhythmias and sudden cardiac death. *Heart rhythm, 3*(1), 108-113.

Zoccal, D. B., et al. (2011). Coupling between respiratory and sympathetic activities as a novel mechanism underpinning neurogenic hypertension. *Current hypertension reports, 13*(3), 229.

Zucker, I. H. (2006). Novel mechanisms of sympathetic regulation in chronic heart failure. *Hypertension, 48*(6), 1005-1011.

Zucker, I. H., et al. (1985). Impaired atrial receptor modulation or renal nerve activity in dogs with chronic volume overload1. *Cardiovascular research, 19*(7), 411-418.

Zucker, I. H., et al. (2004). The origin of sympathetic outflow in heart failure: the roles of angiotensin II and nitric oxide. *Progress in biophysics and molecular biology, 84*(2-3), 217-232.

Zucker, I. H., et al. (2001). The regulation of sympathetic outflow in heart failure: the roles of angiotensin II, nitric oxide, and exercise training. *Annals of the New York Academy of Sciences, 940*(1), 431-443.